

Role of Mitochondrial Dynamics and Autophagy in Removal of Helix-Distorting

Mitochondrial DNA Damage

by

Amanda Smith Bess

Environment
Duke University

Date: _____

Approved:

Joel N. Meyer, Supervisor

William C. Copeland

Richard T. Di Giulio

David E. Hinton

Dissertation submitted in partial fulfillment of
the requirements for the degree of Doctor of Philosophy in
Environment in the Graduate School
of Duke University

2012

ABSTRACT

Role of Mitochondrial Dynamics and Autophagy in Removal of Helix-Distorting

Mitochondrial DNA Damage

by

Amanda Smith Bess

Environment
Duke University

Date: _____

Approved:

Joel N. Meyer, Supervisor

William C. Copeland

Richard T. Di Giulio

David E. Hinton

An abstract of a dissertation submitted in partial
fulfillment of the requirements for the degree
of Doctor of Philosophy in
Environment in the Graduate School
of Duke University

2012

Copyright by
Amanda Smith Bess
2012

Abstract

Mitochondria are the primary energy producers of the cell and play key roles in cellular signaling, apoptosis and reactive oxygen species (ROS) production.

Mitochondria are the only organelles that contain their own genome which encodes for a small subset of electron transport chain (ETC) proteins as well as the necessary tRNAs and ribosomal subunits to translate these proteins. Over 300 pathogenic mitochondrial DNA (mtDNA) mutations have been shown to cause a number of mitochondrial diseases emphasizing the importance of mtDNA maintenance and integrity to human health. Additionally, mitochondrial dysfunction and mtDNA instability are linked to many wide-spread diseases associated with aging including cancer and neurodegeneration. Mitochondria lack the ability to repair certain helix-distorting lesions that are induced at high levels in mtDNA by important environmental genotoxins including polycyclic aromatic hydrocarbons, ultraviolet C radiation (UVC) and mycotoxins. These lesions are irreparable and persistent in the short term, but their long-term fate is unknown. Degradation of mitochondria and mtDNA is carried out by autophagy. Autophagy is protective against cell stress and apoptosis resulting from exposure to mitochondrial toxicants suggesting that it plays an important role in removal of unstable mitochondria that can serve as a source of ROS or initiate apoptotic cell death. Furthermore, dysfunctional mitochondria can be specifically targeted for

degradation by the more specific process of mitophagy influenced in part by the processes of mitochondrial dynamics (i.e., fusion and fission).

The goals of this dissertation were to investigate the long-term fate of helix-distorting mtDNA damage and determine the significance of autophagy and mitochondrial dynamics in removal of and recovery from persistent mtDNA damage. Removal of irreparable mtDNA damage and the necessity of autophagy, mitophagy, fusion and fission genes in removal of this damage were examined using genetic approaches in adult *Caenorhabditis elegans*. In order to investigate the significance of autophagy, fusion and fission genes in recovery from mtDNA damage-induced mitochondrial dysfunction *in vivo*, an experimental method was developed to specifically induce persistent mtDNA damage and mitochondrial dysfunction without persistent nDNA damage in developing *C. elegans*. Additionally, the effect of persistent helix-distorting DNA damage on mitochondrial morphology, mitochondrial function and autophagy was investigated in *C. elegans* and in mammalian cell culture. The rate and specificity of mitochondrial degradation was further examined in cell culture using live-cell fluorescence microscopy and transmission electron microscopy.

Removal of UVC-induced mtDNA damage was detectable by 72 hours in *C. elegans* and mammalian cell culture, and required mitochondrial fusion, fission and autophagy, providing genetic evidence for a novel mtDNA damage removal pathway. UVC exposure induced autophagy with no detectable effect on mitochondrial

morphology in both systems; mitochondrial function was inhibited in the *C. elegans* system but not in the cell culture system in which the degree of mtDNA damage induced was less. Furthermore, mutations in genes involved in these processes as well as pharmacological inhibition of autophagy exacerbated mtDNA damage-mediated larval arrest, illustrating the *in vivo* relevance of removal of persistent mtDNA damage. Mutations in genes in these pathways exist in the human population, demonstrating the potential for important gene-environment interactions affecting mitochondrial health after genotoxin exposure.

Dedication

This work is dedicated to my husband Scott whose love, support, friendship and sacrifice have made all of this possible. Bunches of Kashi.

Contents

Abstract	iv
Dedication	vii
Contents.....	viii
List of Tables.....	xiii
List of Figures	xiv
Acknowledgements	xvi
1. Introduction	1
1.1 Mitochondria.....	3
1.1.1 Mitochondrial DNA.....	4
1.1.1.1 Susceptibility to damage.....	5
1.1.1.2 Consequences of persistent mtDNA damage	6
1.1.2 Mitochondrial dynamics	8
1.1.3 Mitochondrial turnover.....	11
1.1.3.1 Macroautophagy and non-specific mitochondrial degradation	11
1.1.3.2 Mitophagy.....	13
1.2 <i>Caenorhabditis elegans</i>	16
1.2.1 Basic biology and advantages as a model organism	16
1.2.2 Use as a model organism for mitochondrial function.....	17
1.3 Dissertation Objectives and Outline	18
2. Mitochondrial dynamics and autophagy aid in removal of persistent mitochondrial DNA damage in <i>Caenorhabditis elegans</i>	23

2.1 Introduction.....	23
2.2 Materials and Methods.....	26
2.2.1 C. elegans Strains and Culture	26
2.2.2 Quantitative PCR.....	27
2.2.3 DNA Damage and Repair Quantification.....	28
2.2.4 Mitochondrial Copy Number Analysis.....	28
2.2.5 RNA Interference.....	29
2.2.6 Mitochondrial morphology and autophagy analysis.....	30
2.2.7 Larval Arrest Protocol.....	31
2.2.8 Relative ATP Analysis	32
2.2.9 Oxygen consumption analysis.....	33
2.3 Results	34
2.3.1 UVC-induced mtDNA damage is removed over time	34
2.3.2 Mitochondrial dynamics and autophagy are involved in removal of persistent mtDNA damage	35
2.3.3 Persistent mtDNA damage induces autophagy without detectable changes in mitochondrial morphology	36
2.3.4 Serial UVC exposure results in accumulated mtDNA damage and dose-dependent larval arrest.....	38
2.3.5 mtDNA replication is critical for recovery from persistent mtDNA damage ..	41
2.3.6 Recovery from UVC-induced mtDNA damage involves mitochondrial fusion and autophagy	42
2.4 Discussion.....	44

2.4.1 Mitochondrial dynamics and autophagy play critical roles in the response to persistent mitochondrial DNA damage	44
2.4.2 Mitochondrial fusion, fission, and autophagy are required for removal of persistent mtDNA damage	45
2.4.3 Persistent mtDNA damage induces autophagy without detectable changes in mitochondrial morphology	48
2.4.4 Recovery requires mtDNA replication and mitochondrial fusion and is aided by removal of damaged mtDNA via autophagy	50
2.4.5 Potential role of NER proteins and mitochondrial nucleases	54
2.4.6 Broader implications of persistent mtDNA damage removal	55
3. UVC-induced mitochondrial degradation via autophagy correlates with mtDNA damage removal in primary human fibroblasts.....	69
3.1 Introduction.....	69
3.2 Materials and Methods	71
3.2.1 Cell Culture, thymidine block, and UVC/Chemical exposures	71
3.2.2 DNA synthesis analysis.....	72
3.2.3 Cell Viability.....	73
3.2.4 DNA Damage, removal quantification and quantitative PCR	74
3.2.5 Mitochondrial Copy Number Analysis.....	74
3.2.6 Mitochondrial mass, membrane potential, ROS analyses	75
3.2.7 LC3II protein quantification by Western blot	75
3.2.8 RNA extraction, reverse transcription and real-time PCR analysis.....	76
3.2.9 Mitochondrial and lysosomes colocalization	77
3.2.10 Mitochondrial morphology analysis	78

3.2.11 Transmission electron microscopy.....	78
3.3 Results	79
3.3.1 UVC-induced mtDNA damage is removed slowly.....	80
3.3.2 Autophagy is induced by UVC exposure within 24 h	82
3.3.3 No change in mitochondrial mass or mtDNA content	83
3.3.4 Increased lysosomal degradation of mitochondrial at 72 h post exposure.....	84
3.3.5 No significant change in mitochondrial ROS production or membrane potential	84
3.3.6 Mitochondrial morphology is not affected by UVC exposure.....	85
3.3.7 Mitochondrial degradation via autophagy increases during recovery	87
3.4 Discussion.....	89
4. Conclusion	106
4.1 Summary.....	106
4.2 Implications and Future Directions	108
4.2.1 Role of proteins involved in the nuclear DNA damage response pathway ...	108
4.2.2 Susceptibility of aged populations to helix-distorting mtDNA damage.....	110
Appendix A – Identification and tracking of UVC-induced mtDNA damage in mammalian cell culture.....	113
A. 1 Damaged mtDNA tracking in live cells using cyclobutane pyrimidine dimer (CPD) GFP-tagged mutant photolyase.....	113
A.1.1 Gene insert confirmation.....	113
A.1.2 Cloning using the In-Fusion system.....	114

A.1.3 Visualization and confirmation of N378S photolyase mitochondrial localization and DNA binding following UVC exposure	114
A.2 Damaged mtDNA tracking in fixed cells using cyclobutane pyrimidine dimer (CPD) antibody	115
A.2.1 Antibody details	115
A.2.2 Optimization of immunocytochemistry parameters in UVC treated cells	115
A.2.2 Results.....	116
Appendix B – Effects of UVC exposure on mitochondrial membrane potential, mass, relative superoxide level and mtDNA copy number in replicating primary human fibroblasts.....	119
B.1 Methods.....	119
B.2 Results and Discussion.....	119
Appendix C – Studies with low-dose rapamycin and mtDNA damage removal and mitochondrial mass, membrane potential and ROS.	122
C.1 Methods	122
C.2 Results and Discussion	122
References	126
Biography.....	146

List of Tables

Table 1: Primer sequences and RT-PCR conditions for gene expression and mtDNA copy number analyses.	105
--	-----

List of Figures

Figure 1: Mitochondrial morphology differs by cell type.....	20
Figure 2: Molecular process of macroautophagy.....	21
Figure 3: Hypothesized mechanism of removal of persistent mtDNA damage by selective fusion, fission and autophagy.....	22
Figure 4: Mitochondrial DNA lesion frequency slowly decreases after a single dose of UVC in post-mitotic adult <i>C. elegans</i> (<i>glp-1</i>).....	57
Figure 5: Fusion, fission and autophagy gene knockdown inhibits mtDNA damage removal.....	58
Figure 6: Nuclear DNA damage is repaired after a single dose of UVC in post-mitotic adult <i>C. elegans</i> (<i>glp-1</i>).....	59
Figure 7: mtDNA copy number does not increase 120 h post UVC exposure (0, 50 J/m ²) in RNAi-treated <i>C. elegans</i> (<i>glp-1</i>).....	60
Figure 8: UVC exposure induces no detectable changes in mitochondrial morphology in adult <i>C. elegans</i>	61
Figure 9: UVC exposure induces autophagy.....	62
Figure 10: Serial UVC exposure results in mtDNA damage accumulation.....	63
Figure 11: Serial UVC exposure results in dose-dependent L3 arrest, lower steady state ATP level and reduced O ₂ consumption.....	64
Figure 12: Co-exposure to UVC and mitochondrial replication or translation inhibitors exacerbates L3 arrest.....	65
Figure 13: Mutations in fusion and autophagy genes exacerbate L3 arrest following serial UVC exposure.....	66
Figure 14: Mutations in endonuclease genes do not exacerbate L3 arrest following serial UVC exposure.....	67

Figure 15: Proposed model of the effect of mitochondrial fusion, fission, and autophagy processes on persistent mtDNA damage-induced mitochondrial dysfunction and removal of mtDNA damage.....	68
Figure 16: Excess thymidine arrests cells in S-phase and blocks nDNA synthesis within 24 h.	94
Figure 17: UVC-induced mtDNA damage is removed slowly.....	95
Figure 18: UVC exposure increases LC3II expression.	96
Figure 19: No detectable changes in mitochondrial mass or biogenesis.....	97
Figure 20: Increased lysosomal degradation of mitochondria after exposure to UVC.....	98
Figure 21: No detectable changes in mitochondrial MP and ROS level.....	99
Figure 22: Mitochondrial morphology analysis method.....	100
Figure 23: No detectable change in mitochondrial number or mitochondrial morphology in UV exposed cells.....	101
Figure 24: Autophagic degradation of mitochondria is enhanced during recovery.....	102
Figure 25: Toluidine blue stained semi-thin sections of human primary fibroblasts.....	104
Figure 26: Mito-N378S-GFP localizes to the mitochondrial network in MEFs	117
Figure 27: UVC treated cells with a CPD signal in nDNA and Mitotracker Red stained mitochondria.	118
Figure 28: Mitochondrial MP, mass and relative level of superoxide increase after UVC exposure without changes in mtDNA copy number.....	121
Figure 29: Low-dose rapamycin treatment has little effect on mitochondrial mass, MP or ROS in control or UVC exposed cells.....	124
Figure 30: Low-dose rapamycin does not significantly affect the rate of mtDNA damage removal.....	125

Acknowledgements

I have been truly blessed in my graduate school experience with an amazing group of people whose support, encouragement and friendship have been invaluable to the success of this project and maintaining my sanity over the last five years.

First and foremost, Dr. Joel Meyer, thank you for your constant support and patient mentorship over the last four years. Your enthusiasm for science is contagious! So many times I have entered your office completely discouraged and left uplifted with new interest. Thank you for supporting this project through the hiccups and always having your door open for intriguing and sometimes tangential and lengthy discussions. Thank you for being patient with me as I learned how to do research and struggled with the art of public speaking. Your unbiased approach to people and science has helped me to see the value in considering every idea and person with an open mind. It has been a honor to spend my graduate years as a member of your lab and as a small part of the lab's beginning.

To my committee, Rich Di Giulio, David Hinton and Bill Copeland, thank you for your guiding me, challenging me and helping me to see the bigger picture.

For the last four years, I've had the privilege as Black Fusion to work side-by-side with the amazing Environmental Justice League. To everyone both current and past, I thank you for making the lab environment most enjoyable and supporting and

accommodating my “Type A” requests. To Wonder Woman (Tracey Crocker), you have forever made an impression on me. I will change my inner dialogue! Maggie the White (Maggie Gustafson), your friendship means so much to me. You opened my world to the magic of Terry Pratchett, Naomi Novik and Jim Butcher all of which helped me pass long, tedious hours in the lab. Your encouragement and example gave me the confidence to push boundaries in so many areas of my life and I am forever thankful for your influence and friendship. Free Radical (Ian Ryde), how do I thank you for all of your hard work? It has been a privilege to work with you on these projects. And I have thoroughly enjoyed our discussions on lab dynamics. I owe a special thank you to Electrophoresa (Senyene Hunter). You brought a real sense of professionalism to our group and I am deeply grateful for your mentorship, advice and friendship which guided me through the development of my project and those difficult months of uncertainty. To my lab mates, Tox Knight (Maxwell Leung) and Nano Ninja (Candy Yang), you helped me consider different perspectives and the bigger picture in our long discussions of this work. Your enthusiasm and boundless energy have made our time together so entertaining and I will never forget your hilarious stories (e.g., *Stupid Fat*).

I was blessed to begin my graduate career with two amazing ladies, Autumn Bernal and Chelsea Landon. Thank you for your support and friendship from the very beginning. Your friendship means so much to me and I will never forget the long lunches, basketball campouts and birthday celebrations!

Mom, Nicole, Heather and Joey, your love and support have been so uplifting and constant over these last eleven years apart. Thank you for being patient with me when I am at my worst, listening to my concerns and reminding me of my roots.

Last, but certainly not least, to my husband Scott. There is no doubt in my mind that I am here today because you are in my life. You have stuck by me through eleven years of exams, deadlines, terrifying speeches, manuscripts and late night experiments. You have understood that my education should be top priority and put life on the backburner until it could be finished. As my faithful weekend study buddy and reliable late night lab assistant, you have made this entire experience manageable. I am forever grateful for your friendship, love, support and honest criticism. Thank you for hanging in there.

1. Introduction

Mitochondria are present in all nucleated eukaryotic cells and provide approximately 95% of the energy needed to sustain cellular function. These organelles contain multiple copies of circular DNA, which encodes 13 subunits of the oxidative phosphorylation (OXPHOS) system. Over the last three decades, mitochondrial dysfunction and mutations in mitochondrial DNA (mtDNA) have been shown to cause a number of mitochondrial diseases¹ and are linked to many wide-spread pathologies including cancer²⁻⁴, neurodegeneration⁵⁻⁸, type 2 diabetes mellitus⁹, cardiovascular disease¹⁰ and aging¹¹. Although it is not clear what initiates mitochondrial dysfunction and mtDNA mutations, evidence suggests that toxicant exposure may play a role¹²⁻¹⁶. mtDNA has been shown to be more susceptible than nuclear DNA (nDNA) to damage induced by a variety of environmental and endogenous genotoxins¹⁷⁻³⁸, some of which are known to concentrate in mitochondria. While oxidative damage to mtDNA, proteins and lipids can be an important trigger for mitochondrial dysfunction and disease progression, mitochondria house a number of mechanisms to combat oxidative stress including base excision repair, the repair mechanism necessary to repair most oxidative DNA lesions. However, mitochondria lack nucleotide excision repair (NER), the repair mechanism utilized in the nuclear genome to remove “bulky” or helix-distorting damage induced by a variety of environmental toxicants^{37, 39, 40} and ultraviolet C

radiation (UVC) ⁴¹⁻⁴³. Therefore, these lesions are expected to be persistent in mtDNA and their fate in mtDNA and effects on mitochondrial function are not well-understood.

Although there is no known repair mechanism for irreparable helix-distorting mtDNA damage, recent evidence suggests that removal of this damage may occur via a non-repair mediated mechanism. It is now well accepted that mitochondria exist as a network of organelles that undergo fusion and fission at variable rates ⁴⁴. Mutations in or inhibition of the mitochondrial electron transport chain (ETC), acute and chronic ROS production, depletion of ATP or sudden dissipation of the mitochondrial membrane potential (MP) trigger changes in mitochondrial morphology suggesting that fusion and fission rates change with mitochondrial function ⁴⁵⁻⁵⁶. Recent studies suggest that mitochondria with reduced MP cannot undergo fusion and, in most cases, are degraded selectively via autophagy over mitochondria with average MP indicating that removal of mitochondria from the cell may be a selective process ⁵⁷⁻⁶⁷. Toxicants known to induce persistent, helix-distorting mtDNA damage have been shown to result in reduced mitochondrial function ^{31, 68-74} and reduced membrane potential ^{70, 71}. The resulting mitochondrial dysfunction may serve as a signal for selective autophagy of mitochondria with damaged mtDNA. This project is focused on elucidating the role of fusion, fission and autophagy in removal of helix-distorting mtDNA lesions.

1.1 Mitochondria

Although mitochondria are best-known for their role in oxidative phosphorylation, these organelles also play a role in the Krebs cycle, apoptosis, calcium homeostasis, and biosynthesis of heme, iron-sulfur proteins, nucleotides, steroid hormones, and amino acids ⁷⁵. The rate of mitochondrial turnover ranges from 2 – 4 days and mitochondrial morphology varies from many, small spheres to a single mitochondrion consisting of long, tubular networks ⁷⁶⁻⁷⁸. Both turnover and morphology, along with mitochondrial biogenesis, dictate the number of mitochondria per cell which is typically between 100 and 1000 ⁷⁹.

Mitochondria are the primary producers of reactive oxygen species (ROS) ⁸⁰ stemming from generation of superoxide primarily at NADH-ubiquinone oxidoreductase (complex I) and ubiquinol-cytochrome c oxidoreductase (complex III) of the electron transport chain (ETC) located along the inner membrane of the mitochondrion ⁸¹. The production of ROS by the ETC has been estimated to be between 1-2% of the oxygen consumed ^{82, 83}; however, due to the high nonphysiological concentrations of O₂ present *in vitro*, this is likely to be an overestimate ^{83, 84}. Under physiologic O₂ concentrations, approximately 0.1% of O₂ consumed is converted to ROS, typically as superoxide anion ^{80, 85, 86}. Superoxide anion is neutralized by superoxide dismutases to form hydrogen peroxide (H₂O₂). H₂O₂ can then be converted to water by

catalase or peroxidases, or react with superoxide to form the hydroxyl radical, a highly reactive ROS that attacks lipids, proteins and DNA. Formation of the hydroxyl radical from H₂O₂ and superoxide can be catalyzed by transition metals, most commonly iron and copper. Several xenobiotics can enhance the production of superoxide by inhibiting electron flow through respiratory complexes or acting as an electron acceptor including, but not limited to, complex I inhibitors rotenone and MPP⁺ ⁸⁷, complex III inhibitor antimycin ⁸³, and redox cyclers paraquat ⁸⁰ and doxorubicin ^{22, 83}.

1.1.1 Mitochondrial DNA

Mitochondria contain double-stranded circular DNA that is approximately 16.5 kb in length (in mammals) and organized into nucleoid structures each containing 1-10 mtDNA molecules ^{88, 89}. mtDNA encodes 13 polypeptides involved in four of the five complexes of the OXPHOS system, 2 rRNAs and 22 tRNAs ⁹⁰. The number of mtDNA molecules per cell is highly variable and dependent upon cell type and developmental stage ^{79, 91-93}. Somatic cells contain from a few hundred copies of mtDNA in low energy tissues to several thousand mtDNA molecules in more energy demanding tissues such as muscle and neurons ^{93, 94}. Significantly more variation has been observed in mature oocytes with numbers reported from 10⁴ to 10⁶ copies of mtDNA ⁹⁵⁻⁹⁷.

mtDNA copy number is maintained by the competing processes of mtDNA replication and degradation. mtDNA replication occurs in both proliferating and post-mitotic cells independent of the cell cycle and nuclear DNA replication ⁹⁸. Peroxisome

proliferator-activated receptor gamma coactivator 1 α (PGC1 α) regulates both mitochondrial biogenesis and mtDNA replication in part by increasing the expression of nuclear respiratory factors 1 and 2 (NRF1, NRF2) and by increasing the transcriptional activity of NRF1^{99,100}. NRF1 and 2 are nuclear transcription factors which regulate the expression of many OXPHOS genes as well as genes encoding proteins involved in mtDNA replication and transcription such as mitochondrial transcription factor A (TFAM). TFAM is the most abundant nucleoid protein with estimates of 1000 TFAM molecules per molecule of mtDNA¹⁰¹ and is necessary for maintenance of mtDNA copy number acting to both stabilize mtDNA and initiate replication through transcription initiation¹⁰¹. PGC1 α activity is responsive to external stimuli including, but not limited to, exercise¹⁰², low temperatures¹⁰⁰, caloric restriction¹⁰³, hypoxia¹⁰⁴ and ROS¹⁰⁵. Thus it may serve as a link between mitochondrial biogenesis, mtDNA replication and environmental stressors^{11,99}.

1.1.1.1 Susceptibility to damage

mtDNA is particularly susceptible to damage via environmental contaminant exposure. Due to the high lipid content and electro-chemical gradient of the mitochondria, several lipophilic and/or cationic environmental contaminants including benzo[a]pyrene²⁹, alkylating agents^{24,25} and a variety of divalent cationic metals¹⁰⁶⁻¹⁰⁸ have been found at higher concentrations within mitochondria as compared to other cellular compartments, potentially exposing mtDNA to higher concentrations of a

contaminant compared to nDNA. Furthermore, mitochondria contain the necessary phase I metabolic enzymes responsible for activation of some of these contaminants to their DNA reactive form ¹⁰⁹⁻¹¹¹. Additionally, mtDNA molecules are located near the inner membrane within the mitochondrial matrix and, therefore, in close proximity to the electron transport chain (ETC) and ROS ^{18, 30}.

Studies indicate that mtDNA is three to five times more susceptible to oxidative damage than nDNA ¹⁷⁻²³. However, most oxidative damage in mtDNA is repairable by BER which occurs at a similar rate in both mitochondrial and nuclear DNA ^{18, 30}. On the other hand, mitochondria lack NER, the repair mechanism utilized in the nuclear genome to remove most “bulky” or helix-distorting DNA damage induced by PAHs ^{39, 40}, mycotoxin (aflatoxin B₁) ³⁷, UVC ⁴¹⁻⁴³, cisplatin ¹¹² and aldehydes resulting from lipid peroxidation ¹¹³. Consistent with this, mitochondria display a two to 100 times greater susceptibility to bulky adducts created by cisplatin ³¹⁻³³, metabolically-activated polycyclic aromatic hydrocarbons (PAHs) ^{26-29, 34, 35} and aflatoxin B₁ ^{36, 37}, and M₁GD induced by malondialdehyde (MDA) ³⁸.

1.1.1.2 Consequences of persistent mtDNA damage

Helix-distorting mtDNA lesions resulting from exposure to these genotoxins are persistent and have been shown to reduce mtDNA replication ^{28, 114-117} and transcription/translation ^{36, 114}, possibly by stalling mitochondrial polymerase γ ¹¹⁸ and/or mitochondrial RNA polymerase as these lesions have been well-documented to do in

nDNA^{113, 119, 120}. Stalling replication or transcription could have several effects that ultimately result in overall mitochondrial dysfunction including induction of mutations in mtDNA, an imbalance of nuclear vs. mitochondrial DNA encoded subunits potentially resulting in oxidative stress or reduced ATP synthesis¹⁹, and mtDNA depletion. Aflatoxin B₁ has been shown to reduce the activity of cytochrome c oxidase (Complex IV)^{72, 73}, decrease mtDNA encoded cytochrome *b*⁷² and induce lipid peroxidation in mitochondria¹²¹. PAH exposure results in both hyperpolarization¹²² and depolarization^{70, 71}, loss of cytochrome *c*^{70, 71}, decreased ATP synthesis⁶⁹ and production of superoxide^{70, 74}. UVC exposure reduces both oxygen consumption and steady-state ATP levels¹²³ while cisplatin reduces the activity of respiratory complexes II, III and IV^{31, 68} and ATP level³¹.

Helix-distorting lesions induce nDNA mutations^{124, 125} and *in vitro* evidence supports the potential for these lesions to be mutagenic in mtDNA^{118, 126}. However, exposure to BaP diol epoxide (BPDE) or UVC in cell culture resulted in little to no increase in mutation frequency above background^{117, 127, 128}. UVC exposure has been shown to result in a ten-fold increase in single nucleotide mutations in mtDNA *in vitro*¹¹⁷; however, it is not clear if these mutations resulted from incorrect nucleotide incorporation opposite the lesion, from oxidative lesions due to production of ROS, or if non-damaged, mutation carrying mtDNAs were replicated at a higher rate. While the low frequency of mutations observed following exposure to these mutagenic agents may

be the result of insensitive detection methods combined with high background mutation frequency, degradation of mtDNAs harboring helix-distorting lesions has been proposed as an alternate explanation ^{129, 130}.

1.1.2 Mitochondrial dynamics

Mitochondria exist as highly dynamic organelles whose morphology and distribution are driven by the opposing processes of fusion and fission ^{44, 76, 131}. Fusion and fission are primarily regulated by the actions of four key proteins consisting primarily of membrane-bound and cytosolic GTPases. Mitofusins (MFN1 and MFN2) and OPA1 control mitochondrial outer and inner membrane fusion while dynamin related protein 1 (DRP1) and FIS1 control outer membrane fission of mitochondria as well as fission of other tubular membranes such as peroxisomes ^{44, 132}. Fusion is essential for normal development ^{131, 133}, maintenance of mtDNA ^{134, 135}, exchange of mitochondrial proteins, lipids and nucleoids ^{46, 136-139}, and mtDNA replication ¹⁴⁰⁻¹⁴² and repair ¹⁴¹⁻¹⁴³. Mutations in *OPA1* and *MFN2* cause neurodegenerative diseases ¹⁴⁴⁻¹⁴⁶ further emphasizing the importance of mitochondrial fusion for cellular function particularly in post-mitotic cells. Fission is required for development, particularly the proper segregation of mtDNA during mitosis ^{147, 148} and plays a key role in mitochondrial-mediated apoptosis ¹⁴⁹⁻¹⁵¹. Mitochondrial morphology and dynamics are highly variable depending on cell type ranging from long, branched networks in fibroblasts to small compact spheres in hepatocytes to highly compact rods in cardiomyocytes (Figure 1) ¹⁵².

Variation in mitochondrial morphology and interconnectivity in part dictate the functional role of mitochondria within a specific cell type and result in functional heterogeneity of mitochondria within a single cell ^{152, 153}.

Mitochondrial dynamics may serve as a compensatory mechanism for mitochondrial dysfunction. As stated previously, fusion allows mitochondrial contents to mix which creates a relatively homogenous mitochondrial network rather than a population of genetically and metabolically discrete units. Phenotypic consequences of mtDNA mutations have been repeatedly noted to occur only when the occurrence of the mutation is high (over 40-90%) ¹⁵⁴ and functional complementation via nucleoid (mtDNA) mixing between fused mitochondria is one explanation for this observation ^{137, 138, 141, 155, 156}.

Although no studies have addressed the role of mitochondrial dynamics and morphology in recovery from irreparable DNA damage, there have been many studies on the response to other types of insult. Mitochondrial fragmentation results from rapid or sudden dissipation of MP or decreased ATP level triggered by mitochondrial respiratory chain inhibitors and/or uncouplers commonly resulting in apoptosis ⁴⁵⁻⁵⁰. Additionally, high level or prolonged oxidant treatment or significant depletion of complex I protein results in mitochondrial fragmentation ⁵¹ accompanied by depletion of ATP, ROS formation and lipid peroxidation ⁵²⁻⁵⁶. These data suggest the hypothesis that a loss of MP or ATP due to persistent mtDNA damage will result in fragmentation.

While excessive fragmentation can be detrimental and result in apoptosis, when transient or limited to a subpopulation of mitochondria it can isolate damaged mitochondria from the main network thus preventing the dilution of damage through fusion. Furthermore, fragmentation and isolation of damaged mitochondria (e.g., harboring damaged mtDNA) is particularly important for degradation of these mitochondria by mitophagy, as discussed in more detail below.

Significant or sudden loss of mitochondrial function (caused by the treatments listed above) is not the effect one would expect from persistent helix-distorting mtDNA damage. Inhibition of protein synthesis via UVC-irradiation, cycloheximide and actinomycin D triggers stress-induced mitochondrial hyperfusion which results in activated ATP synthesis via oxidative phosphorylation and protection from secondary exposure to apoptotic stimuli ⁴⁷. Additionally, treatment with the DNA intercalator ethidium bromide results in mitochondrial fusion followed by nucleoid remodeling while levels of MP, oxygen consumption and cytochrome *c* are maintained ¹⁵⁷. In contrast to high level oxidant exposure, exposure to chronic low levels of H₂O₂ ¹⁵⁸ and rotenone ^{51, 53, 54} and sub-lethal UVA-UVB exposure ¹⁵⁹ increase mitochondrial fusion and interconnectivity. These data suggest that stressors which induce low-level or slow-onset mitochondrial stress in the form of mild ROS production, reduced mtDNA copy number and/or reduced transcription of mtDNA-encoded proteins may trigger

increased mitochondrial interconnectivity, possibly allowing for the exchange of matrix contents and mtDNA needed for optimal energy production ¹⁶⁰.

1.1.3 Mitochondrial turnover

Initial investigations into mitochondrial turnover dating back to the 1960s indicated that mitochondria and mtDNA turn over on average every 5 to 25 days depending on the tissue ¹⁶¹⁻¹⁶⁴. Later work reported that mitochondria have a half-life closer to 3 to 4 days ¹⁶⁵. However, most recent studies indicate a mitochondrial and mtDNA half-life of 2 days ^{166, 167}, with more rapid turnover observed under conditions of dietary restriction as a consequence of increased macroautophagy ¹⁶⁶.

1.1.3.1 Macroautophagy and non-specific mitochondrial degradation

Macroautophagy (herein referred to as autophagy) is the lysosomal-driven intracellular degradation of cytoplasmic materials and is the primary mechanism for mitochondrial degradation ^{57, 168}. Autophagy, shown in Figure 2 ¹⁶⁹, proceeds through three primary steps: initiation or induction, autophagosomes nucleation and elongation, and autophagosome maturation and degradation. Initiation involves the formation of the ULK1 complex and a crescent-shaped phagophore. This is followed by nucleation requiring the formation of the Beclin I/Class III phosphatidylinositol 3-kinase (PI3K) complex. This activates PI3K leading to phosphatidylinositol 3-phosphate (PI3P) formation, which associates with the developing autophagosomal membrane and recruits additional proteins required for autophagy ^{169, 170}. Elongation and encapsulation

of the mitochondrion requires the formation of two additional complexes that eventually conjugate phosphatidylethanolamine to LC3I converting it to LC3II, which localizes to newly forming autophagosomal membrane and facilitates elongation ¹⁶⁹. Once the autophagosome has completely formed, it “matures” fusing with a lysosome or late endosome resulting in degradation of the autophagosome and mitochondria contained within it ¹⁶⁸⁻¹⁷⁰.

Induction of autophagy by nutrient deprivation/starvation or energy depletion is mediated by AMPK/mTOR signaling^{170, 171}. mTORC1 is considered a primary regulator of autophagy ^{170, 171}. Under non-stimulating conditions, mTOR phosphorylates ULK1 preventing its interaction with AMPK and inhibiting autophagy. When AMP and ADP levels increase as they do during energy depletion, activated AMPK phosphorylates ULK1 and inhibits the interaction of ULK1 with mTOR thus promoting autophagy ¹⁷⁰. As suggested above, starvation and nutrient deprivation trigger degradation of mitochondria as well as other organelles and cytoplasmic materials, a process which has been generally thought to be non-selective ¹⁶⁸. However, recent research shows that upon amino acid starvation, degradation of cytoplasmic materials is ordered with mitochondrial degradation occurring 30 h into starvation after the degradation of cytosolic and proteasomal proteins and ribosomes ¹⁷². This was supported by the recent observation that within the initial hours of amino acid starvation, mitochondrial degradation by autophagy is inhibited by mitochondrial elongation ^{173, 174}; however, this

phenotype may be limited to amino acid deprivation. Complete glucose or serum starvation results in mitochondrial fragmentations followed by mitochondrial degradation as well as degradation of other cytoplasmic materials ^{174, 175}.

1.1.3.2 Mitophagy

Unlike macroautophagy, selective autophagy of mitochondria or “mitophagy” ⁵⁸ is entirely specific in that it does not result in the degradation of other cytoplasmic materials. Two key discoveries initiated an explosion of interest and research in the field of mitophagy, which has now emerged as an established, compensatory mechanism by which dysfunctional mitochondria can be selectively degraded. The first was the observation that mitochondria with reduced membrane potential are preferentially degraded by autophagy ^{57, 58, 176, 177}. While mitophagy had been established for some time in yeast, this was the first evidence of mitophagy in higher organisms. The second was the discovery that PTEN-induced kinase 1 (PINK1) and Parkin, both of which are commonly mutated in those with early-onset familial Parkinson’s disease (PD) ^{178, 179}, mediate targeted degradation of depolarized mitochondria ^{63, 64, 180-182}. While abnormal mitochondrial autophagy and accumulation of dysfunctional mitochondria had been well documented in several neurodegenerative disorders including Parkinson’s, Alzheimer’s and Huntington’s disease ¹⁸³⁻¹⁸⁵, this finding suggested that defective mitochondrial degradation may drive pathogenesis rather than occur as a secondary effect.

Despite significant data publication on this topic since 2008, the mechanism of mitophagy is still unclear. Twig et al. (2008) elegantly demonstrated that upon mitochondrial fission, one of the two daughter mitochondria is commonly hypopolarized, isolated from the mitochondrial network by inhibition of fusion, and selectively degraded by autophagy if the MP does not recovery⁶². This suggested not only that fission yields functionally different daughter mitochondria but also that dysfunctional mitochondria exhibiting decreased MP may be removed by this process. Complete dissipation of the MP induced by carbonyl cyanide *m*-chlorophenyl hydrazone (CCCP; 10 μ M or higher) exposure or targeted photoirradiation with 488 nm light results in selective degradation of depolarized mitochondria by mitophagy under high glucose conditions^{63-65, 186}. In many of these studies, mitophagy is dependent upon the stabilization of PINK1 on the outer membrane of depolarized mitochondria and subsequent recruitment of parkin by stabilized PINK1^{64, 66, 67}. Recently, the applicability of these observations to mitochondrial clearance *in vivo* has been questioned by the observation that in non-immortalized primary neuronal cell lines or in immortalized cell lines grown in galactose media, CCCP treatment does not induce translocation of parkin or mitophagy¹⁸⁷ suggesting that a dependence on OXPHOS inhibits mitophagy.

Also, it is important to emphasize that localization of PINK1 and parkin, mitochondrial dysfunction and induction of autophagic machinery are dissociated events but each is required for mitophagy^{64, 65, 188}. For example, while mitochondrial

fragmentation commonly occurs following loss of MP, it alone is not necessary or sufficient for parkin recruitment⁶³; however, inhibition of fragmentation impairs mitophagy^{62, 189, 190} suggesting that mitochondrial size may influence the ability to degrade dysfunctional mitochondria even with parkin accumulation. In several cell lines harboring pathogenic mtDNA mutations and in WT cells with a mild chemically-induced decrease in MP, neither parkin translocation, decreased membrane potential nor autophagic induction via mTOR inhibition were sufficient to induce mitophagy. Furthermore, surprisingly, cells with mutant mtDNAs did not exhibit increased autophagy (despite compromised mitochondrial function) and had little to no endogenous parkin expression¹⁸⁸.

Despite conflicting reports regarding the mechanism of mitophagy, there is ample evidence to support the protective role of autophagy, mitophagy, PINK1 and parkin against mitochondrial dysfunction, apoptosis and cell death following toxicant exposure or cell stress¹⁹¹⁻²⁰¹ and inhibition of autophagy results in accumulation of dysfunctional mitochondria^{202, 203}, increased ROS production^{204, 205} and cell death^{191, 196, 206}. Furthermore, abnormal mitochondrial autophagy coupled with mitochondrial dysfunction occurs in a variety of pathologies including mitochondrial diseases^{52, 196, 206}, lysosomal storage disorders^{193, 207}, type 2 diabetes mellitus²⁰⁸, cardiac aging²⁰⁹ and neurodegenerative disorders¹⁸³⁻¹⁸⁵. Therefore, it is of significant importance that more

research be done to understand the mechanism by which these processes and proteins integrate to protect against mitochondrial dysfunction *in vivo*.

1.2 Caenorhabditis elegans

1.2.1 Basic biology and advantages as a model organism

C. elegans is a free-living nematode that is found throughout the world in nutrient and bacteria-rich decaying organic materials²¹⁰. This species was first established as a research model by Sydney Brenner in 1974 and it has led to important advances in our understanding of neurobiology, development, cell death, RNAi and cell signaling²¹¹. *C. elegans* has a number of characteristics that make it a powerful laboratory model. *C. elegans* is easy and inexpensive to maintain as it is grown on agar plates or in liquid culture with a diet of *Escherichia coli*^{212, 213}. Its short, hermaphroditic lifecycle and large number of offspring (~300 eggs) allow for studies to be executed with a high number of individuals in a short period of time. The existence of two large gene knockout consortia²¹¹, comprehensive RNAi libraries, a sequenced genome²¹⁴ and extensively described methods in mutagenesis, transgenesis and RNA interference provide a variety of genetic approaches to investigate molecular pathways. Most importantly, *C. elegans* has been shown to have homologues for 60-80% of human genes and to display similar physiologic and behavioral responses to stress and toxicity²¹⁵.

1.2.2 Use as a model organism for mitochondrial function

Mitochondrial biology and function are highly conserved between *C. elegans* and higher eukaryotes²¹⁶⁻²¹⁸. mtDNA in *C. elegans* is slightly smaller than that of mammalian eukaryotes at 13,794 nt and codes for 12 of the 13 subunits encoded by mammalian mtDNA²¹⁸. While *atp-8* has not been definitively identified in *C. elegans*, it is probably present in an unusual form, as is the case in other nematodes²¹⁹. *C. elegans* develop initially through four larval stages before reaching the adult stage marked by sexual maturity²¹². The role of mitochondrial function and the resulting changes in mtDNA copy number throughout development have been well-characterized^{218, 220}. This information can be utilized to better understand consequences of toxicant-induced mitochondrial dysfunction on whole-organism endpoints (behavior, development, reproduction, survival, damage to sensitive tissue types, cell-to-cell interactions) that are difficult or impossible to observe in cell culture. Additionally, the transparency of *C. elegans* allows one to monitor potential changes in mitochondrial morphology *in vivo* following the induction of mtDNA damage. Conservation of mitochondrial biology, the well-described role of mitochondria function and mtDNA in the *C. elegans* lifecycle and unique techniques available to investigate the consequences of mitochondrial dysfunction make *C. elegans* a convenient and advantageous model for research of mitochondrial toxicity.

1.3 Dissertation Objectives and Outline

The primary goals of this dissertation are to identify if autophagy and mitochondrial dynamics play a role in removal of persistent, helix-distorting mtDNA and to investigate the significance of these processes in recovery from mtDNA damage – induced mitochondrial dysfunction. I hypothesized that sub-lethal persistent mtDNA damage initially distributed across the entire mitochondrial network causes mitochondrial dysfunction. Slow-onset dysfunction will induce fusion slowing down degradation of mitochondria but allowing for the recovery of mitochondrial function. Upon restoration of fission, allocation of damaged and undamaged mtDNAs will be random, resulting in some daughter mitochondria with a high proportion of damaged mtDNAs resulting in reduced MP for that mitochondrion. This reduction in MP will trigger mitophagy and the damaged mtDNA will be degraded (depicted in Figure 3).

This dissertation is divided into the following two research chapters which address this hypothesis:

Chapter 2: Mitochondrial dynamics and autophagy aid in removal of persistent mitochondrial DNA damage in *Caenorhabditis elegans*

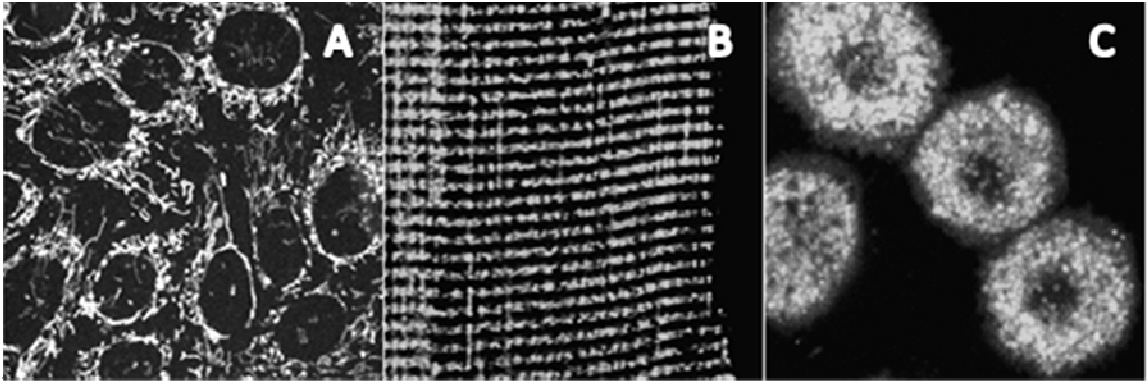
Removal of irreparable mtDNA damage and the necessity of autophagy, mitophagy, fusion and fission genes in removal of this damage were examined using genetic approaches in adult *C. elegans*. An experimental method was developed to specifically induce persistent mtDNA damage and mitochondrial dysfunction without

persistent nDNA damage in developing *C. elegans*. This protocol allowed for investigation of the significance of autophagy, fusion and fission genes in recovery from mtDNA damage-induced mitochondrial dysfunction *in vivo*. The effects of persistent helix-distorting DNA damage on mitochondrial morphology, mitochondrial function and autophagy in adult and developing *C. elegans* were also investigated.

Chapter 3: UVC-induced mitochondrial degradation via autophagy correlates with UVC-induced mitochondrial DNA damage removal in primary human fibroblasts.

In this work, we investigated the effects of UVC exposure on autophagy, mitophagy, mitochondrial morphology, and indicators of mitochondrial ETC function in mammalian cell culture.

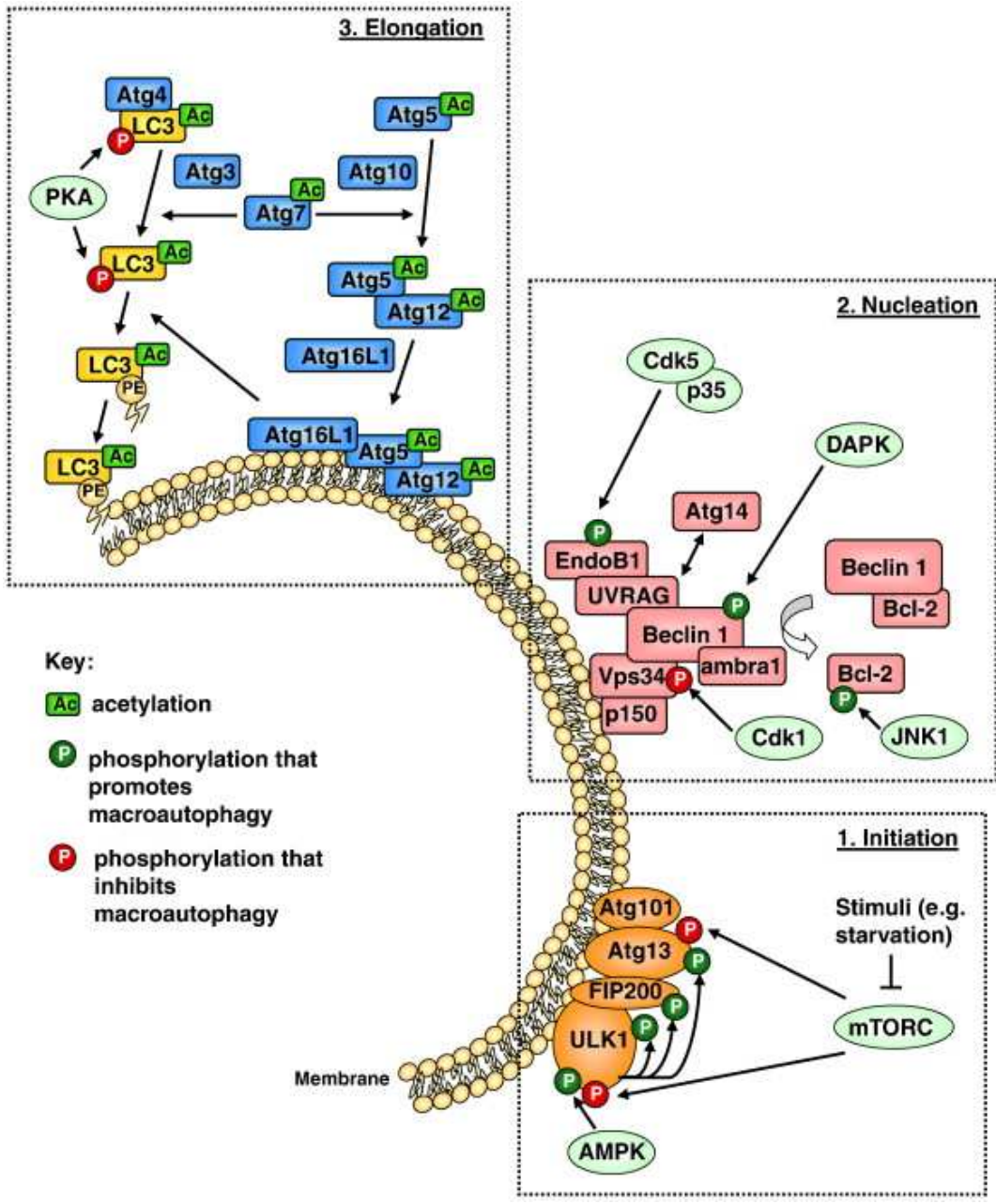
To conclude, the results of this dissertation, their broader implications and future directions are summarized in Chapter 4.



Adapted from Kuznetsov et al. (2009) ¹⁵².

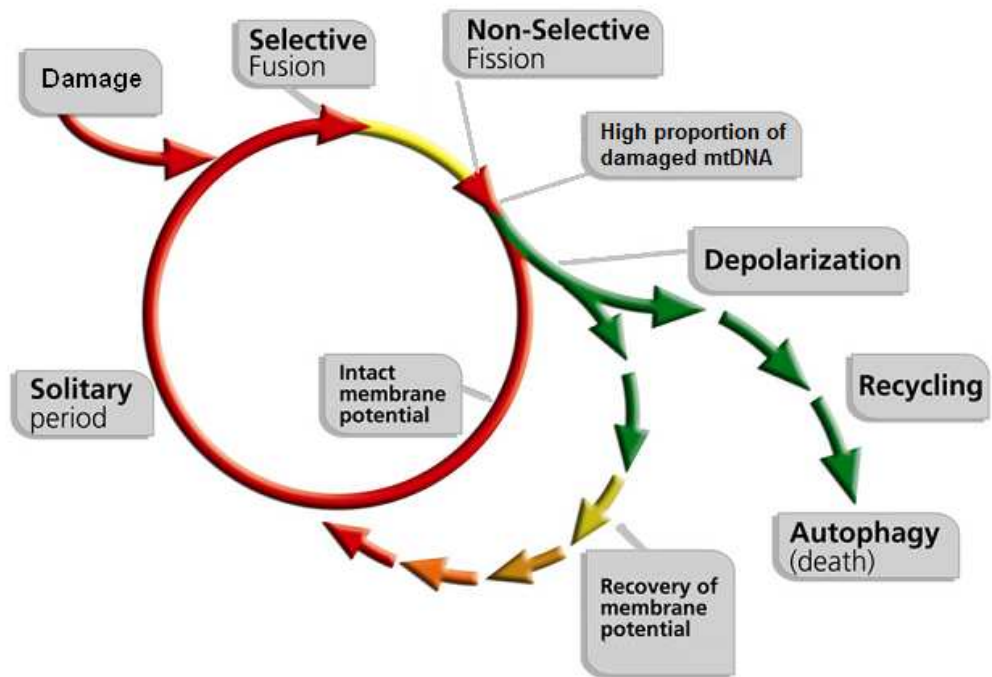
Figure 1: Mitochondrial morphology differs by cell type.

(A) HF-1 cells display long, interconnected networks of mitochondrial while (B) skeletal muscle and (C) hepatocytes have compact, small individual mitochondria.



Wong et al. (2011) ¹⁶⁹.

Figure 2: Molecular process of macroautophagy.



Adapted from Mouli et al. (2009) ²²¹.

Figure 3: Hypothesized mechanism of removal of persistent mtDNA damage by selective fusion, fission and autophagy.

2. Mitochondrial dynamics and autophagy aid in removal of persistent mitochondrial DNA damage in *Caenorhabditis elegans*

The majority of this chapter was published under the same title in *Nucleic Acids Research* 2012. The authors are Amanda S. Bess, Ian T. Ryde, Tracey L. Crocker, and Joel N. Meyer.

2.1 Introduction

Mitochondria serve several critical cellular functions, including energy production via oxidative phosphorylation (OXPHOS) and key roles in apoptosis. The majority of mitochondrial proteins involved in these processes are encoded by nuclear DNA (nDNA), but a small subset, 13 polypeptides that are incorporated into four of the five complexes of the OXPHOS system plus 2 rRNAs and 22 tRNAs, are encoded by mitochondrial DNA (mtDNA). A large and growing number of inherited mitochondrial diseases result from mutations in or depletion of mtDNA and likely affect more than 1 in 6,000 people ¹, emphasizing the importance of mtDNA integrity to human health. Furthermore, there is substantial evidence to support a role of mitochondrial dysfunction and mtDNA mutation in the pathogenesis of more common diseases such as neurodegenerative conditions ^{5,6}, type 2 diabetes mellitus ⁹ and cancer ³.

Compared to nDNA, mtDNA is particularly susceptible to damage from prevalent environmental contaminants. For instance, depending on exposure conditions,

mtDNA is 2- 100 times more susceptible to bulky adducts when exposed to the carcinogenic, polycyclic aromatic hydrocarbon (PAH) benzo(a)pyrene (BaP) ^{26, 28, 29, 34, 127, 222}. This susceptibility is partially due to the fact that mitochondria lack nucleotide excision repair (NER), the repair pathway utilized to repair many helix-distorting or “bulky” nDNA damage induced by common environmental agents including PAHs, mycotoxins and ultraviolet C radiation (UVC) ^{37, 39, 41, 112}. Thus, helix-distorting mtDNA lesions resulting from exposure to these genotoxins are persistent and reduce mtDNA replication ^{28, 115-117} and transcription ³⁶. The resulting reduction of mtDNA copy number or protein synthesis could result in mitochondrial dysfunction, as suggested by cytochrome c release, reduced mitochondrial membrane potential (MP), decreased respiration and increased lipid peroxidation reported in studies with PAHs and the mycotoxin, Aflatoxin B₁ ^{71, 72, 121}.

Helix-distorting lesions induce nDNA mutations ^{124, 125} and *in vitro* evidence supports the potential for these lesions to be mutagenic in mtDNA ^{118, 126}. However, exposures to BaP diol epoxide (BPDE) and UVC in cell culture have resulted in little to no increase in mutation frequency above background ^{117, 127, 128} prompting the hypothesis that mtDNAs harboring helix-distorting lesions are degraded and mutations resulting from these lesions are rare ^{129, 130}. Mitochondrial degradation is carried out by macroautophagy ^{57, 168}. Non-selective autophagy of mitochondria as well as other organelles and cytoplasmic materials ¹⁶⁸ is triggered by starvation and nutrient

deprivation. On the other hand, selective autophagy of mitochondria or “mitophagy”⁵⁸ is responsible for clearance of paternal mtDNA in sperm of *C. elegans*^{223, 224}, of mitochondria during erythrocyte maturation²²⁵ and has emerged as a more specific degradation mechanism for dysfunctional mitochondria in somatic cells^{57, 58, 226-228}. Although the detailed mechanism of dysfunctional mitochondrial clearance by mitophagy has yet to be resolved, current research suggests that spontaneous or stress-induced depolarization results in isolation of dysfunctional mitochondria followed by removal by autophagy^{57, 62, 63, 186, 195, 196}. The Parkinson’s-associated genes encoding Parkin and PINK1 have been shown to selectively accumulate on mitochondria with reduced membrane potential and facilitate mitophagy under certain conditions^{64, 66, 181, 188}. The role of mitophagy in removal of dysfunctional mitochondria with damaged DNA has not been previously addressed but this could play an important role in preventing fixation of mtDNA mutations and mitochondrial-mediated apoptosis or necrosis via removal of unstable mitochondria^{229, 230}.

The goals of this research were to determine the long-term fate of helix-distorting mtDNA damage and investigate the role of autophagy and mitochondrial dynamics in removal of and recovery from this mtDNA damage. Using ultraviolet C radiation, we induced helix-distorting mtDNA lesions in adult *Caenorhabditis elegans* with and without RNAi knockdown of autophagy, fusion and fission genes and measured mtDNA damage over time using quantitative polymerase chain reaction (QPCR). We show that

UVC-induced mtDNA lesions are removed slowly over 72 h in adult *C. elegans* and that this removal is dependent upon genes involved in autophagy and mitochondrial dynamics. In order to better understand the implications of persistent mtDNA damage removal *in vivo*, we investigated in *C. elegans* the effect of UVC-induced mtDNA damage on the frequency and duration of larval arrest, a well-described phenotype mediated by mitochondrial function that serves as an indicator of overall mitochondrial health^{220, 231-233}. We show that high levels of persistent mtDNA damage induce L3 larval arrest and mitochondrial dysfunction in *C. elegans*. Furthermore, recovery from larval arrest is dependent upon mitochondrial fusion, mtDNA replication and removal of damaged mtDNA via autophagy. Thus, we show for the first time that although persistent, UVC-induced mtDNA lesions are removed gradually, and that mitochondrial dynamics and autophagy are involved in removal of and recovery from persistent mtDNA damage.

2.2 Materials and Methods

2.2.1 C. elegans Strains and Culture

Populations of *C. elegans* were maintained on K agar plates seeded with OP50 bacteria unless otherwise stated. N2 (wild-type), JK1107 *glp-1(q224)*, VC893 *atg-18(gk378)*, VC517 *bec-1(ok691)*, VC1253 *cps-6(ok1718)*, CB1392 *nuc-1(e1392)*, VC1024 *pdr-1(gk448)*, CB369 *unc-51(e369)* were obtained from the *Caenorhabditis* Genetics Center (University of Minnesota). *crn-6(tm890)* was obtained from The National Biosource Project for the Nematode (Tokyo, Japan). DA631 *eat-3(ad426)* and BC10210 *fzo-1(tm1133)*

were provided by Alexander van der Blik, University of California (Los Angeles, CA). *drp-1(tm1108)*, *fis-1(tm1867)*, VC801 *fis-2(gk363)* were provided by Ding Xue, University of Colorado (Boulder, CO). Guy Caldwell, University of Alabama (Tuscaloosa, AL), provided UA86 *pink-1(tm1779)*; Pdat-1::GFP; Pdat-1:: α -syn [baIn11]. Luminescent PE255 (*feIs5*) were provided by Christina Lagido, University of Aberdeen (Aberdeen, UK). Alicia Melendez, Queens College, City University of New York (Flushing, NY) kindly provided QU1 izEx1[P_{lgg-1}::gfp::lgg-1 + rol-6].

2.2.2 Quantitative PCR

DNA damage analysis was performed using quantitative polymerase chain reaction (QPCR) optimized for whole *C. elegans* as described in Boyd et al. (2009)²³⁴ with some modifications. *glp-1* adults were picked at a 1 worm to 15 μ l lysis buffer ratio. In RNAi experiments, nuclear and mitochondrial DNA copy number for each QPCR sample determined by quantitative, real-time PCR was used to normalize for copy number variation between samples. This assay relies on the ability of DNA damage to block progression of the DNA polymerase used for PCR; thus, the amount of amplification is inversely related to the amount of DNA damage^{235, 236}. In each sample, a long (~10 kb) nuclear and mitochondrial genomic region is amplified. The long product is used to calculate lesion frequency as compared to control samples.

2.2.3 DNA Damage and Repair Quantification

Synchronized *glp-1* L1 larvae were obtained by bleach-sodium hydroxide isolation of eggs and liquid egg hatch in K⁺ medium ²³⁴. Nematodes were grown to young adult stage at 25°C then transferred to K-agar plates without OP50 and exposed to 50 J/m² UVC using an ultraviolet lamp (UVLMS-38 EL Series 3UV Lamp, UVP, Upland, CA, USA) with peak emission at 254 nm. Doses were quantified using a UVX digital radiometer. Nematodes were lysed at 0, 24, 48 and 72 h after exposure. Nematodes were incubated at 25°C during recovery periods. Analysis was performed on 7-12 sample tubes (6 nematodes/tube) for each treatment condition generated from at least two independent, time-separated experiments creating an “n” of 7 to 12. At least two PCR technical replicates were carried out for each sample. Lesion frequency in UVC treated samples was calculated relative to RNAi clone untreated controls. Global ANOVA analysis was used to determine effects and interactions of treatment, recovery and RNAi clone (Statview 5.0.1). When warranted by global ANOVA, Fisher’s PLSD was used to determine the effect of individual variables.

2.2.4 Mitochondrial Copy Number Analysis

Absolute mitochondrial copy number was measured by quantitative, real-time PCR as described in Bratic et al. (2009) ²³⁷ using the lysed worm samples collected for QPCR as described above. For each sample, three technical replicates were averaged from a single real-time PCR run.

2.2.5 RNA Interference

RNAi-mediated interference was carried out by feeding. HT115 (DE3) RNase III-deficient *E. coli* engineered to express dsRNA for *eat-3* (D2013.5), *drp-1* (T12E12.4), *pink-1* (EEED8.9), and *pdr-1* (K08E3.7) were obtained from Geneservice (Cambridge, UK) or Open Biosystems (Huntsville, AL). *atg-18* (F41E6.13), *bec-1* (T19E7.3), *fzo-1* (ZK1248.14) and *unc-51* (F41E6.13) were retrieved from the Vidal *C. elegans* RNAi library²³⁸ and pL4440 (empty vector, negative RNAi control) and *unc-22* (ZK617.1, positive RNAi control) were retrieved from the Ahringer *C. elegans* RNAi library²³⁹. All RNAi vectors were sequenced to verify the identity of the insert.

RNAi stocks were selected on LB plates containing 15 µg/ml tetracycline and 100 µg/ml ampicillin (Sigma Aldrich). Bacteria were grown in LB containing 50 µg/ml ampicillin (final concentration) for 8 h and were added to NGM plates containing 50 µg/ml ampicillin and 1mM isopropyl β-D-1-thiogalactopyranoside (IPTG, Sigma Aldrich). With the exception of *eat-3*, *fzo-1* and *drp-1* RNAi knockdown, L1 *glp-1* nematodes were synchronized as described above and grown on RNAi-seeded NGM plates for two generations. Nematodes were grown at 15°C throughout the experiment except for a 15 hour period between the L3 and L4 stage during which nematodes were transferred to 25°C for sterilization²⁴⁰. At the adult stage of the second generation, *glp-1* nematodes were dosed with 50 J/m² UVC and lysed immediately and 120 h after the UVC dose for DNA damage analysis. For *eat-3*, *fzo-1* and *drp-1* RNAi knockdown, an

identical procedure was carried out except over one generation instead of two due to embryonic lethality and larval arrest in F1 progeny of nematodes treated with *eat-3*, *fzo-1*²⁴¹ and *drp-1*¹⁴⁷ RNAi.

2.2.6 Mitochondrial morphology and autophagy analysis

Synchronized young adult, N2 *myo-3::matrixGFP* and N2 *LGG-1::GFP* nematodes were maintained and UVC exposed as described above except at 20°C instead of 25°C. At recovery periods, 6-10 nematodes were picked onto 10% agar pads with 10 µl of 10 mM levamisole (Sigma Aldrich, dissolved in water). Single-plane images were taken of muscle cell mitochondria and seam cells from five to ten nematodes per experiment in two, time-separated experiments on a Zeiss 780 confocal microscope at 63x magnification. Between 9-15 seam cells and 25-50 muscle cells were analyzed per treatment per time-point. *LGG-1::GFP* foci in each seam cell were counted manually. An overall effect of treatment determined by ANOVA ($p < 0.0001$) (Statview 5.0.1) and a difference between specific treatments was determined by Fisher's PLSD. Images of muscle cell mitochondria were analyzed using MetaMorph Premier and methods described in ^{242,243}. Briefly, background subtraction, a top hat morphological filter and a threshold were applied to images. After converting to a binary image, mitochondrial area excluding the area of "holes", perimeter and form factor for each muscle cells were measured using Integrated Morphology Analysis.

2.2.7 Larval Arrest Protocol

L1 worms were plated in equal amounts on unseeded, non-peptone (to prevent growth of bacterial contamination), K-agar plates with or without ethidium bromide, doxycycline or chloramphenicol (Sigma Aldrich) for 48 h. L1 nematodes were starved during this period to prevent development. L1 worms were exposed to UVC at 0, 24, and 48 h after plating. Immediately following the 48 h UVC dose, worms were transferred to 24-well, seeded, K-agar plates (1 – 3 worms/well, 12 wells/treatment, one plate/strain) with or without ethidium bromide, doxycycline or chloramphenicol. For 3-MA exposure following the 48 h UVC dose, worms were transferred to 24-well, seeded, liquid K+ as described above with or without 3-MA (Sigma Aldrich, dissolved in dH₂O). Every 24 h for 96 h, each worm was staged and the percentage of nematodes that reached L4 was determined based on the presence of the vulval crescent. All mutant strains and/or treatments were screened in a minimum of three time-separated experiments and the % \leq L3 from each experiment was considered a biological replicate. % \leq L3 across all time points was compared between strains (if applicable) and treatments by repeated measures ANOVA (Statview 5.0.1). Given a significant interaction in the repeated measures ANOVA, ANOVA was used to determine overall effects and interactions at each time point followed by Fisher's PLSD, if warranted.

2.2.8 Relative ATP Analysis

PE255 nematodes were dosed according to the UVC dosing scheme described above (Larval Arrest Protocol) and ATP analysis was conducted immediately after the third UVC dose (0 h) or 24 h after the third dose and placement on food as described in Lagido et al. (2008) ²⁴⁴. In short, each experiment had two biological replicates dosed on separate no-peptone, no-food plates and three time-separated experiments were performed (n=6). Luminescence and GFP were measured using a FLUOstar Optima (BMG Labtech) on ~100 nematodes in 100 µl of K-media added to a 96-well plate with 2-4 technical replicates/ biological replicate. GFP was measured initially using 485/520 filter set. Following GFP measurement, 50 µl of luminescence buffer (citrate phosphate buffer pH 6.5, 0.1 mM D-luciferin, 1% DMSO and 0.05% triton-X, final concentrations) was injected into each sample and luminescence was measured three minutes after injection using a 590 nm emission filter. Luminescence was normalized to GFP fluorescence intensity to account for differences in number of worms per well. Two-way ANOVA was used to determine if there was an effect of treatment and/or recovery on % control luminescence (Statview 5.0.1). After establishing that there was a treatment by recovery effect ($P = 0.0017$), the effect of treatment at each time point was assessed using Fisher's PLSD.

2.2.9 Oxygen consumption analysis

N2 nematodes were treated with 10 J/m² UVC as described above (Larval Arrest Protocol) and oxygen consumption was measured at 0, 24 and 48 h post the third UVC exposure using a Mitocell (MT200) respiration chamber with magnetic stirrer and 1302 Clark-type microcathode oxygen electrode attached to a 782 oxygen meter (Strathkelvin Instruments, Glasgow, UK) essentially as described ²⁴⁵. At 0 and 24 h, 1000 nematodes were sorted into four 1.5 ml microcentrifuge tubes using a COPAS Biosort (Union Biometrica, Holliston, MA, USA) with the same gate used for untreated and treated samples. At 48 h, 500 nematodes were sorted. The UVC exposed group was sorted into two populations: large (non-arrested) and small (arrested). The large or non-arrested gate was defined using the control population which is at L4 or older. The small or arrested gate was defined as any nematode smaller than the control population. Immediately before measurement worms were centrifuged, 100 µl of pelleted worms were added to the Mitocell chamber and oxygen consumption was measured for four minutes once linear. The rate of oxygen consumption was calculated within the linear range for each sample and two-way ANOVA followed by Fisher's PLSD (if applicable) were used to identify significant effects of treatment and recovery (Statview 5.0.1).

2.3 Results

2.3.1 UVC-induced mtDNA damage is removed over time

Studies in cell culture and *C. elegans* have established the persistence of mtDNA damage up to 48 h post exposure to UVC^{116, 246, 247} but further time points have not been investigated, partially due to the confounding effect of dilution of mtDNA damage encountered with proliferating cells in culture. We utilized the germ-line proliferation defective mutant strain, *glp-1(q224)* to investigate the persistence of UVC-induced mtDNA damage. Adult *glp-1* raised at 25°C have post-mitotic somatic cells and few (6-8) germ cells²⁴⁸, such that changes in DNA damage can be attributed to repair or removal rather than dilution following cell replication²⁴⁷. 254 nm radiation (UVC) serves as an excellent model for bulky adducts because it similarly induces helix-distorting lesions and it is primarily absorbed by nucleic acids, with little damage to other macromolecules; thus we utilized UVC to induce helix-distorting mtDNA lesions throughout our studies. Post-mitotic young adult *glp-1* nematodes raised at 25°C were exposed to 0 – 100 J/m² UVC and both nuclear and mitochondrial DNA damage was analyzed at 0, 24, 48 and 72 h post exposure via a highly sensitive quantitative PCR (QPCR) assay that does not require differential extraction of nuclear and mitochondrial DNA^{235, 236, 249}. Over 72 h 30-40% removal of mtDNA damage was observed at 50 and 100 J/m² (Figure 4a). Nuclear DNA damage was repaired to control level by 72 h (Figure 4b). mtDNA replication occurs independently of nDNA replication, and while UV-induced

lesions are likely to block replication¹²⁶, it is unlikely that all of the mitochondrial genomes per cell were damaged even at our highest doses. Assuming a Poisson distribution of lesions and a similar mtDNA copy number per cell, even at 50 and 100 J/m² approximately 35% and 20% (respectively) of mtDNA genomes would be predicted to remain undamaged. Thus, in principle, the reduction in mtDNA damage observed here could result from dilution of damage rather than removal; however, mtDNA copy number did not increase during the recovery period at any UV dose as measured by real-time PCR (Figure 4c). In fact, there was a significant decrease in copy number across treatments by 48 h post-exposure (including controls; Figure 4d); this decrease was not altered by the level of damage ($P = 0.3246$ for treatment x time interaction). Therefore, the decrease in mtDNA damage levels cannot be explained by dilution alone, and must be a result at least in part of removal of damaged genomes.

2.3.2 Mitochondrial dynamics and autophagy are involved in removal of persistent mtDNA damage

We next tested whether mitochondrial fusion, fission and autophagy assist in removal of mtDNA damage. Fusion, fission and autophagy genes were knocked down using RNAi in adult *glp-1 C. elegans*. Adult *C. elegans* were then dosed with 50 J/m² and nuclear and mitochondrial DNA damage was measured immediately and 120 h post exposure. These RNAi experiments were carried out at 15°C except for a 15 h sterilization period at 25°C because we observed higher RNAi efficiency in our RNAi positive control at the lower incubation temperature. We extended the DNA damage

removal period from 72 to 120 h because the lower incubation temperature slowed removal. We considered examining removal at later time points, but chose not to based on our previous observation that mtDNA copy number declines with age^{220, 247}, as does mitochondrial function in general²⁵⁰, effects which could confound our measurements. While the damage removal observed during this timecourse was not complete, it was sufficient for analysis and replicable in multiple experiments.

In our empty vector control (L4440), there was ~30% removal of mtDNA damage 120 h after a single UVC exposure (Figure 5). RNAi knockdown of fusion genes *fzo-1* and *eat-3*, fission genes *drp-1* and *fis-1*, and autophagy/mitophagy genes *bec-1*, *unc-51* and *pink-1* abolished detectable removal of UVC-induced mtDNA damage. No increase in mtDNA copy number was observed in any sample as measured by real-time QPCR (Figure 7), and decreases were observed in some cases. Repair of UVC-induced nDNA damage was not affected by RNAi (Figure 6). These data demonstrate that fusion, fission and autophagy are required for removal of UVC-induced mtDNA damage.

2.3.3 Persistent mtDNA damage induces autophagy without detectable changes in mitochondrial morphology

Given the requirement for mitochondrial dynamics and autophagy genes in removal of mtDNA damage, we evaluated the effect of persistent mtDNA damage on mitochondrial morphology and autophagy following UVC exposure in adult *C. elegans*. To assess mitochondrial morphology, young adult wild-type nematodes containing an extrachromosomal Pmyo-3::matrixGFP, which express GFP in the mitochondrial matrix

of muscle cells ¹⁴⁷, were exposed to a single dose of 50 J/m² and mitochondrial morphology was assessed via confocal fluorescence microscopy at 24 and 48 h post exposure. Mitochondrial morphology was quantified using form factor as a measure of mitochondrial elongation and mean area/perimeter ratio as a measure of mitochondrial interconnectivity ^{242, 243}. As shown in Figure 8a-b, no clear differences were observed in mitochondrial elongation or interconnectivity between control and UVC exposed nematodes at any time point. We observed that within individual nematodes and across treatments there was significant variability in mitochondrial morphology (Figure 8c-e).

To evaluate induction of autophagy following UVC exposure, young adult nematodes that express a GFP-tagged LGG-1 protein ²⁵¹ were exposed to 50 J/m² and LGG-1::GFP foci were quantified in hypodermal seam cells 24 h after the exposure. Lgg-1 is the *C. elegans* homolog to mammalian MAP-LC3 and is incorporated into autophagosomal membranes ²⁵¹. Appearance of LGG-1::GFP foci in hypodermal seam cells has been extensively used as an indicator of autophagy in *C. elegans* ²⁵¹⁻²⁵⁵. UVC treatment induced a mild but statistically significant increase in LGG-1::GFP foci 24 h after exposure (Figure 9). Interestingly, we observed a much greater number of LGG-1::GFP foci in untreated N2 nematodes than has been previously reported ²⁵¹⁻²⁵⁵. To confirm that foci were in fact autophagosomal structures, we inhibited autophagosome formation with 10 mM 3-methyladenine (3-MA), a widely-used class III phosphatidylinositol-3 kinase inhibitor ²⁵⁶, previously shown to inhibit autophagy in *C.*

elegans at this concentration ²⁵⁷. The number of LGG-1::GFP foci decreased significantly with 3-MA treatment (Figure 9) indicating that the foci observed in our untreated and UVC treated nematodes did represent induction of autophagy. Therefore we conclude that UVC exposure induced a mild increase in autophagy without persistent changes in mitochondrial morphology. Whether this increase in autophagy signifies a greater mitochondrial clearance requires further research.

2.3.4 Serial UVC exposure results in accumulated mtDNA damage and dose-dependent larval arrest

We next sought to investigate the in vivo importance of persistent mtDNA lesions and removal of those lesions. *C. elegans* develop through four larval stages before reaching adulthood, and mitochondrial function and mtDNA copy number throughout development have been well-characterized ²²⁰. Development from L3 to L4 entails a dramatic three- to five-fold increase in mtDNA copy number and a switch from anaerobic respiration to oxidative phosphorylation, both of which are associated with somatic and germ cell development ^{220, 237}. Several researchers demonstrated that either knockdown of ETC components or chemical inhibition of mtDNA replication or protein translation early in larval development (L1-L2) results in developmental arrest at or before L3 ^{220, 232, 233}. The authors concluded that larval development serves as an indicator of overall mitochondrial function. This conclusion was further supported by Addo et al (2010) who utilized L3 larval arrest as a screen-able phenotype for genes involved in mtDNA maintenance ²³¹.

We utilized this L3 arrest phenotype to address the role of removal of persistent mtDNA damage in recovery of mitochondrial function following UVC exposure. In order to address specifically the effects of mtDNA damage and not nDNA damage, we developed an experimental protocol (Figure 10a) that results in accumulation of mtDNA damage in early larval development but permits repair of nDNA damage. In this protocol, age-synchronized L1 nematodes are dosed three times with UVC over the course of 48 h, with 24 h recovery periods to allow nDNA damage repair. This larval arrest protocol results in time-dependent accumulation of mtDNA damage to a level similar to that induced in adult experiments above, while nDNA damage levels were reduced to close to the limit of detection (0.1 lesions/10 kb, ²³⁶; Figure 10b). Following the third exposure to UVC, L1 nematodes were provided with food and screened at 48, 72, and 96 h to assess the frequency and duration of L3 arrest. A UVC dose-dependent increase in L3 arrest was observed with significant inhibition starting at 7.5 J/m² (Figure 11a). Steady state ATP levels, quantified 24 h after the third dose and prior to detectable larval arrest, were significantly lower at all UVC exposures (Figure 11b).

As a more specific measure of mitochondrial respiration, oxygen consumption was assessed at 0, 24 and 48 h after exposure to 10 J/m² UVC and addition of food. UVC-exposed nematodes displayed significantly lower oxygen consumption by 24 h (Figure 11c) with a more significant effect in treated nematodes at 48 h. At 48 h when larval arrest is first quantified, control nematodes are at young adult stage while

approximately 40% of nematodes in the UVC treated group are L2-L3. We separated these two populations based on size in the UVC exposed group using a COPAS Biosort, defining large or non-arrested nematodes as those which were the same size as untreated nematodes and smaller or “arrested” nematodes as those smaller than untreated nematodes. Both the arrested and non-arrested nematodes had significantly lower oxygen consumption compared to controls, but oxygen consumption in arrested nematodes was significantly lower than non-arrested UVC treated nematodes.

Thus, accumulated mtDNA damage resulted in an overall decrease in mitochondrial function as indicated by increased L3 arrest, lower steady state ATP level and reduced oxygen consumption. To further test whether the L3 arrest was mediated by mitochondrial dysfunction, we evaluated the severity of L3 arrest after co-exposure to UVC plus chloramphenicol or doxycycline. Doxycycline and chloramphenicol are antibiotics that specifically block mitochondrial protein synthesis²⁵⁸. If UVC-induced larval arrest is mediated by mitochondrial dysfunction then co-exposure to these mitochondrial inhibitors should exacerbate larval arrest. Co-exposure with UVC and chloramphenicol (750 µg/ml) or doxycycline (10 µg/ml) exacerbated L3 arrest across all time points compared to UVC or chemical alone (Figure 12), supporting that L3 arrest following the larval screen protocol is mediated by mitochondrial dysfunction.

Although nDNA damage is repaired throughout larval exposure and the recovery period, we cannot entirely rule out the possibility that L3 arrest is influenced

by lingering low (below our limit of detection) levels of nDNA damage. We note, however, that in a previous study that employed a single 10 J/m² dose of UVC, which should result in a similar maximal level of nDNA damage to that which we measured throughout the larval arrest protocol (~0.8 lesions/10 kb) but a much lower level of mtDNA damage (also ~0.8 lesions/10 kb), no effect on larval development was observed²⁵⁹.

2.3.5 mtDNA replication is critical for recovery from persistent mtDNA damage

At serial UVC doses less than 25 J/m², nematodes recover from larval arrest over time (Figure 11a). This recovery may be facilitated by replacement of UVC-damaged mitochondrial genomes. Ethidium bromide is a DNA intercalating agent that preferentially targets mtDNA over nDNA and blocks replication²⁶⁰. Previous studies indicate that inhibition of mtDNA replication by ethidium bromide results in L3 arrest and depletion of mtDNA²²⁰. If recovery from UVC-induced L3 arrest is aided by dilution of damaged mtDNA via replication of undamaged genomes, then co-exposure to UVC and ethidium bromide should exacerbate larval arrest. We selected an ethidium bromide concentration (5 µg/ml) that results in a similar frequency and duration of larval arrest as UVC 10 J/m². Co-exposure with UVC (10 J/m²) and ethidium bromide (5 µg/ml) dramatically exacerbated L3 arrest across all time points compared to UVC or chemical alone (Figure 12). This demonstrates the importance of mtDNA replication in recovery of mitochondrial function resulting from persistent mtDNA damage.

2.3.6 Recovery from UVC-induced mtDNA damage involves mitochondrial fusion and autophagy

To better understand the role of removal of mtDNA damage in recovery from UVC-induced L3 arrest, we compared L3 arrest in wild-type (N2) *C. elegans* to strains carrying mutations in fusion, fission and autophagy genes. If removal of persistent mtDNA damage plays a significant role in vivo in recovery from UVC-induced mitochondrial dysfunction then knockout of these genes involved in removal will increase the frequency and duration of larval arrest compared to wild-type. As shown in Figure 13, significant exacerbation of L3 arrest was observed in the fusion mutants *fzo-1* and *eat-3* and the autophagy mutant *unc-51*. Mutations in fission genes *drp-1* and *fis-1*, autophagy gene *bec-1* or mitophagy genes *pink-1* and *pdr-1* did not significantly exacerbate L3 arrest at any time point.

It is possible that the lack of effect observed in this mutant is due to retained BEC1 function, given that the larval arrest protocol was performed on *bec-1(ok961)* heterozygotes; this was necessary due to embryonic lethality in homozygous *bec-1(ok961)*. We attempted to perform the larval arrest protocol on *atg-18(gk378)*, another autophagy mutant, but untreated nematodes did not develop following the 48 hour period of starvation. Since we were limited in our ability to test genetically for a role of autophagy in recovery from persistent mtDNA damage due to mutant inviability, we chemically inhibited autophagy with 3-MA. N2 nematodes were exposed to 10 mM 3-MA following the third UVC exposure and placement on food. At this dose, 3-MA

exposure alone did not result in significant larval arrest (data not shown); however, 3-MA exposure did exacerbate UVC-induced L3 arrest (Figure 13).

It is interesting that knockout of fusion resulted in complete larval arrest with no recovery while knockout of autophagy led to a more moderate increase in larval arrest with delayed recovery. If removal of UVC-induced mtDNA damage were the sole driver of recovery then knockout of these two pathways would lead to similar results.

Mitochondrial fusion has been shown to be critical for mtDNA integrity and recovery from mitochondrial dysfunction in part because it aids in mtDNA replication which is critical for recovery from UVC-induced larval arrest as shown above and in functional complementation ¹⁴¹ that results from mixing damaged mtDNA among undamaged mtDNA. These results suggest that removal of damaged mtDNA does aid in recovery from mitochondrial dysfunction; however, mtDNA replication and mitochondrial fusion are necessary for recovery. We suggest that enhanced mitochondrial fusion as a result of *drp-1* or *pink-1* knockout may explain why knockout of these genes did not affect larval arrest or recovery although both of these are involved in mtDNA damage removal.

As previously mentioned, measuring removal of mtDNA damage in proliferating cells is confounded by dilution of damage associated with cell replication. *C. elegans* larval development is marked by a 2-fold increase in somatic cells, a five-fold increase in mtDNA copy number and development of approximately 250 germ cell nuclei ²²⁰. Therefore we were not able to directly test if mutations in these genes

prevented removal of damage or if arrested nematodes had more persistent mtDNA damage compared to non-arrested nematodes, because the developmental changes would have confounded those measurements. Nonetheless, our genetic and pharmacologic data allow us to conclude that mitochondrial fusion and autophagy play an important role in recovery from UVC-induced mitochondrial dysfunction.

2.4 Discussion

2.4.1 Mitochondrial dynamics and autophagy play critical roles in the response to persistent mitochondrial DNA damage

MtDNA integrity is critical to mitochondrial function and is more vulnerable than nDNA to common types of environmentally-induced damage^{26, 28, 29, 34, 127, 222}. This vulnerability is exacerbated by the fact that mitochondria lack NER, the pathway required to repair helix-distorting and bulky DNA damage induced by important environmental genotoxins including UVC, mycotoxins and PAHs^{37, 39, 41, 112}. Thus, at least in most species (fission yeast is an exception:²⁶¹), mtDNA damage induced by such agents is irreparable. Our experiments indicate that mitochondrial dynamics and autophagy protect against persistent mtDNA damage; we suggest that this results both from a role in removal of damaged mtDNAs and from a role in protecting mitochondrial function in the face of mtDNA damage.

We propose a model (Figure 15) whereby persistent mtDNA damage leads to mitochondrial dysfunction. Mitochondrial fusion protects against dysfunction, as does

autophagy, presumably by promoting functional complementation, mtDNA replication and removal of dysfunctional mitochondria (these processes are further discussed below). Mitochondrial genomes carrying persistent damage can be removed by mitochondrial fission and subsequent autophagy of dysfunctional daughter mitochondria, which is observed in our experiments as a mitochondrial fission- and autophagy-dependent removal of mtDNA damage. It is not intuitive that mitochondrial fusion would be required for the removal of damaged mtDNAs, but we propose that fusion is so critical for mitochondrial function (as supported by our larval arrest results) and mitochondrial biogenesis that the lack of fusion results in severe mitochondrial dysfunction that incapacitate the processes required for removal. While additional experiments will be required to fully test this model, it is consistent with our data and supported by a significant body of literature, as discussed below.

2.4.2 Mitochondrial fusion, fission, and autophagy are required for removal of persistent mtDNA damage

Irreparable, helix-distorting mtDNA damage is persistent but our results indicate that this damage is removed slowly in vivo with significant removal observed by 72 h post exposure. This data is consistent with other literature indicating the persistence of UV-induced photodimers up to 48 h ^{112, 116, 117, 246, 247}, although one study reported a 40% reduction in UVC-induced photodimers in mtDNA of mouse cells by 24 h ²⁶². We considered the role of mitochondrial dynamics and degradation via autophagy in this removal. Autophagy is the primary mechanism of removal for mitochondria and can be

both non-selective, such as during starvation¹⁶⁸, or selective meaning that isolated, dysfunctional mitochondria with low MP are degraded preferentially^{57, 62, 63}. Selective autophagy of mitochondria or mitophagy under certain conditions is mediated by accumulation of PINK1, a serine/threonine-protein kinase on dysfunctional mitochondria and subsequent recruitment of Parkin, an E3 ubiquitin ligase to those mitochondria^{64, 66, 181}. However, the necessity and sufficiency of these events to induce mitophagy in vivo is unclear^{187, 188}.

UNC51 is a serine/threonine kinase with a role in autophagy induction; BEC1, a class III phosphatidylinositol 3-kinase (PI3K), is involved in recruiting other autophagy proteins to pre-autophagosomal structures; and ATG18, which binds phosphoinositol-3-phosphate, is required for autophagosomes formation; mutation or knockdown of these genes results in abnormal autophagy in *C. elegans*²⁵¹. We found that RNAi knockdown of autophagy/mitophagy genes *bec-1*, *unc-51* and *pink-1* inhibited removal of UVC-induced mtDNA damage suggesting that autophagy is an important mechanism of degradation of damaged mtDNA. The lack of an effect of knockdown of *atg-18* may result from insufficient knockdown or a degradation mechanism independent of *atg-18*. We noted that knockdown of autophagy proteins *bec-1* and *unc-51* prevented the trend of an age-dependent decrease in mtDNA copy number; however, *atg-18* knockdown did not prevent this decrease. This is consistent with incomplete knockdown of *atg-18*, which might permit residual mitochondrial turnover and explain why knockdown did

not inhibit damage removal. Interestingly, knockdown of *pink-1* but not *pdr-1*, the *C. elegans* Parkin homolog, inhibited mtDNA damage removal. Parkin is thought to act downstream of PINK1 and in other model systems compromised function of either reduces mitophagy^{64, 66}. In *C. elegans*, few studies have investigated the role of these genes in relation to mitochondrial function. *pdr-1* mutants have reduced oxygen consumption and are sensitive to mitochondrial complex I inhibitors²⁶³, *pink-1* mutants have reduced cristae length and are sensitive to oxidative stress²⁶⁴ and expression of wild-type *pink-1* and *pdr-1* rescued α -synuclein induced mitochondrial fragmentation²⁶⁵. These reports are consistent with those in other models suggesting conserved function of these proteins between *C. elegans* and mammals²⁶⁴. Further research is needed to better understand mitophagy in *C. elegans* and the role of *pink-1* and *pdr-1* in that process.

Knockdown of fusion genes *fzo-1* and *eat-3* and fission genes *drp-1* and *fis-1* also inhibited removal of UVC-induced mtDNA damage. The role of mitochondrial morphology and dynamics in mediating mitophagy is unclear. Inhibition of fission via manipulation of fission genes Fis1 and Drp1 results in reduced mitophagy while overexpression of fission proteins induces mitophagy and decreases mitochondrial mass²⁶⁶. Consistent with these studies, our results indicate that Drp1 and Fis1 are required for removal of damaged mtDNAs. The requirement of Fis1 is particularly interesting because the role of FIS1 and FIS2 in fission in *C. elegans* is still controversial. *fis-1*, *fis-2*

and *fis-1/fis-2* mutants do not have abnormal mitochondrial morphology under unstressed conditions, suggesting that these proteins may not retain a role in mitochondrial fission, despite homology with *fis1*, the yeast and mammalian fission gene¹⁴⁹.

It may be tempting then to assume that knockdown of fusion genes would enhance mitophagy and removal of mtDNAs. Certainly OPA1 deficiency results in a general increase in autophagy and mitochondria targeted for degradation exhibit OPA1 depletion^{62, 267}. However, loss of mitochondrial mass resulting from nicotinamide treatment is partially inhibited by fusion knockdown rather than enhanced as might be predicted²⁶⁸ and studies that inhibit fusion without compromising membrane potential or mitochondrial function show that fission alone without accompanying mitochondrial dysfunction does not result in increased mitophagy^{63, 269}. Consistent with our data, human fibroblasts harboring a missense mutation in the fusion gene MFN2 exhibit significantly reduced repair efficiency of oxidative mtDNA damage and DNA instability¹⁴³. Our data suggests that fusion is required for removal of mtDNA damage; whether this is by facilitating autophagy or another mechanism requires further research.

2.4.3 Persistent mtDNA damage induces autophagy without detectable changes in mitochondrial morphology

We considered that slow removal of UVC-induced mtDNA damage may reflect the natural turnover rate of mitochondria and not an induction in autophagy. We therefore evaluated the level of autophagy following UVC exposure in LGG-1::GFP

expressing *C. elegans*. We observed a mild increase in the number of autophagosomes in the UVC exposed nematodes 24 h after treatment suggesting that UVC exposure does induce autophagy. Whether this increase in autophagy signifies a greater mitochondrial clearance requires further research.

Mitochondrial dynamics are responsive to mitochondrial function. Loss of membrane potential inhibits fusion and results in an overall fragmented morphology and treatment with pro-oxidants or mitochondrial respiratory chain uncouplers triggers fragmentation⁴⁵⁻⁴⁷. On the other hand, mitochondrial hyperfusion has been observed following treatment with DNA intercalators or UV^{47,159} highlighting the complex responses of mitochondrial dynamics to mitochondrial stressors. We evaluated the effect of UVC exposure on mitochondrial morphology. We did not observe a difference in mitochondrial interconnectivity or elongation with UVC treatment at 24 or 48 h after treatment. There remains the possibility that changes in morphology occurred between the time points analyzed; however, given the persistence of this damage we would expect any morphological changes induced by this damage would also be persistent. Thus, while our genetic data demonstrate the importance of mitochondrial dynamics in responding to persistent mtDNA damage, such damage did not lead to changes in mitochondrial morphology that were easily observable by microscopy.

2.4.4 Recovery requires mtDNA replication and mitochondrial fusion and is aided by removal of damaged mtDNA via autophagy

Mitochondria contain multiple copies of DNA thus recovery from helix-distorting mtDNA damage could be achieved by both removal of the damaged copies and dilution of damaged copies with undamaged genomes. In adult *glp-1 C. elegans* raised at 25°C (^{220, 247} and Fig 1d) and 15°C (Fig S1), mtDNA copy number decreases with age. This indicates that degradation of mtDNA is occurring and the resultant decline in copy number is not compensated for by increased biogenesis. This decrease in copy number likely relates to the decreased metabolic rate and ATP production shown in aging nematodes ²⁵⁰. We therefore used developing rather than adult *C. elegans* to determine the significance of removal of damaged mtDNAs in recovery from UVC exposure. During the L3-L4 transition, nematodes switch to oxidative phosphorylation to produce energy; this is accompanied by a significant increase in energy demand and mtDNA copy number ²²⁰. Inhibition of mitochondrial replication or translation or mutations in mitochondrial electron transport chain components all result in arrest at or before the L3 stage ^{220, 232, 233}. Using a novel protocol designed to permit accumulation of a high level of mtDNA damage early in L1 (Figure 10a), we showed that UVC-induced mtDNA damage caused dose-dependent increases in mitochondrial dysfunction as indicated by L3 arrest, reduced steady state ATP level, and reduced oxygen consumption. Treatment with low levels of ethidium bromide nearly abolished recovery

from UVC-induced L3 arrest suggesting that recovery of mitochondrial function is facilitated by dilution of damaged mtDNA via mtDNA replication.

unc-51 mutants displayed a significant increase in L3 arrest as did nematodes in which autophagy was inhibited with 3-MA. These data indicate that autophagy (and presumably removal of damaged mtDNA via autophagy) is involved in functional recovery from persistent mtDNA damage. Autophagy provides protection against mitochondrial dysfunction, apoptosis and cell death following toxicant exposure or cell stress¹⁹⁵⁻¹⁹⁸ and abnormal mitochondrial autophagy coupled with mitochondrial dysfunction occurs in a variety of pathologies including mitochondrial diseases¹⁹⁵, lysosomal storage disorders²⁰⁷ and neurodegenerative disorders including Parkinson's, Alzheimer's and Huntington's disease¹⁸³⁻¹⁸⁵. It is not unlikely that autophagy protects against mitochondrial stressors, in part, by removing mitochondria that would otherwise generate reactive oxygen species (ROS) and trigger apoptosis or necrosis^{229, 230}. Thus, the reduction in autophagy with age particularly in post-mitotic cells may result in persistence of unstable mitochondria potentially leading to development of age-related disorders¹¹. Surprisingly, *pink-1* mutants did not exhibit increased larval arrest despite the role of this protein in removal of damaged mtDNA in adult *C. elegans*. This may indicate that removal of damage in replicating cells is not PINK1 dependent. On the other hand, PINK1 knockdown in *C. elegans* increases mitochondrial fusion (unpublished observations) and in other model organisms is associated with increased

mitochondrial fusion^{270, 271} which is critical for recovery from L3 arrest as discussed below.

Mutations in the fusion genes *fzo-1* and *eat-3* resulted in complete arrest of larval development following serial UVC, suggesting that mitochondrial fusion is critical in recovery of mitochondrial function following UVC-induced mtDNA damage. While it is likely that the complete larval arrest observed in these mutants is partially due to inhibition of damage removal, the degree of exacerbation suggests failure of other recovery mechanisms. Fusion is critical for recovery of mitochondrial function following toxicant exposure and cell stress. Loss of fusion capacity increases susceptibility to loss of membrane potential¹³¹, respiratory deficiency^{131, 272}, oxidative stress^{241, 273}, apoptosis and cell death^{189, 241, 274}. Additionally, enhanced mitochondrial fusion has been shown to be protective against UV irradiation induced depletion of ATP^{47, 159} and blockage of mtDNA replication by mtDNA intercalators¹⁵⁷.

Fusion provides protection against the effects of mtDNA mutations by facilitating “functional complementation”^{137, 155}, the mixing of lipids, proteins and mtDNA to compensate for mutated DNA¹⁴¹ and this mechanism may explain the lack of phenotypic expression of mtDNA mutations until the occurrence is high (over 40-90%)¹⁵⁴. This function of fusion also equally distributes proteins involved in mtDNA replication and repair¹⁴¹. Mice harboring mutations in fusion proteins exhibit severe depletion of mtDNA¹⁴⁰ due to defects in mtDNA replication¹⁴¹ and *polg-1* mutant C.

elegans exhibit increased mitochondrial fusion in response to mtDNA depletion²³⁷. As described above, mtDNA replication is a particularly important mechanism of recovery from L3 arrest. Therefore, mitochondrial fusion may aid in recovery from UVC-induced larval arrest by promoting functional complementation, mtDNA replication and removal of damaged mtDNAs.

Consistent with this idea, mutation in the fission genes *drp-1* and *fis-1* did not increase L3 arrest. While this could suggest that mtDNA damage removal does not require fission in developing *C. elegans*, we hypothesize that enhanced fusion resulting from the *drp-1* or *fis-1* mutation may compensate for lack of mtDNA damage removal. Decreased mitochondrial fragmentation has been shown to be protective against toxicant-induced mitochondrial dysfunction, ATP depletion and apoptosis^{47, 268, 269}. Conversely, Yang et al. (2011) found that *drp-1* nematodes are more sensitive to heat stress and paraquat²⁷⁵ and, in mammalian cells, knockdown of drp1 results in mitochondrial dysfunction, loss and disorganization of mtDNA and decreased membrane fluidity^{45, 190}.

We were unable to directly test in developing *C. elegans* if mutations in fusion, fission and autophagy/mitophagy genes inhibit removal of UVC-induced mtDNA damage or if lack of damage removal correlates with the frequency and duration of L3 arrest due to developmental changes (i.e., somatic and germ cell proliferation and substantial increases in mtDNA copy number) that would have confounded those

measurements. Assuming that larval *C. elegans* employ the same mechanism as adults to remove UVC-induced mtDNA damage, our genetic and pharmacologic data suggest that removal of mtDNA damage aids in recovery from UVC-induced mitochondrial dysfunction facilitated by autophagy and mitochondrial fusion.

2.4.5 Potential role of NER proteins and mitochondrial nucleases

Our model assumes that mitochondria in *C. elegans*, like other metazoans studied to date, lack NER such that UVC-induced mtDNA damage is irreparable and persistent^{37, 39, 41, 112}. Recently, however, NER proteins CSA and CSB have been shown to localize to mitochondria and to have a direct role in sensing and responding to oxidative mtDNA damage^{276, 277}, as well as inducing mitochondrial turnover via autophagy in response to cell stress²⁷⁸. Based on these studies, an interesting future research direction will be to determine if CSA/CSB aid in the response to helix-distorting mtDNA damage and facilitate the removal of these lesions via autophagy.

There is evidence mtDNA harboring double strand breaks (DSBs) resulting from high levels of oxidative lesions can be degraded in vitro by nucleases residing in mitochondria²⁷⁹⁻²⁸², of which endonuclease G, involved in nDNA degradation during apoptosis, and EXOG, involved in mitochondrial long patch BER²⁸², remain the primary candidates. Additionally, fission yeast possesses a UV-damaged DNA endonuclease-dependent excision repair that drives repair of UV photodimers in mtDNA by nicking the phosphodiester bond 5' to the UV-induced photodimers to initiate BER²⁶¹. This

repair mechanism has not been observed in higher organisms. Still, it is possible that degradation of mtDNA harboring irreparable UVC-induced photodimers may in part involve nuclease-dependent degradation. We considered this less likely than our current model for two reasons. Firstly, the degradation rate reported for mtDNA with strand breaks is significantly faster than that reported here, with significant degradation reported within an hour of oxidant exposure²⁸¹. Secondly, when we screened viable *C. elegans* mutants of known endonucleases including *cps-6*, the *C. elegans* homolog of endonuclease G using the larval arrest protocol, we found that mutations in *cps-6*, *crn-6* and *nuc-1* did not exacerbate larval arrest (Figure 14). This indicates that these nucleases are not necessary for recovery from UVC-induced mtDNA damage in larval *C. elegans* and suggests that they are not involved in removal of UVC-induced mtDNA damage. However, due to the potential redundancy in mitochondrial nucleases, we cannot exclude a role of nucleases in recovery from and removal of UV-induced mtDNA damage.

2.4.6 Broader implications of persistent mtDNA damage removal

In summary, our results suggest a model whereby mitochondrial dynamics and autophagy play a role both specifically in removal of mtDNA damage, and more broadly in the response to mtDNA damage and mitochondrial dysfunction (Figure 15). This research shows that UVC-induced mtDNA damage can be removed, and furthermore demonstrates that mitochondrial dynamics and autophagy are part of a

novel pathway for the removal of otherwise irreparable mtDNA damage. Based on this and published literature, we hypothesize that initial recovery of mitochondrial function from such mtDNA damage requires mitochondrial fusion and mtDNA replication, and is assisted by removal of this damage via autophagy. Upon recovery from mtDNA damage, mitochondrial fission is restored creating a heterogeneous population of mitochondria, some with a high proportion of damaged mtDNA which are removed by autophagy, potentially in a selective fashion involving PINK1. This pathway is of potentially great significance due to the fact that many common environmental contaminants cause high levels of mtDNA damage that, like UVC-induced damage, is not repaired in the mitochondrial genome. This pathway may also be important for removal of a subset of oxidative mtDNA damage²⁸³ and damage induced by certain biological aldehydes³⁸ that are repaired in the nucleus by NER, extending the importance of our findings to damage caused by normal metabolism. Finally, mutations in genes in these pathways are associated with human disease states, demonstrating the potential for important gene-environment interactions affecting mitochondrial health after genotoxin exposure.

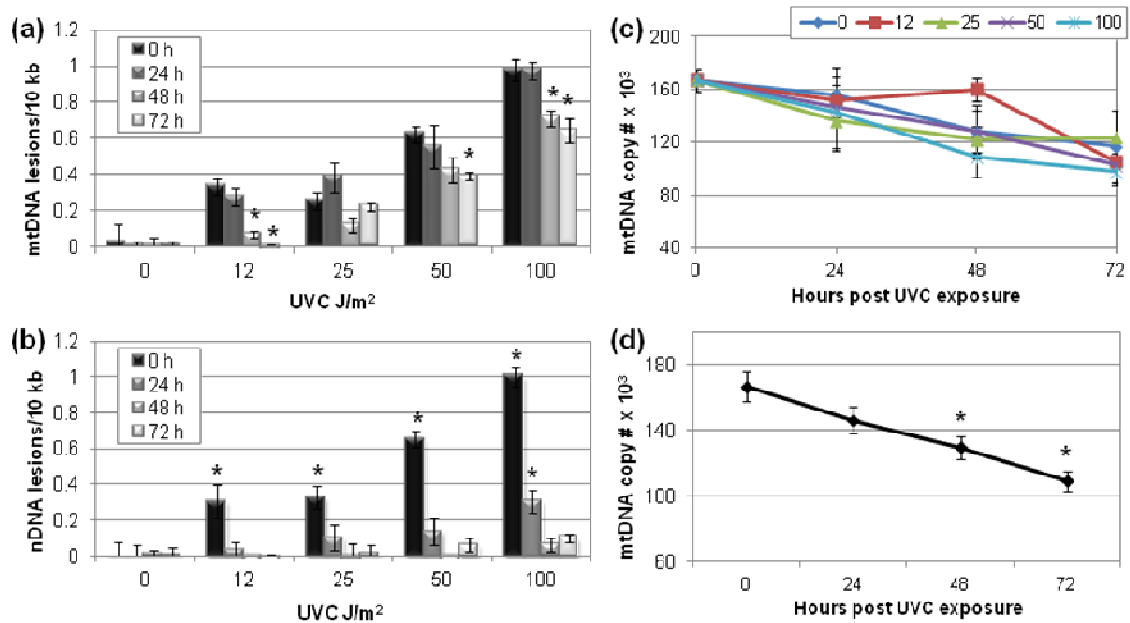


Figure 4: Mitochondrial DNA lesion frequency slowly decreases after a single dose of UVC in post-mitotic adult *C. elegans* (*glp-1*).

Nematodes were exposed to UVC and analyzed for DNA damage immediately (0 h), or after 24, 48, or 72 h via QPCR (a) mtDNA damage is removed by ~40% over 72 h at 50 and 100 J/m². Two-way ANOVA indicated a significant effect of recovery ($P < 0.0001$) and a recovery x treatment interaction ($P < 0.05$). Asterisks denote a significant difference compared to 0 h lesion frequency within each UVC treatment (Fisher's PLSD, $P < 0.05$). (b) nDNA damage is repaired following a single dose of UVC. Two-way ANOVA indicated a significant effect of treatment ($P < 0.0001$) and a recovery x treatment interaction ($P < 0.0001$). Asterisks denote a significant difference compared to undosed control lesion frequency at each recovery timepoint (Fisher's PLSD, $P < 0.05$). (c) No significant increase in mtDNA copy number was observed during the recovery period. (d) mtDNA copy number significantly decreased over the recovery period irrespective of UVC exposure. Two-way ANOVA indicated a significant effect of time ($P < 0.0001$) but no significant treatment effect ($P = 0.4714$) or treatment x time interaction ($P = 0.3246$). Asterisks denote a significant difference compared to 0 h mtDNA copy number (Fisher's PLSD, $P < 0.05$). Bars \pm s.e.m.

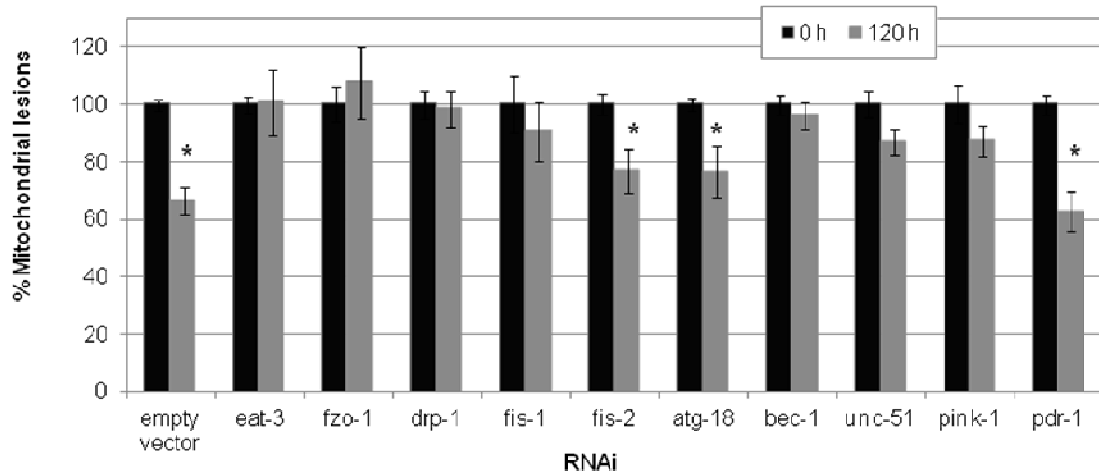


Figure 5: Fusion, fission and autophagy gene knockdown inhibits mtDNA damage removal.

Mitochondrial DNA lesions are removed in empty vector control (L4440) by 30-40% 120 h post a single UVC exposure in post-mitotic adult *C. elegans* (*glp-1*). RNAi knockdown of *eat-3*, *fzo-1*, *drp-1*, *fis-1*, *bec-1*, *unc-51* and *pink-1* inhibited mtDNA damage removal (inhibition of removal was determined by a lack of a significant difference between 0 and 120 h lesion frequency within each RNAi treatment). Two-way ANOVA indicated a significant interaction between RNAi and recovery ($P < 0.05$). Asterisks denote a significant difference between 0 h and 120 h mtDNA lesions within RNAi treatment (Fisher's PLSD, $P < 0.05$). Percent mtDNA lesions remaining after 120 h was calculated based on 0 h lesion frequency within each RNAi treatment. Bars \pm s.e.m.

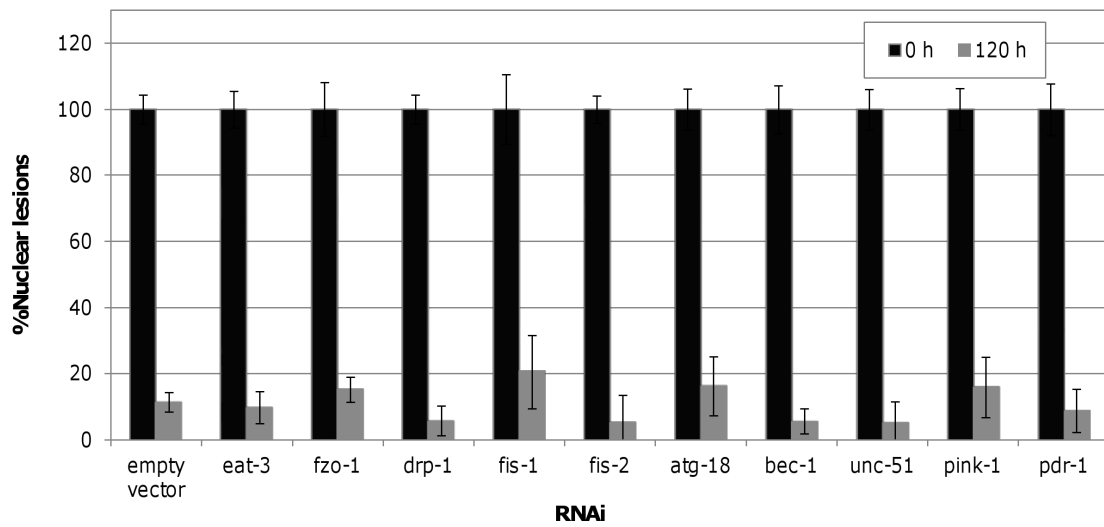


Figure 6: Nuclear DNA damage is repaired after a single dose of UVC in post-mitotic adult *C. elegans* (*glp-1*).

Nematodes were exposed to UVC and analyzed for DNA damage immediately (0 h), or after 24, 48, or 72 h. Percent nDNA lesions remaining after 120 hours was calculated based on 0 h lesion frequency within each RNAi treatment. Bars \pm s.e.m.

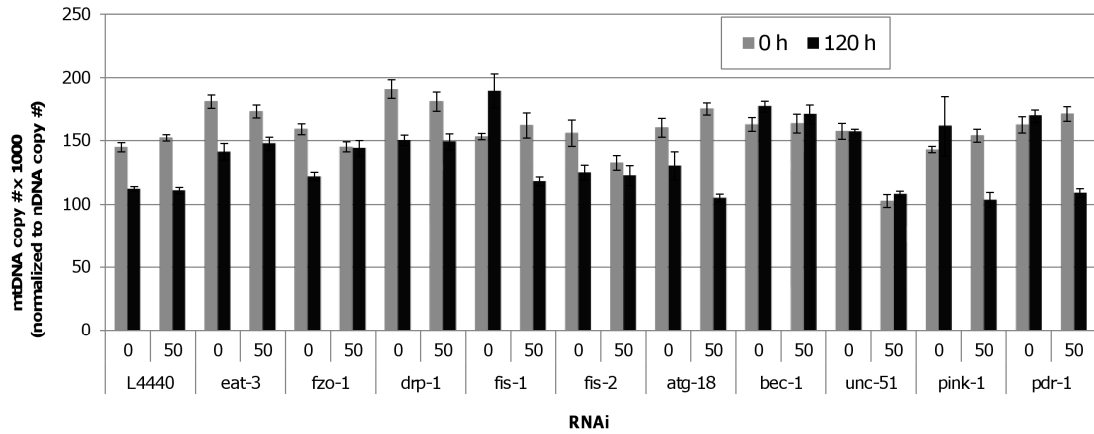


Figure 7: mtDNA copy number does not increase 120 h post UVC exposure (0, 50 J/m²) in RNAi-treated *C. elegans* (*glp-1*).

Three-way ANOVA indicated a significant effect of strain ($P = 0.0009$) and time ($P < 0.0001$) but no significant effect of UVC exposure ($P = 0.1018$) and no significant interactions of strain, time and exposure. Bars \pm s.e.m.

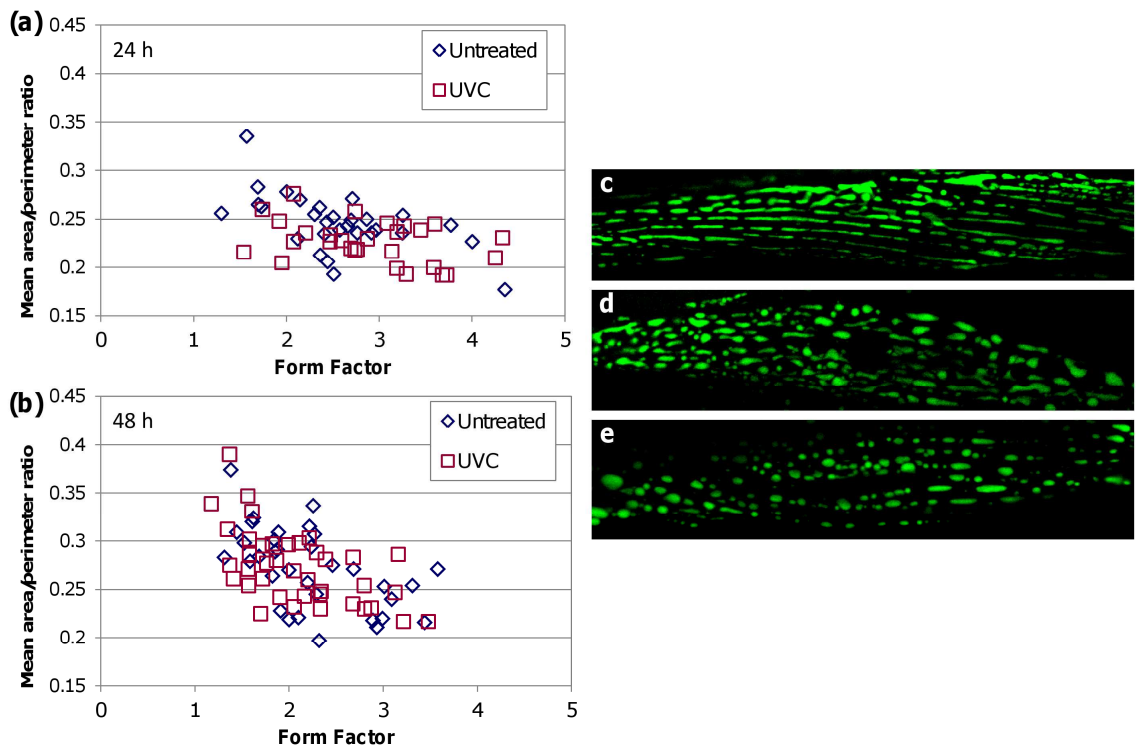


Figure 8: UVC exposure induces no detectable changes in mitochondrial morphology in adult *C. elegans*.

Mitochondrial morphology was assessed using form factor as a measure of elongation (perfect circles = 1) and mean area/perimeter ratio as a measure of interconnectivity. No detectable differences were observed at (a) 24 h or (b) 48 h following UVC exposure. Each data point represents the mean area/perimeter ratio and form factor of mitochondria within a single muscle cell. Mitochondrial morphology was highly variable within each treatment group. Representative images show a (c) tubular, (d) intermediate and (e) fragmented mitochondrial morphology in muscle cells of untreated controls 48 h after UVC exposure. Bars \pm s.e.m.

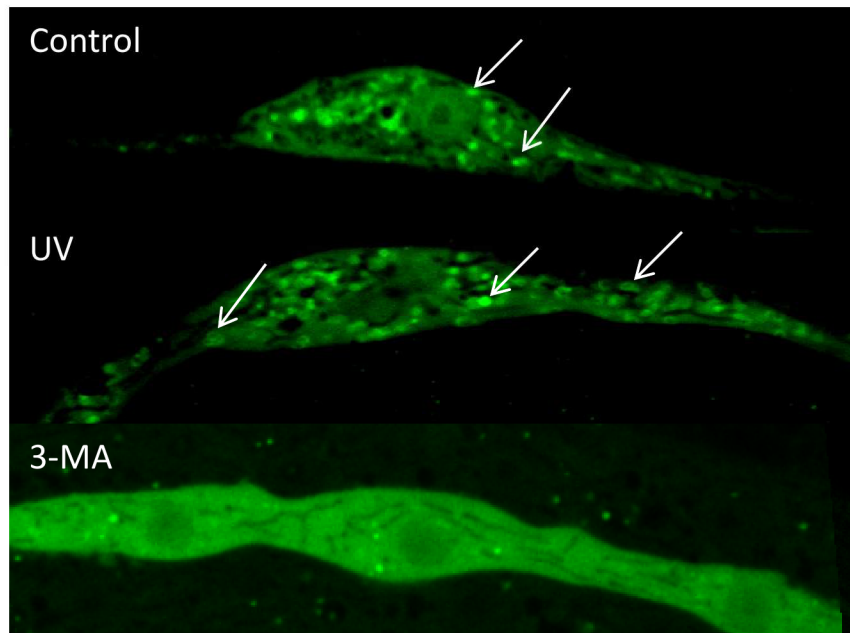
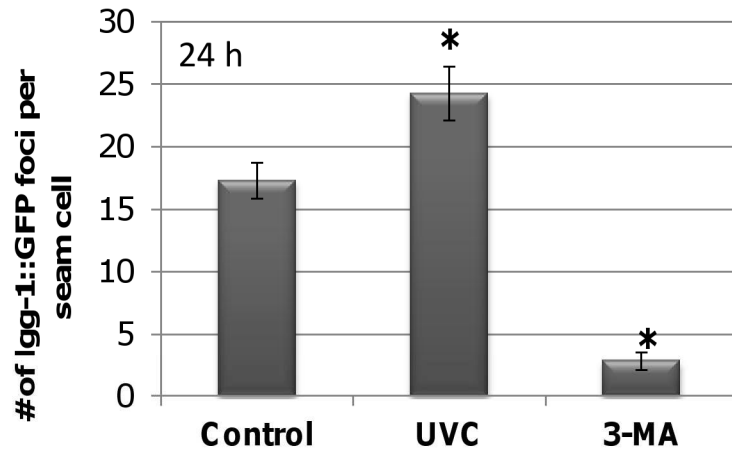


Figure 9: UVC exposure induces autophagy.

The number of LGG-1::GFP foci per seam cell increased 24 h following UVC exposure compared to untreated controls (Fisher's PLSD, $P = 0.004$). Inhibition of autophagy with 3-MA exposure reduced the formation of LGG-1::GFP foci compared to untreated controls (Fisher's PLSD, $P < 0.0001$). Arrow indicate LGG-1::GFP foci. An overall effect of treatment was determined by ANOVA ($P < 0.0001$). Bars \pm s.e.m.

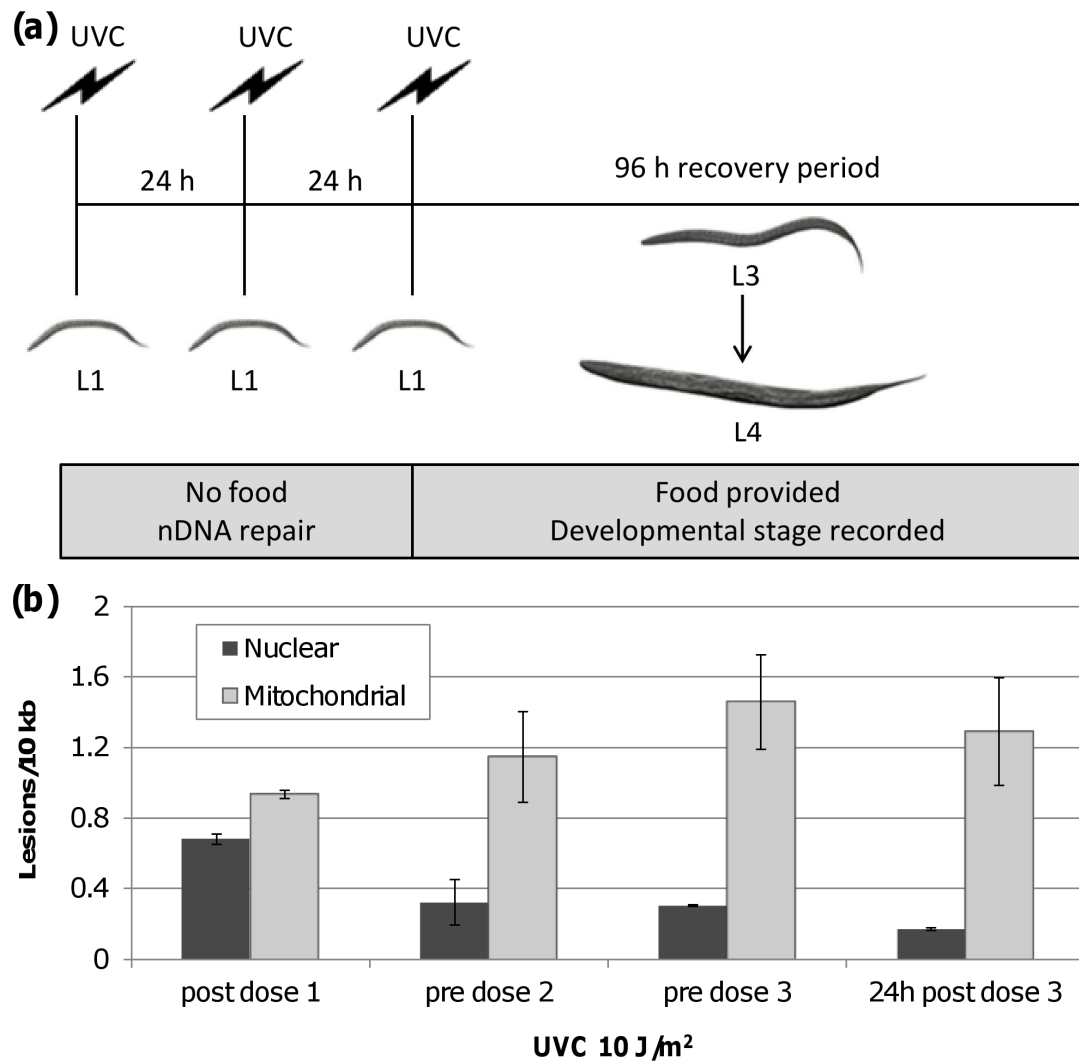


Figure 10: Serial UVC exposure results in mtDNA damage accumulation.

(a) Schematic of serial UVC protocol. L1 nematodes on unseeded plates are dosed with UVC at 254 nm every 24 h for a total of three doses. Following the third dose, nematodes are provided with food and developmental stage recorded at 48, 72 and 96 h post UVC exposure. (b) mtDNA damage accumulates over serial UVC exposure and persists 24 h after the last UVC exposure and addition of food. Following 24 h recovery periods, nDNA damage was repaired. Bars \pm s.em.

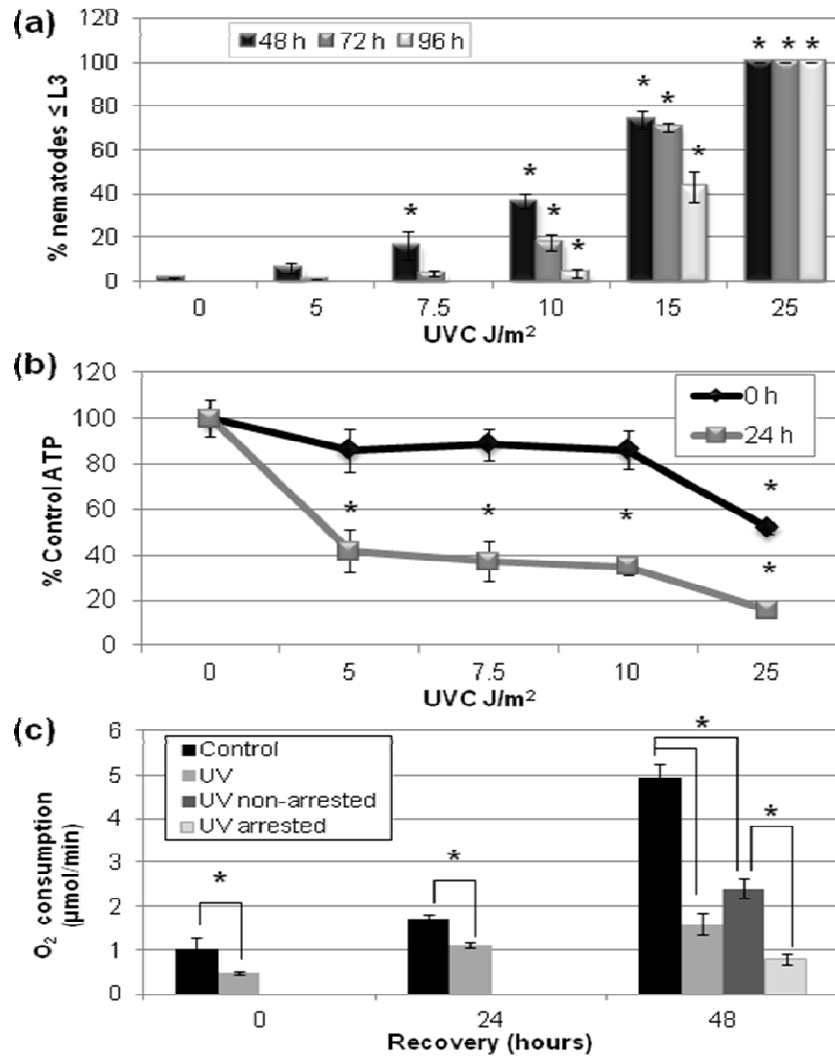


Figure 11: Serial UVC exposure results in dose-dependent L3 arrest, lower steady state ATP level and reduced O₂ consumption.

(a) Larval arrest increased in a dose-dependent manner following serial UVC exposure. (b) Steady state ATP levels were significantly lower by 24 h after UVC exposure and addition of food. Asterisks denote a significant treatment effect compared to untreated control (Fisher's PLSD, $P < 0.05$). (c) Nematodes exposed to serial UVC 10 J/m² had significantly lower O₂ consumption compared to untreated nematodes at 0, 24 and 48 h post exposure and addition of food. At 48 h, O₂ consumption was further decreased in arrested nematodes compared to non-arrested nematodes and both were decreased compared to the untreated group. Two-way ANOVA indicated a significant treatment x recovery interaction ($P < 0.0001$) and asterisks denote significant differences at each time point (Fisher's PLSD, $P < 0.05$). Bars \pm s.e.m.

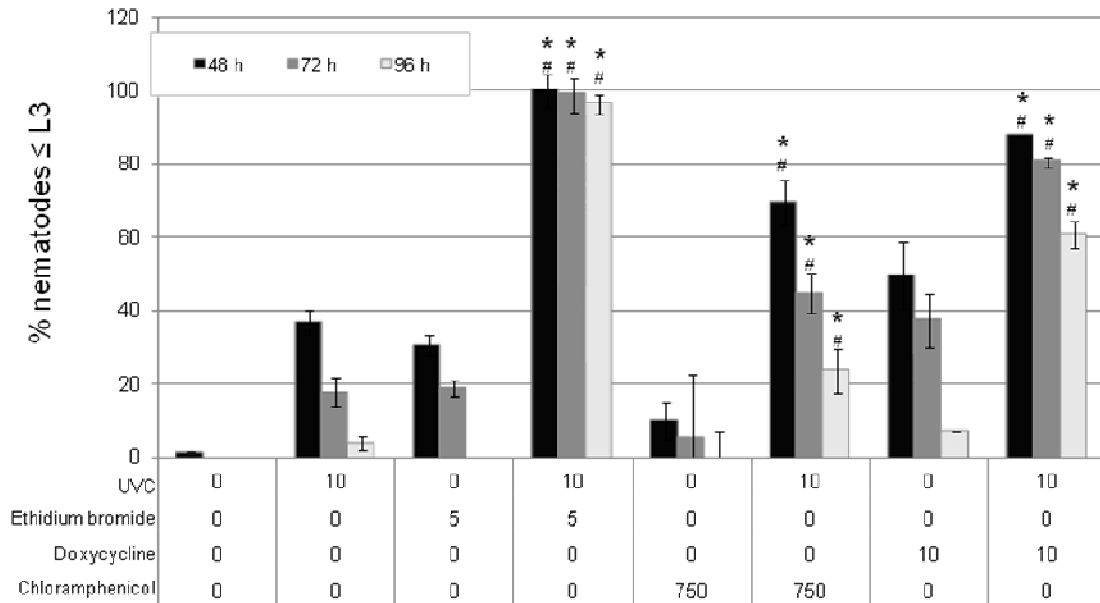


Figure 12: Co-exposure to UVC and mitochondrial replication or translation inhibitors exacerbates L3 arrest.

Co-exposure to UVC (10 J/m²) and ethidium bromide (5 µg/ml), doxycycline (10 µg/ml) or chloramphenicol (750 µg/ml) further exacerbates L3 arrest compared to UVC (asterisks) or chemical (hash) exposure alone at every time point (Fisher’s PLSD, *P* < 0.05). Bars ± s.e.m.

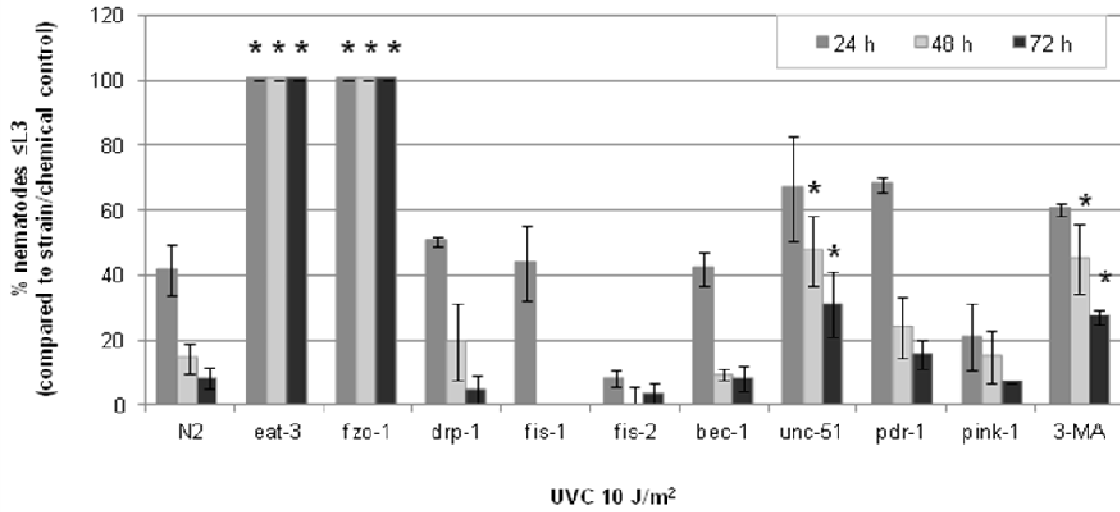


Figure 13: Mutations in fusion and autophagy genes exacerbate L3 arrest following serial UVC exposure.

Mutations in fusion genes *fzo-1* and *eat-3* and autophagy gene *unc-51*, as well as inhibition of autophagy with 3-MA, exacerbated L3 arrest compared to wild-type at 72 and 96 h. Asterisks denote a significantly different effect of treatment on mutant compared to wild-type strain (two-way ANOVA, $p < 0.05$). Bars \pm s.e.m.

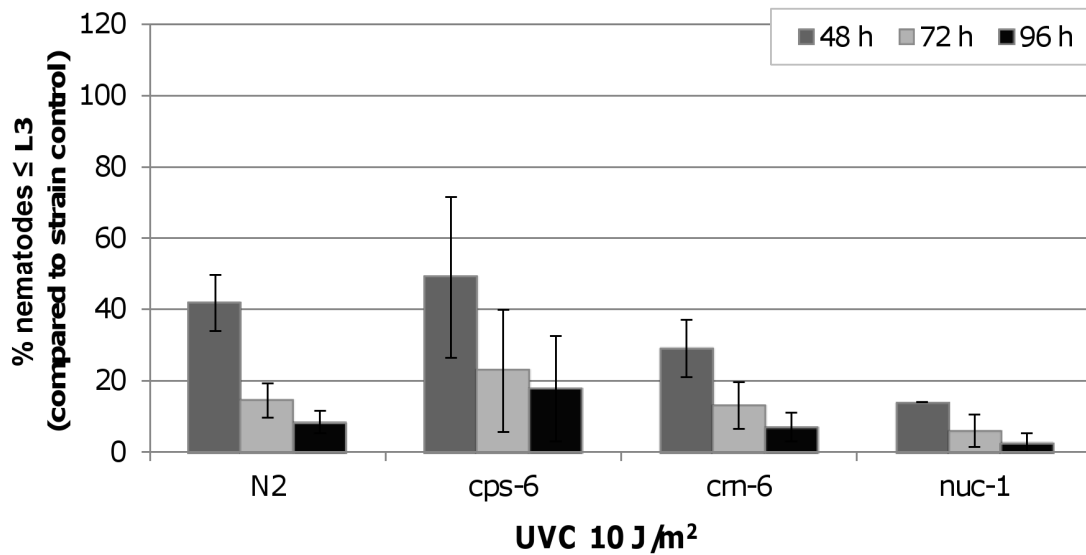


Figure 14: Mutations in endonuclease genes do not exacerbate L3 arrest following serial UVC exposure.

Mutations in endonuclease genes *cps-6* (*C.elegans* homolog to endonuclease G), *cm-6* and *nuc-1* do not exacerbate L3 arrest compared to wild-type at 48, 72 or 96 h. Two-way ANOVA indicated no significant differences in the effect of UVC exposure on larval arrest between mutant and wild-type (Statview 5.0.1). Bars \pm s.e.m.

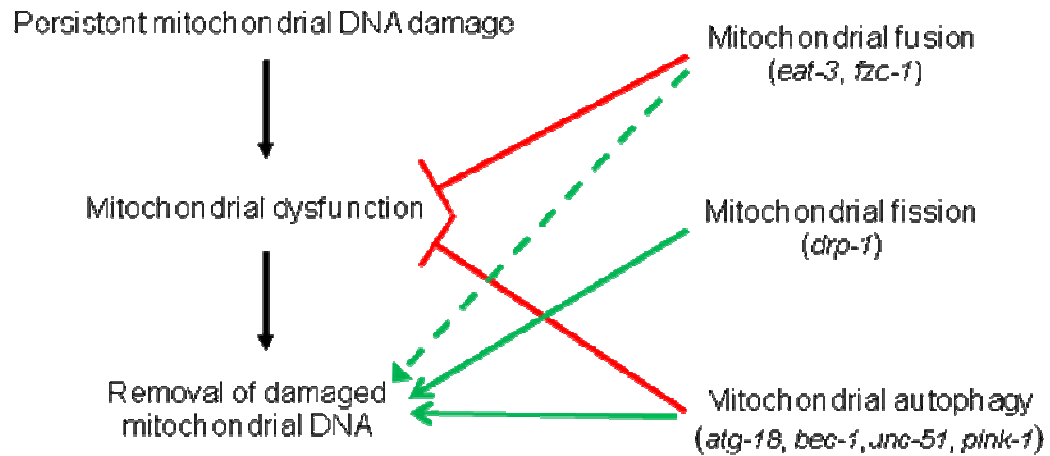


Figure 15: Proposed model of the effect of mitochondrial fusion, fission, and autophagy processes on persistent mtDNA damage-induced mitochondrial dysfunction and removal of mtDNA damage.

Persistent mtDNA damage leads to mitochondrial dysfunction (e.g., reduced ATP levels and larval arrest). Mitochondrial fusion protects against dysfunction, as does autophagy, presumably by promoting functional complementation, mtDNA replication and removal of dysfunctional mitochondria (red solid lines). Mitochondrial fission and autophagy promote mtDNA damage removal (green lines) while mitochondrial fusion is indirectly required for mtDNA damage removal because it is required to preserve basic mitochondrial function and mtDNA replication (dashed green line denotes the indirect effect of fusion on mtDNA damage removal).

3. UVC-induced mitochondrial degradation via autophagy correlates with mtDNA damage removal in primary human fibroblasts

3.1 Introduction

Mitochondria are the site of most energy production within a cell and are key regulators of apoptosis and calcium homeostasis ⁷⁵. Mitochondria contain several hundred copies of their own 16.5 kb genome which encodes for a small subset of mitochondrial proteins including 13 polypeptides that are incorporated into four of the five complexes of the OXPHOS system plus 2 rRNAs and 22 tRNAs, with the remaining proteins encoded by nuclear DNA (nDNA) ⁹⁰. Despite this relatively small contribution, mutations in or depletion of mtDNA are associated with a significant number of inherited mitochondrial diseases which in total are estimated to affect more than 1 in 6,000 people ¹, emphasizing the importance of mtDNA integrity to human health. Significant research also implicates mitochondrial dysfunction and mtDNA mutation in the pathogenesis of widespread disorders such as neurodegenerative conditions ⁵⁻⁸, type 2 diabetes mellitus ⁹, cancer ²⁻⁴ and aging ¹¹.

There is substantial evidence that mtDNA is uniquely susceptible to damage caused by certain ubiquitous environmental genotoxicants including metabolically-activated polycyclic aromatic hydrocarbons ^{26-29, 34, 35} and mycotoxins ^{36, 37}, as well as endogenously produced reactive oxygen species ³⁸. Mitochondria house several

mechanisms to combat oxidative damage including base excision repair, the repair mechanism responsible for repair of most oxidative DNA lesions. However, mitochondria lack nucleotide excision repair (NER), the mechanism necessary to repair helix-distorting chemical adducts and UVC-induced photodimers. Therefore these lesions persist and have the potential to stall DNA replication^{28, 114-117} and transcription^{36, 114} potentially leading to depletion of mtDNA and mtDNA-encoded proteins, mutations and subsequently mitochondrial dysfunction.

Mitochondria and mtDNA are degraded by macroautophagy, the lysosomal-driven degradation of cytoplasmic materials^{57, 168}. It is now well-established that autophagy can selectively degrade dysfunctional mitochondria, referred to as mitophagy, and that this process is dependent in part upon mitochondrial function and morphology and autophagy induction^{57, 58, 176, 177, 188}. Mitochondrial dysfunction resulting from toxicant exposure, mtDNA mutations and ROS can induce autophagy and mitophagy^{63, 64, 180-185} and blocking autophagy and mitophagy results in accumulation of dysfunctional mitochondria and damaged mtDNA^{202, 203} and increased susceptibility to apoptotic cell death^{191, 196, 206}. Therefore, autophagic mitochondrial degradation may serve as an important mechanism to rid the cell of damaged mitochondria that would otherwise trigger apoptosis.

We recently found that UVC-induced mtDNA damage is gradually removed *in vivo* in *Caenorhabditis elegans* and that removal is dependent upon genes involved in

autophagy, mitophagy and mitochondrial dynamics. Additionally, we demonstrated that UVC exposure induces autophagy in *C. elegans*. We hypothesize that UVC-induced DNA damage results in mitochondrial dysfunction resulting in changes in mitochondrial morphology and autophagy induction that result in the removal of damaged mtDNAs. In this work, we investigated the effects of UVC exposure on mitophagy, mitochondrial morphology, and indicators of mitochondrial ETC function. We show that UVC-induced mtDNA damage is removed at a similar rate in primary human fibroblasts as in *C. elegans* and that exposure to UVC induces autophagy within 24 h. Interestingly, significant mitochondrial degradation is not observed until 72 h post exposure. No significant changes in mitochondrial MP, ROS or mitochondrial morphology were observed following UVC exposure. These data further support the idea that persistent mtDNA damage is removed by autophagy; however, future research is needed to elucidate the factors which trigger removal.

3.2 Materials and Methods

3.2.1 Cell Culture, thymidine block, and UVC/Chemical exposures

Primary human skin fibroblasts (CCD-1139sk, ATCC) were maintained in Iscove's Modified Dulbecco's Media supplemented with 10% fetal bovine serum, 5% CO₂, and 5% penicillin/streptomycin at 37°C. We recognize that using a cell culture system to study mitochondrial endpoints is complicated by the tendency of cells cultured in high glucose to utilize glycolysis for energy production rather than

OXPHOS, thus rendering mitochondrial function less critical for cell survival⁸³. We attempted to avoid this by using non-transformed, primary human skin fibroblasts replaced monthly from a low passage frozen stock.

The thymidine block, which was used for all experiments unless otherwise noted, was performed 24 h before analyses on 90% confluent cells by the addition of 3 mM thymidine (final concentration) to IMDM. Thymidine media was replaced every 24 h for the duration of an experiment. For UVC exposure, cells were washed once in PBS, exposed to 10 J/m² UVC using an ultraviolet lamp with built-in UVC sensor (CL-1000 Ultraviolet Crosslinker, UVP, Upland, CA, USA) with peak emission at 254 nm without media; cell culture media was immediately replaced. For flow cytometry analyses, cells were seeded at 75K cells/2 ml of normal growth media with or without thymidine in six-well plates, collected by 0.25% trypsin incubation, spun down and resuspended in FACS buffer (1% BSA in PBS). For chemical exposures, 100 nM bafilomycin A1 (Sigma) resuspended to 32 µM in DMSO and further diluted into culture media was replaced every 24 h for extent of the treatment period.

3.2.2 DNA synthesis analysis

Cells were exposed to UVC with and without 3 mM thymidine in normal growth media and assessed for DNA synthesis by BrdU incorporation at 24, 48 and 72 h post exposure to UVC. Cells were incubated with 10 µM BrdU (BD Biosciences; Cat. No. 550891) for 1 h; and, after collection were fixed in 70% ethanol for at least 2 hours.

Following pelleting at 1500 g for 5 min and resuspension in 1 ml of denaturation solution (2N HCL and 0.5% Triton-X in PBS) for exactly 30 min, cells were pelleted, resuspended in neutralization buffer (0.1 M Na₂B₄O₇) and incubated for 30 minutes. Next, cells were pelleted and incubated in 1ml of blocking solution (0.5% Tween 20 and 1% BSA in PBS) plus 20 µl of anti-BrdU FITC for 30 min at room temperature and then pelleted and washed once in 1 ml of blocking buffer. After resuspension in 0.5 ml of propidium iodide staining solution (100 µg/ml RNase A, 0.05% Triton-X and 50 µg/ml PI in PBS) and incubation for 40 min at 37°C, cells were analyzed for FITC and PI fluorescence simultaneously using a FACScan flow cytometer (Becton Dickinson). FlowJo 7.6.4 was used to identify BrdU positive cells and perform cell cycle analysis. Two biological replicates were analyzed for each treatment at each time point.

3.2.3 Cell Viability

Cells were collected and resuspended in FACS Buffer (1% BSA in PBS) containing 5 µg/ml (final concentration) Hoechst (Life Technologies) and 1:100 Annexin V APC (Life Technologies) and immediately placed on ice. Fluorescence was measured simultaneously using a FACSVantage Sorter (Becton Dickinson) and acquired data was analyzed using FlowJo 7.6.4. Viable, apoptotic and dead cell populations were defined by unstained and Annexin V APC or Hoechst 33258 individually stained cells and the same quadrants were applied to all samples. Four biological replicates were analyzed for each treatment at each time point. Two-way ANOVA was used to compare the total

percentage of apoptotic/dead cells (Q2 + Q3) between treatments and recovery time (Statview 5.0.1).

3.2.4 DNA Damage, removal quantification and quantitative PCR

At each recovery time point, cells were scraped, pelleted, flash frozen, and stored at -80°C until DNA extraction. Genomic DNA was extracted and quantified as described in ²⁸⁴ using the automated extraction procedure. DNA damage analysis was performed using quantitative polymerase chain reaction (QPCR) as described in Furda et al. (2012) ²⁸⁴. This assay relies on the ability of DNA damage to block progression of the DNA polymerase used for PCR; thus, the amount of amplification is inversely related to the amount of DNA damage ^{235, 236}. In each sample, a long (~10 kb) nuclear and mitochondrial genomic region is amplified. The long product is used to calculate lesion frequency as compared to control samples. A short (~200 bp) mitochondrial genomic region is amplified in order to normalize for sample to sample variation in mtDNA copy number. At least two time-separated QPCR reactions were performed on each sample and at least two biological replicates were analyzed per treatment and time point. Significant removal/repair at recovery time points 72 and 96 h was determined by one-way ANOVA (effect of time point) and subsequent Fisher's PLSD (Statview 5.0.1).

3.2.5 Mitochondrial Copy Number Analysis

Relative mtDNA content was measured by quantitative, real-time PCR as described in Venegas and Halberg (2012) ²⁸⁵ using the QPCR samples described above.

Primers are listed in Table 1. For each sample, three technical replicates were averaged from a single real-time PCR run.

3.2.6 Mitochondrial mass, membrane potential, ROS analyses

Cells were stained in 150 nM Mitotracker Green (Life Technologies) for 30 min at 37°C then washed and stained with either 300 nM TMRE (Life Technologies) or 150 nM Mitotracker Red CM-H₂XROS (Life Technologies) for 30 min at 37°C. Cells were collected for FACS analysis as described above. Samples were immediately placed on ice and Mitotracker Green and TMRE or Mitotracker Red CM-H₂XROS fluorescence were simultaneously measured using a FACScan flow cytometer (Becton Dickinson). Viable cells were gated and geometric mean fluorescence values for MTG, TMRE and Mitotracker Red CM-H₂XROS were obtained using FlowJo 7.6.4. TMRE and Mitotracker Red CM-H₂XROS were normalized to mitochondrial mass. 2-4 biological replicates were analyzed per treatment per time point for each fluorophore.

3.2.7 LC3II protein quantification by Western blot

Cells were incubated with or without bafilomycin (100 nM) for 3 hours then collected and lysed in 100 µl of buffer containing 2% Triton-X and complete protease inhibitor cocktail (Sigma) in PBS for 1 h on ice. Protein concentration was measured by BCA assay (Thermo Scientific). Lysates were resolved by 4-12% LDS-PAGE (NuPage 4-12% Bis-Tris Gels) and electrotransferred onto a PVDF membrane. The membrane was blocked for 1 h in 5% milk then incubated overnight in primary antibodies against LC3B

(Novus Biologicals; Cat. No. NB600-1384; 1:2000) and beta-actin (Abcam; Cat. No. ab8224; 1:2000) and for 2 hours in secondary antibodies: anti-rabbit-HRP (Pierce; Cat. No. 32460, 1: 200) and anti-mouse-HRP (Immuno Jackson Research, Cat.No. 115-035-174, 1:2000). The blots were developed using SuperSignal West Pico Chemiluminescent Substrate (Thermo Scientific) and developed on film. Densitometry was performed using ImageJ (1.43m). Each sample was analyzed by Western blot at least twice and 2-4 biological replicates were analyzed per treatment per time point.

3.2.8 RNA extraction, reverse transcription and real-time PCR analysis

Total RNA was extracted with Qiagene RNeasy Mini Kit and quantified by NanoDrop 8000 spectrophotometer (Thermo Scientific/NanoDrop). 250ng of isolated RNA was converted to cDNA using the High Capacity cDNA Reverse Transcription Kit (Cat. No. 4368814) using the manufacturer's instructions and amplified by real time PCR using the 7300 Real Time PCR System (Applied Biosystems), under the following conditions: 2 min at 50 °C, 10 min at 95 °C, 40 cycles of 15 sec at 95 °C and then 60 sec at 60 °C for *18S*, *36B4*, *BECN1*, *COXI*, *COXIV*, *FIS1*, *MAPLC3*, *MFN1*, *NRF1*, *OPA1*, and *TFAM*, at 62 °C for *PGC1α* and at 64 °C for *DRP1*. A dissociation curve was calculated for each sample at the end of each profile. The 25µl PCR reaction contained 12.5µl of SYBR Green PCR Master Mix, 8.5µl H₂O, 2µl of target-specific primers at 400 nM final concentration, and 2µl of cDNA from the RT reaction already diluted to 2 ng/µl. The ABI PRISM 7300 Sequence Detection System Software, Version 1.1 (Applied Biosystems)

was used to carry out data analysis. The average mRNA fold change of each target gene was calculated by comparing the C_T (cycle threshold) of the target gene to that of the housekeeping gene 36B4. All samples were run in triplicate and were averaged prior to analysis. RT-PCR conditions were optimized for previously published and designed primers; the primer sequences and conditions are listed in Table 1.

3.2.9 Mitochondrial and lysosomes colocalization

HF cells were plated in 35 mm collagen coated, glass bottom dishes (MatTek Corporation) in normal growth media plus thymidine. Cells were stained with Mitotracker Green (300 nM) for 30 min, washed and stained with 50 nM LysoTracker Red (Life Technologies) for 30 min. Cells were incubated in 10 μ M leupeptin (Sigma; stock 10 mM in H₂O), 7.5 μ M pepstatin A (Sigma; stock 2 mM in EtOH) and 50 nM LysoTracker red for 1 h. For imaging, media was replaced with Opti-MEM supplemented with 10 μ M leupeptin, 7.5 μ M pepstatin A and 50 nM LysoTracker Red.

Fluorescence imaging was performed using a Leica Sp5 laser scanning confocal microscope with 63x/1.20 NA plan apochromat water immersion objective lens at 37°C. Z-stacks were acquired (0.38 μ m thickness) at 1024 x 1024 resolution and analyzed in 3D for colocalization using Imaris 7.3. Colocalized areas were converted to “surfaces” and the number of surfaces per cell was compared between treatments and time points by two-way ANOVA. Given the significant treatment x time point interaction ($P < 0.0001$), a treatment effect was analyzed by Fisher’s PLSD at each time point.

3.2.10 Mitochondrial morphology analysis

Cells were plated in 35 mm collagen coated, glass bottom dishes (MatTek Corporation) in normal growth media plus thymidine. Cells were stained with Mitotracker Green (300 nM) for 30 min. For imaging, media was replaced with Opti-MEM. Fluorescence imaging was performed using a Leica Sp5 laser scanning confocal microscope with 63x/1.20 NA plan apochromat water immersion objective lens at 37°C. Z-stacks were acquired (0.38 μm thickness) at 1024 x 1024 resolution. Morphometric analyses were based on those in Koopman et al. (2005)²⁸⁶ but with several modifications for 3D analysis. Using Imaris 7.3, green fluorescence intensity was used to build a “surface” representing the mitochondria within a cell. The total number of surfaces per cell was quantified as well as the surface area, volume and sphericity of each surface. Mitochondria were separated in the following categories based on volume: 0-10 μm^3 (class I), 10-100 μm^3 (class II) and ≥ 100 μm^3 (class III) and average inverse sphericity, average surface area/volume and the number of mitochondria were compared between treatments within each class for each time point. At least 20 cells/treatment/time point/experiment were analyzed and two experiments were performed.

3.2.11 Transmission electron microscopy

Cells were plated in six-well plates for 24 h after which they were dosed with UVC 10 J/m². Three hours before collection cells were incubated with or without bafilomycin (100 nM). Cells were collected using trypsinization, pelleted then

resuspended and placed in the initial fixative, 4% paraformaldehyde, 1% glutaraldehyde (45:1G, pH 7.2-7.4) and stored at 4 ° C until time of processing. Primarily fixed cells were then pelleted, placed in secondary fixative, i.e., 1% osmium tetroxide/0.1 M sodium phosphate buffer (pH 7.2-7.4) for 1 h at room temperature. Resultant secondarily fixed cells were dehydrated in graded ethanol solutions and embedded in Spurr's resin. Semithin sections (500 nm thick) were cut with glass knives, mounted on glass slides, and stained with 1% toluidine blue O in 1% sodium borate. These sections served two purposes. First, to determine presence and relative number of fibroblasts in the block face, and secondly to visualize high resolution light microscopic details of the cells (Figure 25). Ultrathin sections (70-90 nm thick) cut with a diamond knife, stained with uranyl acetate and lead citrate, and examined using a FEI/Philips 208S transmission electron microscope (TEM) at 80kV accelerating voltage. All TEM processing, analysis, and imaging were performed at the Laboratory for Advanced electron and Light Optical Methods (LAELOM), College of Veterinary Medicine, North Carolina State University. Cells were selected at random for imaging. Images were taken at 3300X-5600X to capture the entire cell, at 11000X to capture the majority of the cytoplasmic area and finally at 22000X to investigate the contents of AVs within the cell.

3.3 Results

We recently reported that otherwise irreparable UVC-induced mtDNA damage is removed slowly in adult *C. elegans*, detectable within 72 h, and that this removal is

dependent on autophagy, mitophagy, and mitochondrial dynamics. The goal of this work was to test if removal would also be detectable in a mammalian cell culture system, and elucidate the effect of UVC exposure on mitophagy and mitochondrial function and dynamics. A cell culture system was utilized to address these goals because of the ease of mitochondrial and autophagy visualization via fluorescence and electron microscopy and availability of high-throughput technologies such as flow cytometry (FACS) to analyze mitochondrial function.

3.3.1 UVC-induced mtDNA damage is removed slowly

First, we sought to determine if removal of UVC-induced photodimers in mtDNA occurred at a similar rate in primary human fibroblasts as it does in *C. elegans*. Most studies in cell culture have shown the persistence of bulky adducts and UVC-induced photodimers up to 48 h^{116, 246, 247} but further time points have not been investigated. One challenge associated with examining later time points is the potential confounding effect of cell replication on removal quantification due to mtDNA damage dilution. Although mtDNA replication is not dependent on the cell cycle, we wanted to minimize any effect of dilution and so blocked nDNA synthesis with excess thymidine (3 mM), a method referred to as a thymidine block²⁸⁷. A thymidine block arrests cells in S-phase and has been extensively utilized to synchronize cell cultures. BrdU incorporation and propidium iodide-based cell cycle analysis were utilized to test for the effectiveness of the thymidine block. In Figure 16a, the cell cycle profile of 90% confluent

cells without the thymidine block displays a typical cell cycle distribution with most cells in G0/G1 (76%)²⁸⁸. Addition of excess thymidine for 24 h arrested the majority of cells at the beginning of S-phase (Figure 16b). At confluency, nDNA synthesis is very low (~4% of cells positive for BrdU incorporation; Figure 16c) and addition of excess thymidine significantly blocked nDNA synthesis with <1% of cells positive for BrdU incorporation (Figure 16d). At 48 and 72 h after seeding, nDNA synthesis is minimal with or without excess thymidine, presumably due to 100% confluency (Figure 16e).

In thymidine blocked cells, we measured UVC-induced DNA lesions in mitochondrial and nuclear DNA at 0, 72 and 96 h post exposure (10 J/m²). As shown in Figure 17a, mtDNA damage was reduced by ~40 % by 72 h and ~60 % by 96 h. There was a nonsignificant trend towards more mtDNA damage removed without the thymidine block. Additionally, the thymidine block did not inhibit nDNA repair (Figure 17a) which was repaired to baseline by 72 h (earlier timepoints were not examined) nor did it inhibit mtDNA replication (Figure 17b). In order to ensure that loss of damage was not the result of cell death, we measured cell viability via FACS analysis of Annexin V APC and Hoescht 33258 cell uptake. Annexin V APC is an indicator of early apoptosis and Hoescht 33258 is an indicator of cell death. Lack of a significant increase in the proportion of cells positive for the above markers in control or treated cells led us to conclude that cell viability was not diminished at 24, 48 or 72 h post exposure (Figure 17c-d).

3.3.2 Autophagy is induced by UVC exposure within 24 h

The half-life of mtDNA is estimated to be 2-4 days^{165, 166, 167}. Therefore, the removal of damaged mtDNA that we observed may reflect natural turnover rather than the result of induced degradation via autophagy. Increased conversion of microtubule-associated protein 1 light chain 3 (LC3) to LC3II upon phosphatidylethanolamine conjugation is commonly used as an indicator of autophagy²⁸⁹. We measured LC3II protein in control and UVC exposed cells. LC3II was significantly lower in UVC exposed cells compared to controls at each time point (Figure 18a); however, these data reflect the steady-state level of LC3II protein which results from both formation and degradation of the LC3II. Addition of bafilomycin prevents autophagosomal and lysosomal fusion and allows for the measurement of LC3II production specifically (i.e., autophagic flux)²⁹⁰. UVC exposed cells had significantly higher LC3II production compared to control samples indicating that lower steady state LC3II in UVC exposed cells is the result of rapid LC3II degradation and that autophagy is induced. Gene expression of *MAPLC3* and *BECN1*, which encodes for the autophagy protein BECLIN1 required in the early stages of autophagosomes nucleation, were measured. In accordance with the protein data, we observed a small but significant 1.3 fold induction in *MAPLC3* expression (Figure 18b); however, there was no significant change in the expression of *BECN1*.

3.3.3 No change in mitochondrial mass or mtDNA content

Mitochondrial mass can serve as an indicator of both mitochondrial biogenesis and degradation. To determine if the increase in autophagy increased mitochondrial degradation, mitochondrial mass was quantified in control and UVC exposed cells at 0, 48 and 72 h post exposure using the mitochondrial selective dye Mitotracker Green (MTG). MTG selectively accumulates in mitochondria independent of mitochondrial MP and is commonly used to measure mitochondrial mass^{291, 292}. While there was a significant increase in mitochondrial mass with time, there was no significant difference between control and UVC exposed cells at any time point (Figure 19a). As described above, mtDNA content did not change significantly over the course of these experiments (Figure 17b). This suggests that mitochondrial and mtDNA degradation is balanced by mitochondrial biogenesis and mtDNA replication.

To further explore a potential biogenic response, we measured the expression of genes that regulate biogenesis including peroxisome proliferator-activated receptor gamma coactivator 1 α (*PGC1 α*), nuclear respirator factor 1 (*NRF1*) and mitochondrial transcription factor A (*TFAM*), as well as genes regulated by this pathway: mitochondrial proteins cytochrome c oxidase subunit IV (*COXIV*) and COX subunit I (*COXI*). *PGC1 α* regulates both mitochondrial biogenesis and mtDNA replication through enhanced *NRF1* expression and transcriptional activity^{99, 100}. *TFAM*, the downstream target of *NRF1*, is essential for mtDNA stability and directly influences

mtDNA copy number^{101, 293}. *COXIV* and *COXI* expression are mediated by PGC-1 α ²⁹⁴. We observed statistically significant changes in *NRF1* and *TFAM* gene expression over 48 h but these were few and small (Figure 19b). These data indicate that mitochondrial biogenesis was not dramatically induced or repressed by 10 J/m² UVC exposure.

3.3.4 Increased lysosomal degradation of mitochondrial at 72 h post exposure

Given that mitochondrial mass and copy number were not affected by UVC exposure, we questioned whether increased autophagy resulted in increased mitochondrial degradation. To evaluate this, lysosomal degradation of mitochondria was captured via live-cell fluorescence microscopy. LysoTracker Red (LTR; 50 nM) and MTG (300 nM) stained cells were incubated with protease inhibitors, leupeptin and pepstatin A, to prevent mitochondrial degradation within the lysosomes. Colocalization of lysosomes and mitochondria was quantified using Imaris Colocalization. In UVC exposed cells, the number of colocalized spots was significantly lower at 24 h, returned to control level by 48 h and was significantly higher at 72 h (Figure 20). This indicates that initially mitochondrial degradation is reduced following UVC exposure but gradually increases to exceed baseline mitochondrial degradation by 72 h.

3.3.5 No significant change in mitochondrial ROS production or membrane potential

Others have demonstrated that targeting of mitochondria for degradation can be mediated by mitochondrial MP and ROS. We tested whether UVC exposure affected

mitochondrial MP or level of mitochondrial ROS considering that later onset of dysfunction may account for the later onset of mitochondrial degradation at 72 h. FACS analysis of tetramethylrhodamine ethyl ester (TMRE) and Mitotracker Red CMH₂XROS fluorescence were employed. TMRE selectively accumulates in mitochondria based on membrane potential and is widely used for mitochondrial labeling and MP quantification ²⁹⁵. Of the available fluorescent ROS indicators, Mitotracker Red CMH₂XROS has been shown to be the most mitochondrial specific and exhibits relatively high sensitivity ²⁹⁶. Compared to control, there was no significant change in MP or mitochondrial ROS in UVC exposed cells at any time point (Figure 21), after normalizing to total mitochondrial mass. These data indicate that it is unlikely that autophagy was induced by decreased MP or increased ROS production.

3.3.6 Mitochondrial morphology is not affected by UVC exposure

Slow-onset or low level mitochondrial dysfunction can trigger mitochondrial fusion which restores function ^{47, 51, 53, 54, 157-159} and in many cases inhibits degradation ^{62, 189, 190}. We considered that increased mitochondrial interconnectivity may mask low level dysfunction caused by UVC treatment and modulate mitochondrial degradation. Therefore, mitochondrial morphology was analyzed in both treatments at all time points via live-cell fluorescence microscopy and MTG staining. Morphometric analysis was based on Koopman et al. (2005) ²⁸⁶ but several modifications were made for 3D analysis. 3D reconstruction of the mitochondrial network was performed with Imaris 7.3 resulting

in construction of a 3D representative “surface” (Figure 22). To evaluate the effect of UVC on mitochondrial interconnectivity and elongation, the number of surfaces (i.e., mitochondria) per cell as well as the inverse sphericity and surface area/volume ratio of each surface were compared between treatments. Inverse sphericity acts as a measure of both elongation and branching (1=perfect sphere)²⁸⁶. Surface area/volume ratio decreases with size but, within a specific size range, increases with elongation and branching. Size distribution among the mitochondrial population of each cell is heavily skewed toward small mitochondria such that taking the average of these morphology parameters per cell does not accurately represent the morphological variation of the mitochondrial population and reduces the sensitivity to detect slight treatment differences (Figure 22). Therefore, we chose to classify mitochondria by volume (size) into the following groups: 0.1-10 μm^3 (Class I), 10-100 μm^3 (Class II) and <100 μm^3 (Class III) and the number of mitochondria, average surface area/volume and average inverse sphericity were quantified per class for each cell.

Figure 23a displays the average number of mitochondrial per cell within each class for each treatment and time point. There was initially a decrease in the number of mitochondria per cell in UVC treated cells at 24 h. This reflected primarily a decrease in class I and II mitochondria therefore there were less small mitochondria. This could result from an increase in mitochondrial fusion or fewer mitochondria. However, as shown above, mitochondrial mass was unaffected by UVC exposure. At later time

points, there was no significant effect of UVC on the total number of mitochondria per cell or the size distribution of mitochondria. UVC exposure did not significantly affect mitochondrial elongation or interconnectivity as measured by inverse sphericity or surface area/volume ratio at any time point within any class (Figure 23b). Therefore, we concluded that there was not a significant change in mitochondrial morphology in UVC treated cells.

We also addressed the gene expression of *MFN1*, *OPA1*, *DRP1* and *FIS1* which encode for the proteins necessary for mitochondrial fusion and fission. At 6 hr post UVC exposure, *OPA1*, *MFN1* and *DRP1* gene expression were significantly reduced (-1.5, -1.6 and -1.4 fold, respectively; Figure 23c). A reduction in both fusion and fission gene expression could reflect an overall decrease in mitochondrial dynamics and this would have minimal effects on mitochondrial morphology since it reflects the balance between fusion and fission. At 24 hr, endogenous expression was restored in all cases and by 72 hr post exposure, expression of *DRP1* and *OPA1* genes was elevated, significantly so in the case of *DRP1*.

3.3.7 Mitochondrial degradation via autophagy increases during recovery

The mitochondrial/lysosomal colocalization data described above suggests that mitochondrial degradation increases at 72 h post exposure. While this approach provides detailed 3D data it does not lend information regarding the specificity of the degradation process (autophagy vs. mitophagy). Therefore, we next investigated this

using TEM which allows for the visualization of autophagic vacuoles and differentiation of their specific contents. In order to capture autophagosomes and their contents prior to degradation, bafilomycin was added three hours before cell fixation to inhibit fusions of autophagosomes and lysosomes.

As shown in Figure 24A, control cells without bafilomycin contained several autophagic vacuoles (AV) resembling multivesicular endosomes (MVE). Mitochondria in these cells were numerous, well-defined and dense. As expected, AVs representing multiple stages of autophagy including MVE, early and late autophagosomes and lysosomes were present in bafilomycin treated cells. The occurrence of AVs containing recognizable mitochondria was low in control cells and mitochondria in bafilomycin-treated control cells were less dense and had less defined cristae (Figure 24B). In UVC exposed cells mitochondrial ultrastructure was variable ranging from long, dense mitochondria with well-defined cristae to rounded, enlarged mitochondria with less well-defined membranes and cristae (Figure 24C-H). In two cases, mitochondria in UVC exposed cells revealed a focal area of low electron density signifying swelling of the matrix (Figure 24D, F). There was an increasing trend toward occurrence of AVs containing mitochondria at 48 and 72 h post exposure (Figure 24E, H). Of these, many contained other cytoplasmic components. Additionally, there were several AVs without mitochondria that contained general cytoplasmic contents such as glycogen and

membranous tubules. These observations support a UVC-induced increase in non-specific autophagy leading to increased mitochondrial degradation later in recovery.

3.4 Discussion

mtDNA is susceptible to helix-distorting DNA lesions induced by common environmental agents like polycyclic aromatic hydrocarbons, mycotoxins and UV radiation in part because mitochondria lack NER, the mechanism utilized in the nucleus to repair these lesions. Persistence of these lesions in mtDNA has the potential to cause mtDNA instability and mitochondrial dysfunction. Turnover of mitochondria as well as other organelles and cytoplasmic contents is facilitated by autophagy. Autophagy is an important mechanism by which the cell can rid itself of damaged cellular materials and recycle macromolecules. Specific degradation of dysfunctional mitochondria via mitophagy has been illustrated at the level of the mitochondrion and entire mitochondrial population. We recently demonstrated that autophagy was necessary for removal of damaged mtDNA containing UVC-induced photodimers *in vivo*. We also found that recovery from mitochondrial dysfunction caused by accumulated UVC-induced mtDNA damage was mediated by autophagy and mitochondrial fusion. In the present study, we further investigated the effects of UVC exposure on autophagy, mitophagy and mitochondrial function using a mammalian cell culture model.

In adult *C. elegans* ~40% of UVC-induced mtDNA damage was removed within 72 h of exposure. We induced a similar number of mtDNA lesions in non-replicating

(arrested in S-phase) primary human fibroblasts and found that damage removal occurred at a similar rate with ~40% removal by 72 h post exposure. This suggests that the kinetics of removal are conserved between lower eukaryotes and mammals at least in non-replicating cells.

We and others ¹⁹¹ have found that UVC exposure induces autophagy. This was also the case here as shown by increased LC3 expression and LC3II formation. Interestingly, our data suggest that mitochondrial degradation is initially inhibited at 24 h post exposure despite elevated autophagy but recovers and exceeds control level by 72 h. Despite the correlation between the rate of mitochondrial degradation and the rate of damage removal, we can not know with certainty that autophagy is removing damaged mtDNA without inhibiting autophagy. Autophagy inhibition was attempted with 3-methyladenine (3-MA), an inhibitor of autophagosomes formation ²⁵⁶, but there was significant loss of cell viability after 24 h in 3-MA highlighting the importance of autophagy in maintaining cell survival. We also attempted to investigate UVC-induced mtDNA damage removal in mouse embryonic fibroblasts with mutations in autophagy genes; however, wild-type MEFs proved especially sensitive to low-level UVC exposure with cell death observed within 24 h of exposure to $< 5 \text{ J/m}^2$.

A disconnect between induction of autophagy and mitochondrial degradation has recently been reported by others ¹⁷²⁻¹⁷⁴. During autophagy induced by amino acid starvation, degradation of cytoplasmic materials was ordered with mitochondrial

degradation occurring 30 h into starvation, subsequent to the degradation of cytosolic and proteasomal proteins and ribosomes within 12 hr of starvation ¹⁷². This lag time was attributed to enhanced mitochondrial elongation resulting from unopposed fusion due to reduced DRP1 activity ^{173, 174}. Interestingly, at 24h when mitochondrial degradation was suppressed, there was a corresponding decrease in smaller sized mitochondria suggesting increased fusion. However, mitochondrial elongation and interconnectivity at 24 h were not affected by UVC exposure at least at the level that we could detect with our morphological parameters. Thus an exciting future direction of this research is to investigate directly the effect of UVC on fusion and fission events.

UVC exposure in this system induced approximately one lesion per 10 kb or 1.6 lesions per genome. ~20% of mtDNA genomes are predicted to remain undamaged at this UVC dose assuming a Poisson distribution of lesions and a similar mtDNA copy number per cell. Despite greater than 80% of mtDNAs containing at least one lesion, the effects of this damage appear to be within the compensatory range of the mitochondrial population such that mtDNA damage was removed with no significant perturbation of mitochondrial mass, mtDNA content, MP or the level of ROS. Mitochondrial fusion maintains homogeneity of contents among the mitochondrial population ^{137, 141, 155}. However, Twig et al. (2008) demonstrated that following mitochondrial fission one of the daughter mitochondria is often hypopolarized and unable to undergo subsequent fusion if the MP does not recover ⁶². It is therefore likely that mtDNAs harboring UVC-

induced photodimers are distributed randomly and unequally during fission events rendering a subset of mitochondria with a higher proportion of damaged DNA and potentially significantly compromised mitochondrial function. FACS analyses of MP and ROS performed here reflect an average among the entire mitochondrial population of the cell; thus, effects in a subset of mitochondria cannot be ruled out. In fact, the variability in mitochondrial ultrastructure observed in UVC treated cells by TEM suggests that UVC exposure may have compromised a subset of mitochondria within the overall mitochondrial population.

Dysfunctional mitochondria unable to undergo fusion are preferentially removed by autophagy⁶². We observed an increasing trend in AVs containing mitochondria in UVC treated cells at 48 and 72 h post exposure, some of which appeared to contain only mitochondria while others contained mitochondria and other cytoplasmic materials. We also observed several AVs without mitochondria that contained general cytoplasmic materials at these time points. Therefore, non-specific autophagy rather than more specific mitophagy appears to be mediating mitochondrial degradation following UVC exposure. Even so, it is still unclear even in non-specific autophagy how mitochondria are selected for degradation and recent research suggests that there is some level of selectivity. For example, mitochondrial degradation during starvation-induced autophagy is dependent upon the mitochondrial permeability transition (MPT)¹⁷⁵ and can be enhanced by mutations that result in mitochondrial

dysfunction¹⁷⁴. Therefore, we can not rule out the possibility that dysfunctional mitochondria may be degraded preferentially thus facilitating mtDNA damage removal. In future experiments, identification of AVs and their contents could be assisted by the use of antibodies that label specific organelles, autophagic vacuoles and lysosomes. Additionally, identification and use of a positive control for mitophagy would help to distinguish mitochondrial degradation resulting from mitophagy versus general autophagy.

Given that autophagy was increased within 24 h of exposure to UVC without detectable changes in mitochondrial MP or ROS, nDNA damage signaling may be responsible for this response. UVC-induced photodimers in nDNA activate the DNA damage responsive gene *ATR*²⁹⁷. *ATR* can also activate another DDR gene, *ATM*, typically associated with the response to double strand breaks^{298, 299}. Activation of *ATM* or *ATR* as well as their downstream target *p53* increases autophagy³⁰⁰⁻³⁰² and *ATM*-deficient cells exhibit defective mitophagy³⁰³. However, Chen et al. (2012) recently demonstrated that autophagy induction following UVC exposure is *ATR* dependent up to 6 h but is *ATR* independent at 24 and 48 h¹⁹¹. Clearly, an effect of nDNA damage on mitochondrial fate cannot be ruled out even though this damage is repaired relatively quickly. Further research is needed to understand the role of nDNA damage responsive genes in mediating mitochondrial turnover by autophagy and mitophagy.

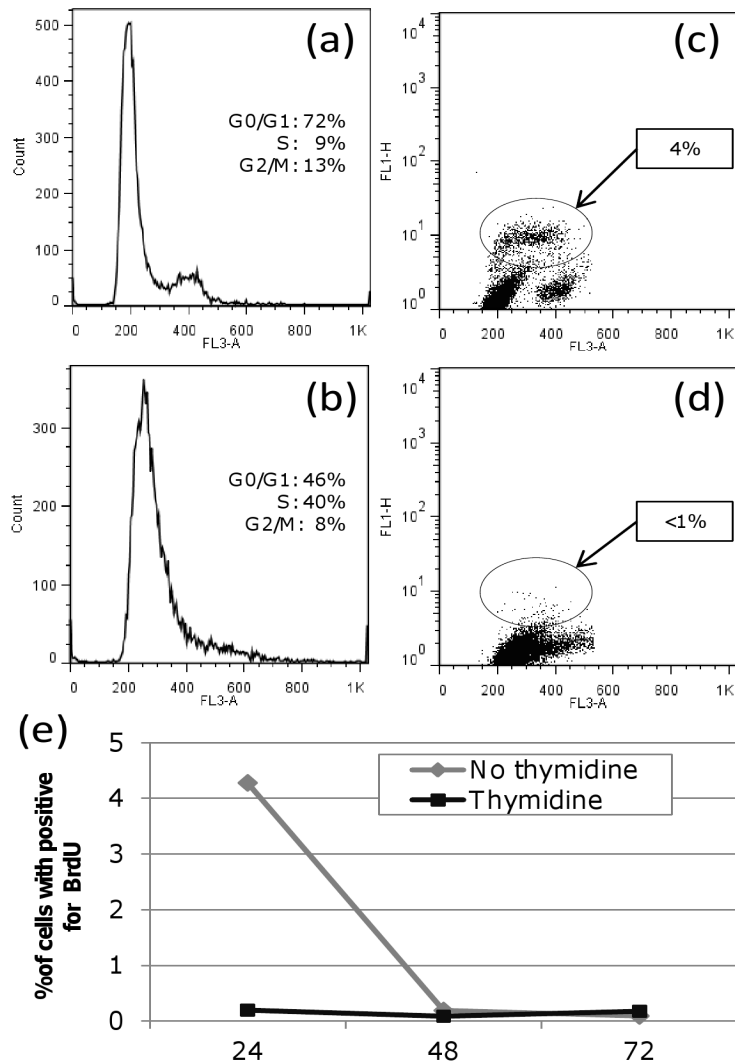


Figure 16: Excess thymidine arrests cells in S-phase and blocks nDNA synthesis within 24 h.

Cell cycle analysis using PI in (a) untreated and (b) thymidine treated cells. 86% of thymidine treated cells are arrested at G0/G1 or S-phase. BrdU incorporation over an hour incubation period was measured in (c) untreated and (d) thymidine treated cells. Confluent untreated cells have a low level of DNA synthesis (4% of cells positive for BrdU incorporation) 24 h after seeding with further reductions in DNA synthesis at later timepoints presumably due to 100% confluency. (e) Thymidine treatment blocked DNA synthesis at 24-72 h.

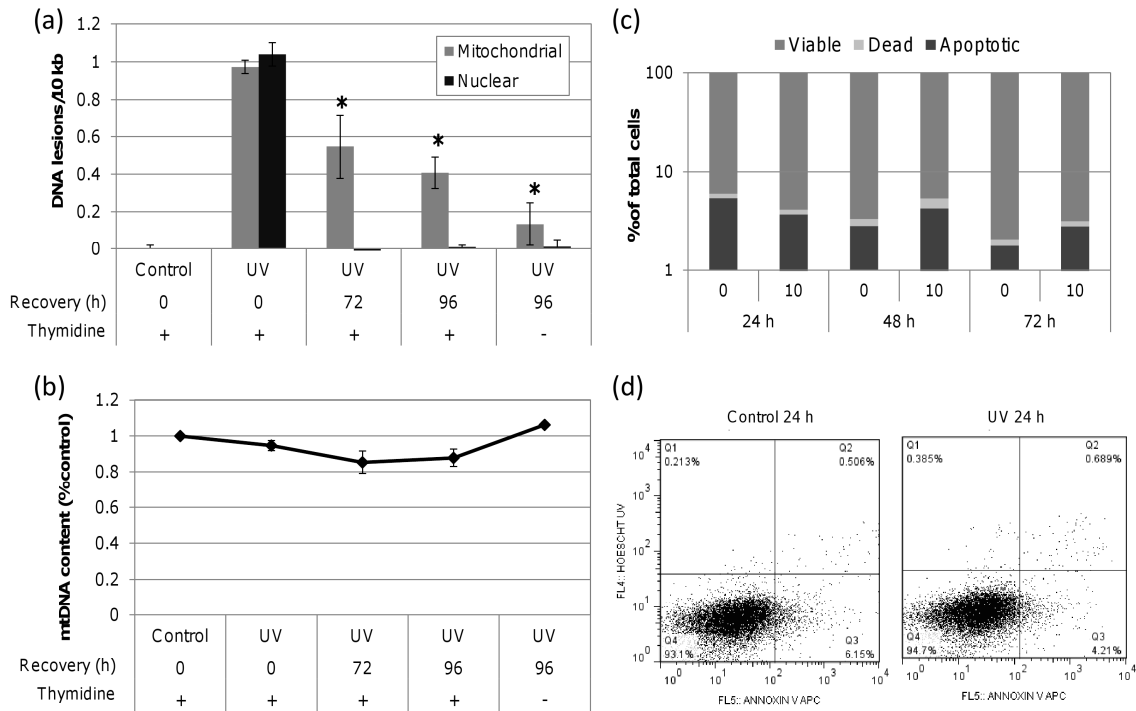


Figure 17: UVC-induced mtDNA damage is removed slowly.

(a) Significant mtDNA damage removal was observed in cells dosed with 10 J/m² UVC by 72 h compared to initial lesion frequency (one-way ANOVA, effect of time point $P = 0.0140$; Fisher's PLSD, $P = 0.0316$ for 72 h and $P = 0.0047$ for 96 h). nDNA damage was repaired to baseline by 72 h. (b) mtDNA content was comparable to control throughout the recovery period. (c) No significant decrease in cell viability was observed in cells exposed to 10 J/m² as measured by Annexin V APC and Hoechst 33258. (d) Representative control and UVC dot plots at 24 h post exposure as measured by FACS with viable (Q4), apoptotic (Q3) and dead (Q2) cell frequencies defined. Bars \pm s.e.m.

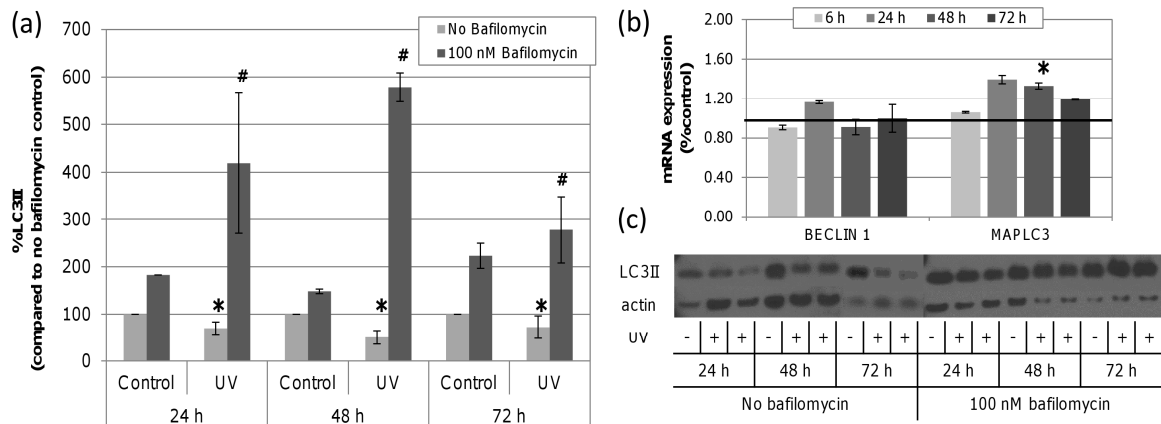


Figure 18: UVC exposure increases LC3II expression.

LC3II protein was quantified by Western blot in control and UVC treated cells with and without bafilomycin and normalized to beta-actin. (a) Steady-state (no bafilomycin) levels of LC3II were significantly decreased by UVC exposure at 24, 48 and 72 h when compared to time point controls (asterisks; two-way ANOVA, effect of treatment $P = 0.0325$). With bafilomycin, UVC exposed cells accumulated more LC3II compared to bafilomycin treated controls at all time points (hash; two-way ANOVA, effect of treatment $P = 0.007$). (b) *MAPLC3* mRNA expression increased by 1.3 fold with UVC exposure 48 h after exposure (asterisks; two-way ANOVA, treatment \times time point $P = 0.03$; Fisher's PLSD, effect of treatment $P < 0.0424$ at 48 h). No significant change in *BECN1* expression was observed in UVC treated cells. The black line signifies baseline expression level. (c) Representative immunoblots of LC3II in control and UVC (10 J/m²) exposed cells with and without bafilomycin at 24, 48 and 72 h. Bars \pm s.e.m.

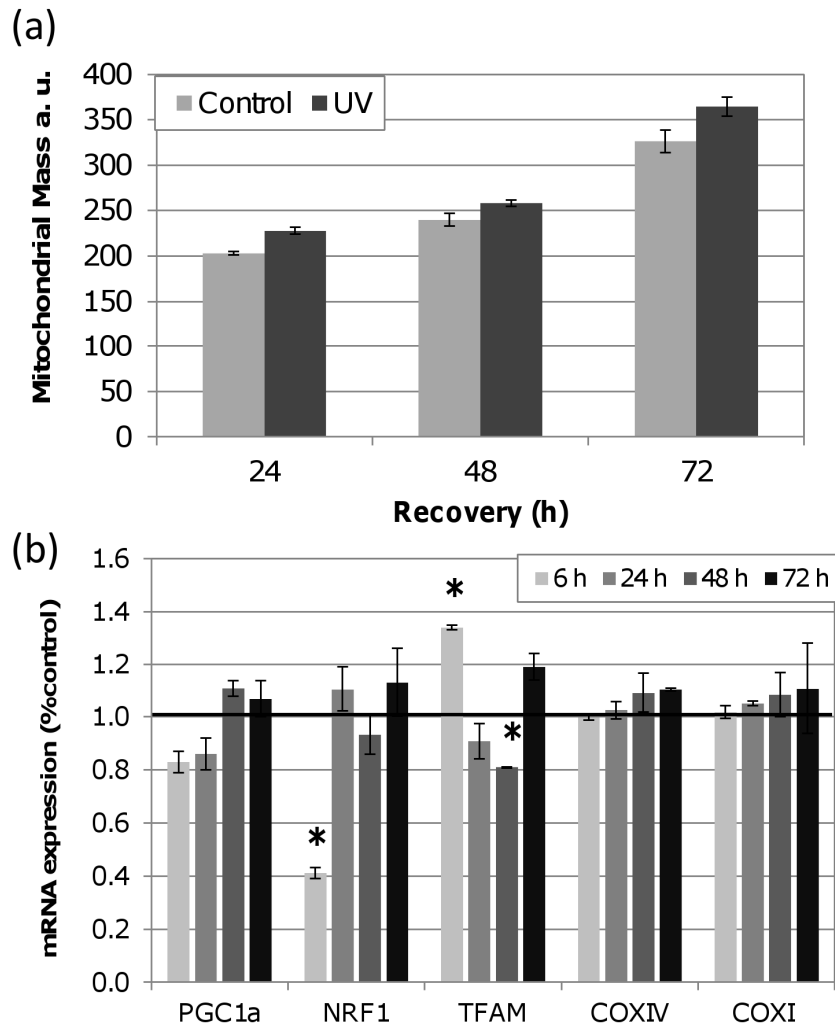


Figure 19: No detectable changes in mitochondrial mass or biogenesis.

(a) No significant change in mitochondrial mass was detected after UVC exposure compared to controls (two-way ANOVA, effect of recovery $P < 0.0001$, treatment \times recovery $P = 0.4730$). (b) mRNA expression of *PGC1a*, *NRF1* and *TFAM*, both involved in mitochondrial biogenesis, and their downstream targets *COXIV* and *COXI*. *NRF1* expression decreased at 6 h ($P = 0.0466$). *TFAM* expression was induced 1.3 fold at 6 h but reduced by -1.20 fold by 48 h (two-way ANOVA, treatment \times time point $P = 0.01$; Fisher's PLSD, effect of treatment $P < 0.05$ at 6 and 48 h). No significant affect of UVC exposure on expression of *COXIV* or *COXI* was observed. The black line signifies baseline expression level. Bars \pm s.e.m.

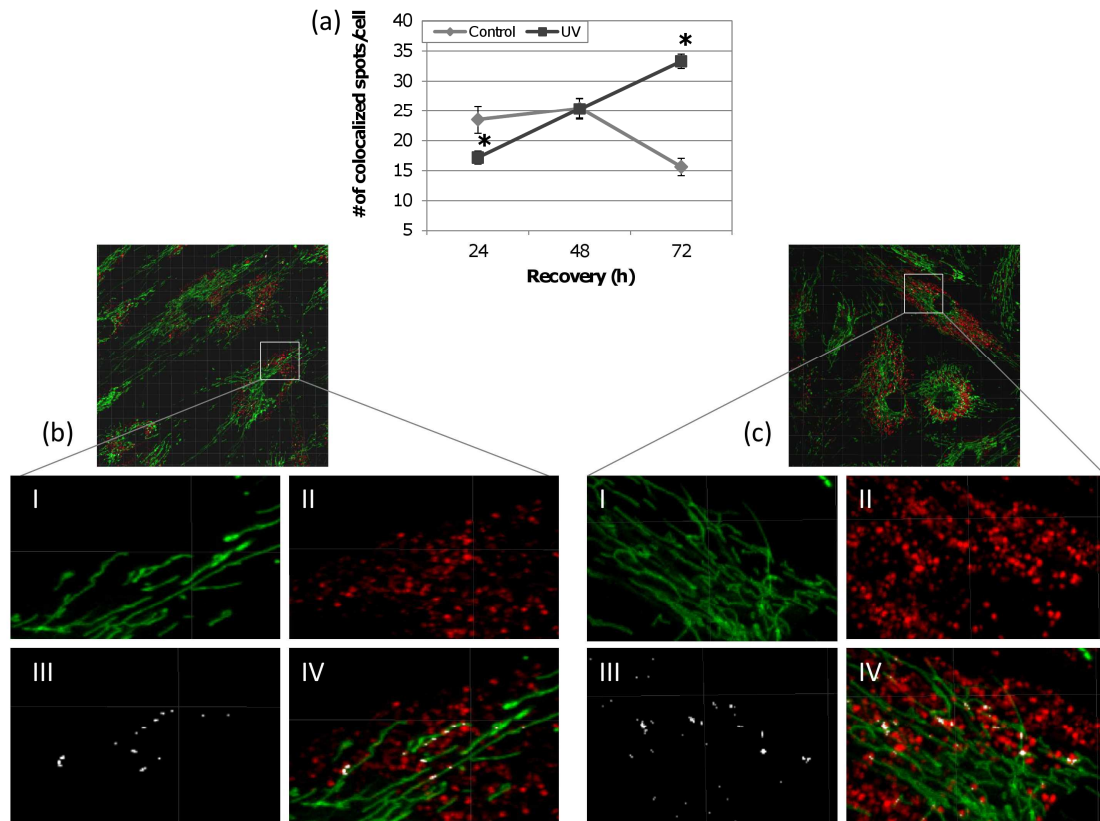


Figure 20: Increased lysosomal degradation of mitochondria after exposure to UVC.

(a) The number of colocalized spots between mitochondria and lysosomes was initially lower at 24 h but significantly exceeded that of control by 72 h (two-way ANOVA, treatment \times time point $P < 0.0001$; Fisher's PLSD, effect of treatment at 24 h $P = 0.0068$ and 72 h $P < 0.0001$). Representative images displaying (I) MTG stained mitochondria, (II) LTR stained lysosomes, (III) colocalized spots and (IV) an overlay of all three as detected by Imaris 3D colocalization analysis in (b) control and (c) UVC treated cells. Bars \pm s.e.m.

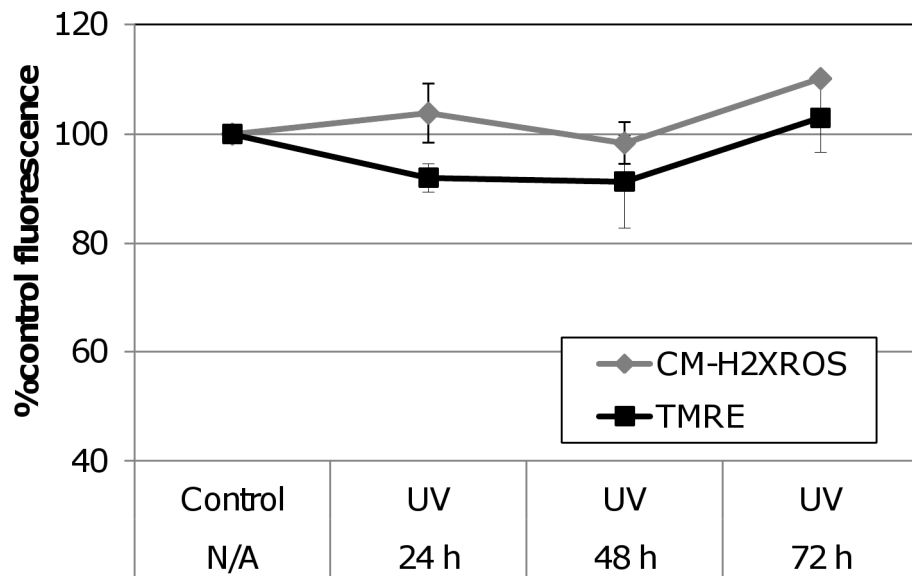


Figure 21: No detectable changes in mitochondrial MP and ROS level

UVC exposure did not induce detectable changes in mitochondrial MP or ROS level at any time point (two-way ANOVA, treatment x recovery for TMRE and CM-H₂XROS $P = 0.2086$ and 0.7312 , respectively). Bars \pm s.e.m.

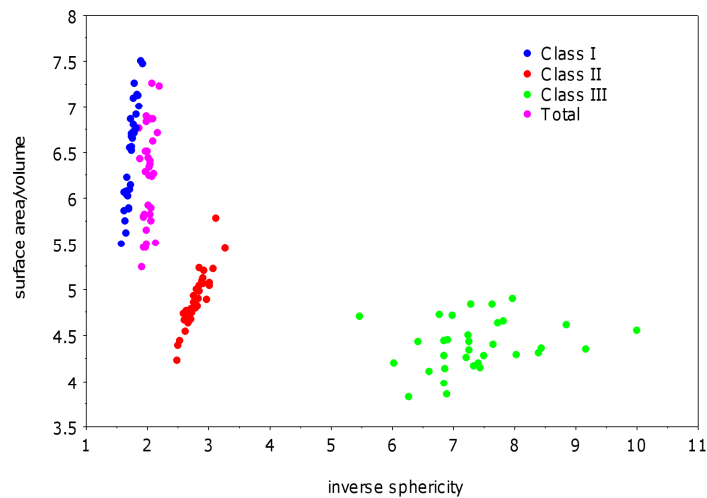
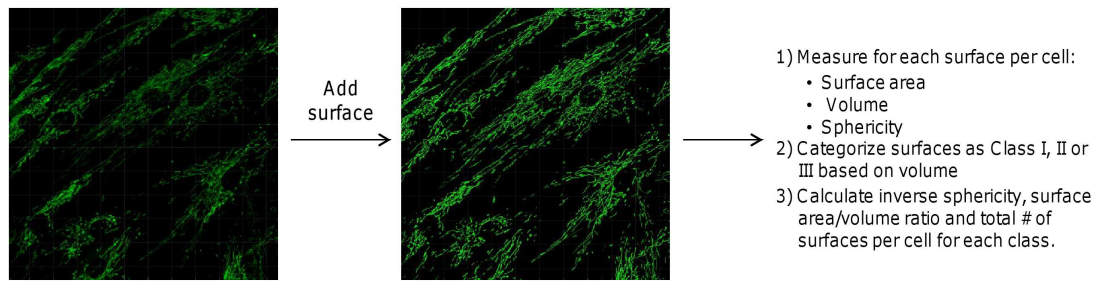


Figure 22: Mitochondrial morphology analysis method.

Mitochondrial were labeled with MTG and captured via live-cell fluorescence imaging on a Leica SP5 laser scanning confocal microscope. Z-stacks at 0.38 μm thickness were taken at 1024 \times 1024 resolution and imported into Imaris 7.3. A representative surface of the mitochondrial network was generated. For each surface the surface area, volume and sphericity was measured. Surfaces were then categorized by volume into three classes: Class I (0-10 μm^3), Class II (10-100 μm^3) and Class III ($\geq 100 \mu\text{m}^3$). Average surface area to volume ratio, inverse sphericity and total number of surfaces were calculated for each class. The scatterplot comparing inverse sphericity to surface area/volume indicates that expressing the average of these parameters in all surfaces (total, pink dots) without volume classification does not accurately represent the variation in the mitochondrial population of each cell. Classes I, II and III (blue, red and green dots, respectively) show distinct relationships between morphology parameters. Therefore, categorizing allows for the identification of treatment-induced shifts in size distribution as well as elongation and interconnectivity.

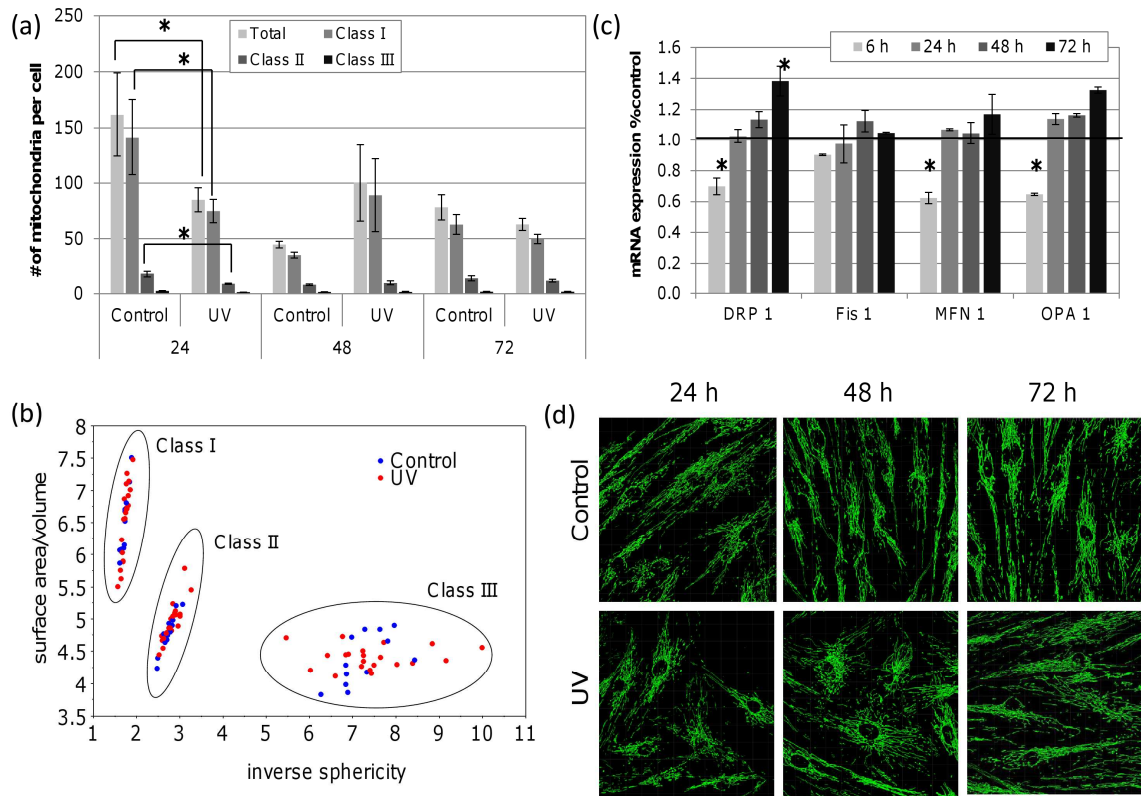


Figure 23: No detectable change in mitochondrial number or mitochondrial morphology in UV exposed cells.

(a) The total number of mitochondria per cell was decreased 24 h after UVC exposure (two-way ANOVA, treatment \times time point $P = 0.0143$; Fisher's PLSD, effect of treatment at 24 h in $P = 0.0345$), particularly in class I and II sized mitochondria (three-way ANOVA, treatment \times time point \times class $P = 0.0034$, two-way ANOVA per class, treatment \times time point $P < 0.05$; Fisher's PLSD effect of treatment at 24 h $P < 0.05$). By 48 h mitochondrial number and size distribution had returned to control levels. (b) Scatterplot displaying the average surface area/volume as compared to the average inverse sphericity of mitochondria in each size class. Mitochondrial interconnectivity and elongation (inverse sphericity or surface area/volume) were not affected by UVC exposure at any time point in any class (three-way ANOVA, treatment \times time point \times class $P > 0.05$). (c) A small but significant ~40 % reduction in *DRP1*, *MFN1* and *OPA1* expression was observed within 6 h of UVC exposure. (d) Representative images of control and UVC exposed mitochondria stained with MTG. Bars \pm s.e.m.

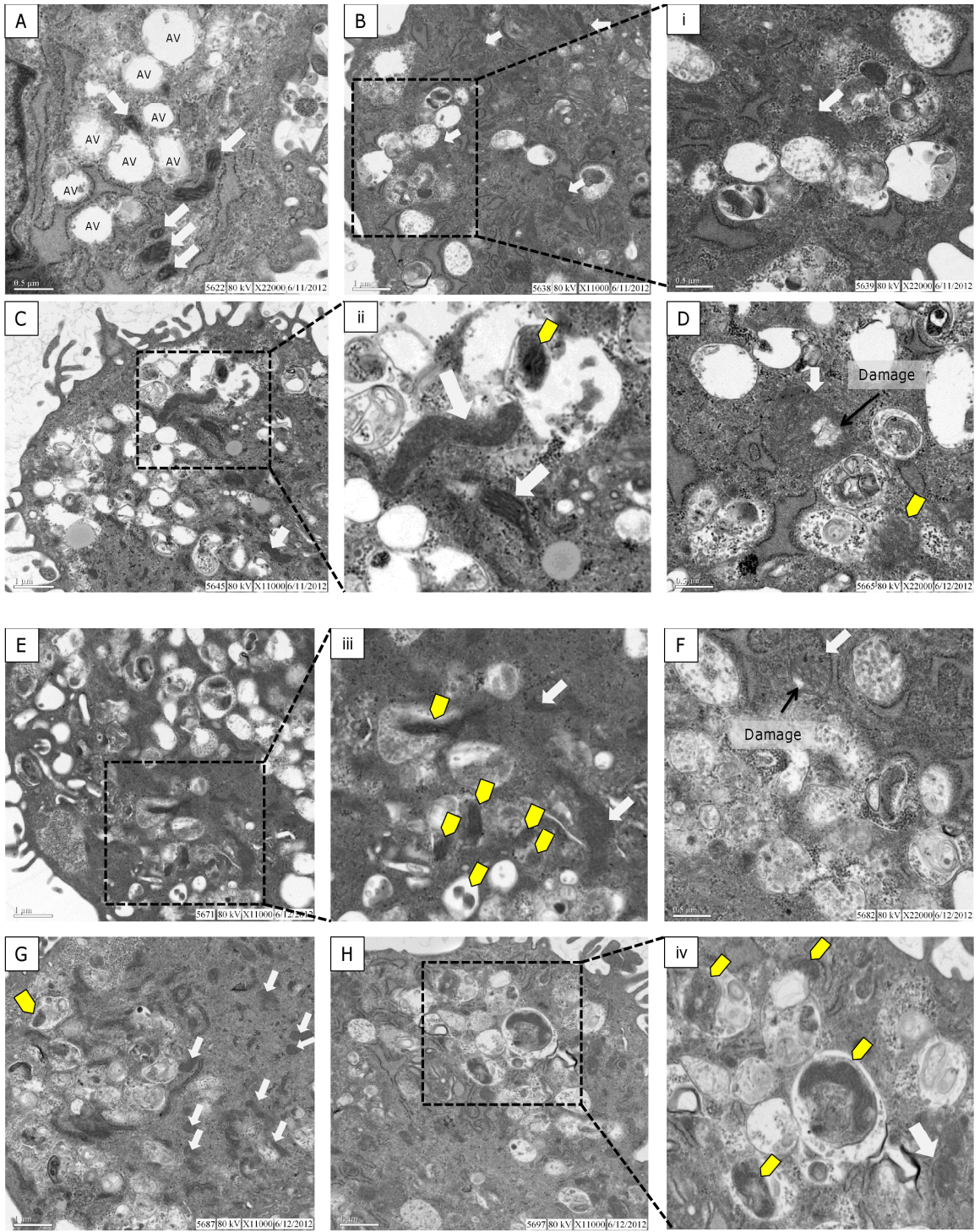


Figure 24: Autophagic degradation of mitochondria is enhanced during recovery.

Electron micrographs of control (A), control + Baf (B), UV 24 h + Baf (C-D), UV 48 h + Baf (E-F) and UV 72 h + Baf (G-H). (A) Control cells without bafilomycin had autophagic vacuoles (AV) that corresponded to multivesicular endosomes (MVE) or early autophagosomes, and several mitochondria with defined cristae (solid white arrows). (B) Mitochondria in control cells with bafilomycin were less defined and several AVs representing MVEs, autophagosomes and lysosomes were present. (i) Higher magnification (22,000 X) of a mitochondrion highlighting a lack of electron density and cristae definition. In UVC-exposed (10 J/m²) cells a range of mitochondrial phenotypes was observed from dense mitochondria with well-defined cristae to enlarged mitochondria with less density and poorly defined cristae. At 24 and 48 h (D,F) large round mitochondria were observed with areas of low electron density suggesting damaged or swollen inner membrane. Autophagosomes containing mitochondria (yellow arrows) were observed at 24, 48 and 72 h with an increasing trend in frequency at 48 and 72 h. Several autophagosomes containing general cytoplasmic materials were also observed throughout the recovery period.

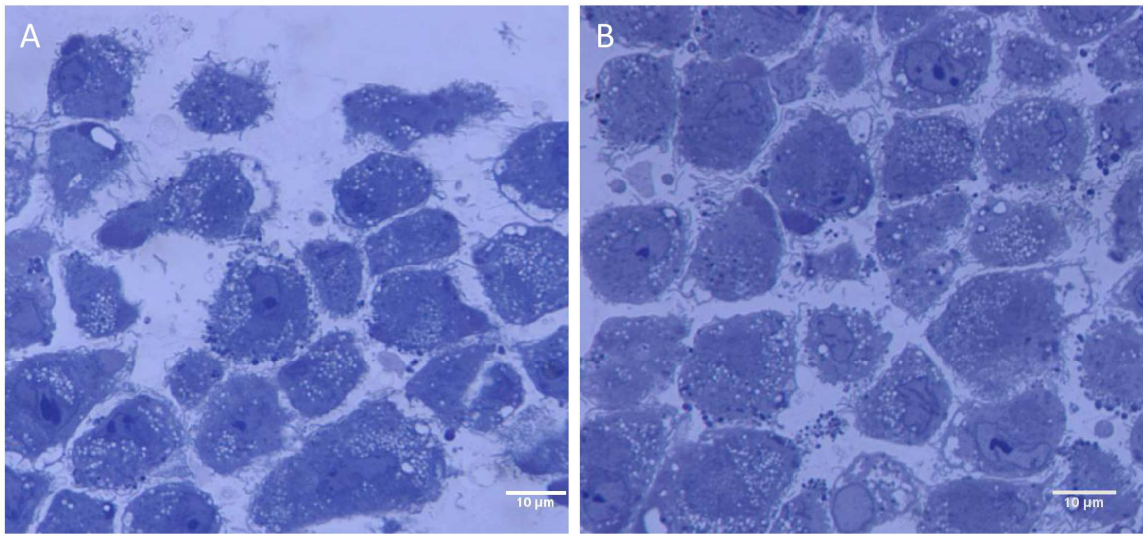


Figure 25: Toluidine blue stained semi-thin sections of human primary fibroblasts.

Representative images of (A) control and (B) UVC-treated cells. Cell pellets were embedded in Spurr's resin, cut into semithin sections (500 nm thick), stained with toluidine blue O and imaged by high resolution (60X) light microscopy. Several cells were present in the block face and few cells were identified that demonstrated apoptotic or necrotic features.

Table 1: Primer sequences and RT-PCR conditions for gene expression and mtDNA copy number analyses.

Gene target	Primer sequence	Temp. °C	final conc. (nM)	source
Gene expression analysis				
<i>18 S</i>	GAG GAT GAG GTG GAA CGT GT	60	400	304
	GGA CCT GGC TGT ATT TTC CA	60	400	304
<i>36B4</i>	GTG ATG TGC AGC TGA TCA AGA CT	60	400	304
	GAT GAC CAG CCC AAA GGA GA	60	400	304
<i>BECN1</i>	GGA TGG ATG TGG AGA AAG GCA AG	60	400	195
	TGA GGA CAC CCA AGC AAG ACC	60	400	195
<i>MAPLC3</i>	GCC TTC TTC CTG CTG GTG AAC	60	400	195
	AGC CGT CCT CGT CTT TCT CC	60	400	195
<i>NRF 1</i>	GGT GCA GCA CCT TTG GAG AA	60	400	304
	CCA GAG CAG ACT CCA GGT CTT C	60	400	304
<i>COXIV</i>	CAT GTG GCA GAA GCA CTA TGT GT	60	400	304
	GCC ACC CAC TCT TTG TCA AAG	60	400	304
<i>COXI</i>	CTG CTA TAG TGG AGG CCG GA	60	400	305
	GGG TGG GAG TAG TTC CCT GC	60	400	305
<i>MFN1</i>	TGT TTT GGT CGC AAA CTC TG	60	400	304
	CTG TCT GCG TAC GTC TTC CA	60	400	304
<i>OPA1</i>	GCA ATG GGA TGC AGC TAT TT	60	400	56
	CAC TGT TCT TGG GTC CGA TT	60	400	56
<i>FIS1</i>	CGA GCT GGT GTC TGT GGA GGA CC	60	400	Designed
	TGT CAA TGA GCC GCT CCA GTT CC	60	400	Designed
<i>PGC1a</i>	CCT TGC AGC ACA AGA AAA CA	62	400	Designed
	TGC TTC GTC GTC AAA AAC AG	62	400	Designed
<i>DRP1</i>	TGG GCG CCG ACA TCA	64	400	306
	GCT CTG CGT TCC CAC TAC GA	64	400	306
<i>TFAM</i>	CCG AGG TGG TTT TCA TCT GT	60	400	Designed
	GCA TCT GGG TTC TGA GCT TT	60	400	Designed
mtDNA copy number analysis				
tRNA F3212	CAC CCA AGA ACA GGG TTT GT	62	400	285
tRNA R3319	TGG CCA TGG GTA TGT TGT TA	62	400	285
B2M F594	TGC TGT CTC CAT GTT TGA TGT ATC T	62	400	285
B2M R679	TCT CTG CTC CCC ACC TCT AAG T	62	400	285

4. Conclusion

4.1 Summary

The overall goal of this dissertation was to broaden our understanding of the fate and effects of irreparable mtDNA damage induced by environmental genotoxicants. Despite the susceptibility of mtDNA to helix-distorting lesions and the potential for this damage to compromise mtDNA integrity, there existed little information regarding the fate of this damage in mtDNA. Furthermore there is little understanding of the role of autophagy and mitochondrial dynamics in removal of and recovery from this persistent mtDNA damage even though these processes in many cases are critical for recovery from other mitochondrial toxicants. Therefore, the first hypothesis addressed in this work was that UVC-induced photodimers in mtDNA are removed and the removal is dependent upon mitochondrial dynamics and autophagy. In Chapter 2, data are presented that show removal of UVC-induced mtDNA damage by 48 h after exposure. This result was supported in Chapter 3 with removal of this mtDNA damage detectable by 72 h after exposure in primary human fibroblasts. Furthermore, in Chapter 2, I show that removal of this damage is dependent upon genes involved in autophagy, mitophagy, fusion and fission. These data demonstrates that mitochondrial dynamics and autophagy are part of a novel pathway for the removal of otherwise irreparable mtDNA damage.

Secondly, I hypothesized that UVC-induced mtDNA lesions would induce mitochondrial dysfunction altering mitochondrial morphology and mitophagy. In both *C. elegans* and primary human fibroblasts a single exposure to a sub-lethal dose of UVC induced autophagy by 24 h. However, data presented in Chapter 3 suggest that mitochondrial degradation is not increased until 72 h after exposure. Interestingly, this induction occurred without detectable changes in mitochondrial function and only mild changes in mitochondrial morphology. These data suggest that mitochondrial morphology, MP and ROS may not be the primary signals leading to induction of autophagy following helix-distorting DNA damage as has been reported with other treatment conditions.

Thirdly, I hypothesized that mitochondrial dynamics and autophagy are important for recovery from UVC-induced mitochondrial dysfunction, at least in part because these processes facilitate damage removal. In order to address this hypothesis an experimental method, described in Chapter 2, was developed to specifically induce persistent mtDNA damage and mitochondrial dysfunction without persistent nDNA damage in developing *C. elegans*. Accumulated mtDNA damage caused moderate larval arrest and significant decreases in steady-state ATP level and oxygen consumption. mtDNA replication and mitochondrial fusion proved to be critical for recovery from larval arrest as indicated by complete larval arrest with ethidium bromide treatment or fusion gene knockout. Genetic and pharmacological inhibition of autophagy increased

the frequency and duration of larval arrest but still allowed for some recovery. These data demonstrate that recovery is aided by autophagy, presumably due to its role in removal of damage; however, mtDNA replication and mitochondrial fusion are essential for recovery.

4.2 Implications and Future Directions

4.2.1 Role of proteins involved in the nuclear DNA damage response pathway

The DNA damage response (DDR) pathway involves identification of nDNA damage and subsequent activation of cell cycle arrest, DNA repair and in some cases apoptosis. Ataxia Telangiectasia Mutated (ATM) gene is responsible for the DDR to DSBs ^{298, 299, 302} and when mutated results in Ataxia Telangiectasia, a disorder marked by neurodegeneration and cancer predisposition ³⁰⁷. ATR on the other hand is responsible for responding to DNA damage that blocks DNA replication such as UVC-induced photodimers and bulky adducts ²⁹⁷. Recent evidence indicates that DNA damage-induced ATM or ATR activation results in increased autophagy which inhibits apoptotic cell death ^{191, 300-302}. ATR, once activated, can activate ATM and both of these activate p53 ^{298, 300}. p53 activation induces autophagy as a result of mTOR inhibition and AMPK activation through activation of TSC2 ^{300, 301}. Interestingly, Chen et al. (2012) recently demonstrated that UVC exposure induces a bi-phasic autophagy response ¹⁹¹. Early on, UVC activates ATR and elevates autophagy markers from 1 to 6 h after exposure. However, there is a secondary increase in autophagy noted at 24 h sustained at least

until 48 h which is independent of ATR activation. Furthermore, ATM-deficient cells demonstrate enhanced basal autophagy but defective mitophagy suggesting that ATM is involved in mitochondrial targeting for autophagy rather than autophagy induction ³⁰³. The data presented in Chapter 3 indicate that autophagy is increased within 24 h of exposure to UVC without detectable changes in MP or ROS level suggesting that nDNA damage signaling may be responsible for this response. Further research is needed to determine the involvement of DDR genes in UVC-induced autophagy at early and late time points and whether or not these proteins play a role in mitophagy signaling.

In addition to their role in autophagy, ATM and p53 are also involved in mtDNA maintenance ³⁰⁸⁻³¹⁰. Tissue specific mtDNA depletion is observed in ATM null mice and ATM knockdown in MEFs results in 50% depletion of mtDNA ³⁰⁸; furthermore, increased mtDNA copy number following γ -irradiation are ATM dependent. p53 localizes to mitochondria and is reported to bind to and mediate the activity of POLG1, TFAM and mitochondrial single stranded binding protein all of which are involved in mtDNA maintenance ³⁰⁹. Additionally, p53 induces expression of ribonucleotide reductase subunit R2 (p53R2) which when mutated causes severe mtDNA depletion ³¹⁰ emphasizing the importance of *de novo* dNTP synthesis in mtDNA replication. A potential role of p53 as a mtDNA damage sensor has been suggested ³⁰⁹ but further research is needed to elucidate the role of ATM and its downstream target, p53, in mediating a mtDNA damage response.

4.2.2 Susceptibility of aged populations to helix-distorting mtDNA damage

The effects of mitochondrial dysfunction in mitochondrial diseases typically occur in high energy post-mitotic tissues such as muscle and nervous tissue ¹. Generally these are thought to be more affected because they are high energy tissues, heavily dependent on OXPHOS and therefore have a greater probability of ROS-induced mitochondrial and mtDNA damage and a greater susceptibility to mtDNA mutations, mitochondrial dysfunction and mitochondrial-mediated apoptosis. Given that these cells cannot be replaced, apoptosis or energy deficiency over a certain threshold leads to tissue wide disease. An overall decrease in autophagy as well as defective mitophagy has been observed in aging post-mitotic nervous and cardiac tissue ^{183-185, 209}. The data presented in this dissertation demonstrate that removal of helix-distorting mtDNA damage is mediated by autophagy, therefore susceptibility to mitochondrial dysfunction and tissue damage resulting from this persistent mtDNA damage will increase with age. Intriguingly, PAH exposure was linked to an abnormal case of a 60 year old man with late-onset Leber's Hereditary Optic Neuropathy (LHON), a disease characterized by mutations in complex I typically resulting in early adult onset of optic neuropathy and blindness ³¹¹. While this individual carried the LHON mutation throughout his life and spent greater than 30 years exposed to high levels of PAH, disease pathogenesis did not occur until later life. Furthermore, a comprehensive review of environmental exposures

in affected and unaffected individuals from 125 LHON pedigrees identified a strong correlation between disease development (i.e., vision loss) and smoking in later life ¹⁵.

The data presented in this dissertation indicate that the removal rate of helix-distorting lesions in mtDNA is roughly comparable between *C. elegans* and non-replicating human fibroblasts. However, it is likely that the rate of damage removal is cell type specific given differences in energy demand, mtDNA copy number and autophagic capacity between cell types. For example, a dependence on OXPHOS has been shown to prevent mitophagy from taking place to any significant degree in primary cells ¹⁸⁷. An interesting future direction of this research would be to compare the rate of mtDNA damage removal in different tissues types.

In many cases, fusion acts to compensate for mitochondrial damage and mtDNA mutations by allowing for complementation of mitochondrial contents and enhancing mitochondrial DNA repair and replication ^{137, 141, 155}. Therefore, it is not surprising that this process was critical in recovery from UVC-induced larval arrest as shown in Chapter 2. However, fusion can inhibit mitophagy thus it was surprising to find that fusion knockdown inhibited removal of UVC-induced mtDNA damage. An exciting future direction of this research is to determine the ability of UVC to induce autophagy and mitophagy in fusion-deficient cells. This is of particular importance because individuals harboring heterozygous mutations in fusion genes, *OPA1* and *MFN2*, exist in the population and exhibit varying degrees of neurodegeneration in optic and

peripheral nerves, respectively, suggesting important gene-environment interactions that could have a direct impact on disease pathogenesis.

Appendix A – Identification and tracking of UVC-induced mtDNA damage in mammalian cell culture

One of the original goals of this dissertation work was to investigate the distribution of damaged mtDNA throughout the mitochondrial network after exposure and determine if mitochondria with a high proportion of damaged mtDNAs are selectively isolated and degraded. In order to test this two approaches were attempted.

A. 1 Damaged mtDNA tracking in live cells using cyclobutane pyrimidine dimer (CPD) GFP-tagged mutant photolyase

A.1.1 Gene insert confirmation

The N378S CPD *Escherichia coli* photolyase was first described by Xu et al. (2008)³¹². This photolyase contains a single base substitution resulting in an amino acid change. It is able to bind to CPDs but cannot reverse the dimer. It was obtained from the Xu lab in a pET-22b(+) vector as a purified plasmid. This was transformed into One Shot TOP10 competent *E.coli* (Invitrogen) using the manufacturer's instructions. Extracted and purified plasmid was sequenced using primers designed for the T7 promoter and terminator sequences that flank the N378S gene insert. Blast results of the resulting sequence confirmed that the gene insert was the *E. coli* photolyase (X57399.1) with the N378S mutation.

A.1.2 Cloning using the In-Fusion system

The In Fusion system utilizes the principals of homologous recombination to ligate DNA fragments into a linearized plasmid. Primers with a short region homologous to a linearized plasmid are used to amplify the gene of interest such that the homologous region was added to the ends of the gene sequence.

In-Fusion primers (below) were designed, optimized and used to amplify N378S photolyase gene sequence adding a short region homologous to the Mito-pAcGFP(Clontech, PT3730-5) plasmid cut with BamHI and AgeI.

forward: ATTCGTTGGGGGATCCAATGACTACCCATCTGGTCTGGTTT

reverse: GCTCACCATGACCGGTTTCCCCTTCCGCGCCG

The In-Fusion reaction was carried out using the manufacturer's instructions. Confirmation of a successful Mito-N378S-pAcGFP clone was carried out by transformation of the In-Fusion products into Stellar *E. coli* (Clontech), plasmid extraction and purification, sequencing and AgeI fragment analysis. Several In-Fusion products yielded the expected AgeI fragments and had the correct sequence. *E. coli* stocks containing successful clones were frozen.

A.1.3 Visualization and confirmation of N378S photolyase mitochondrial localization and DNA binding following UVC exposure

Extracted and purified Mito-N378S-pAcGFP was transfected into mouse embryonic fibroblasts (MEFs) using Lipofectamine LTX (Invitrogen), cells were dosed with 50 J/m² UVC and imaged on a Leica SP5 laser scanning confocal microscope. This

UVC exposure was selected to ensure a high level of CPD lesion frequency in mtDNA. In transfected cells, GFP under the control of a CMV promoter was limited to what appeared to be the mitochondrial network (Figure 26). No change in fluorescence localization was observed in UVC exposed cells. Possible reasons for this observation are that the addition of GFP to the enzyme prevented its ability to bind to CPDs or expression of the plasmid was too high making it difficult to discern matrix-associated and CPD-associated enzyme.

A.2 Damaged mtDNA tracking in fixed cells using cyclobutane pyrimidine dimer (CPD) antibody

A.2.1 Antibody details

Three anti-CPD antibodies have been cited in the literature: UV-2 (not available), TDM-2 (Cosmo Bio Company, Tokyo, Japan) and KTM53 (conjugated to horseradish peroxidase; Kamiya Biomedical Company, Seattle, WA). KTM53, TDM-2, an AlexaFluor 647 conjugated anti-HRP and an AlexaFluor 647 conjugated anti-mouse were purchased.

A.2.2 Optimization of immunocytochemistry parameters in UVC treated cells

Cells were treated with 50 J/m² UVC. Experiments with KTM53 were performed on MEFs and TDM-2 experiments were performed on human fibroblasts. The following ICC parameters were tested:

Fixation: 3.7 % paraformaldehyde 10, 15 and 20 minutes

Permeabilization: 0.1 – 1% Triton-X 5 - 20 min on ice and RT; ice-cold acetone

5 – 10 min

Denaturation: none; 0.4 M NaOH 4 min; 0.5, 1 and 2 M HCL 20 – 30 min RT

Blocking: 10% goat serum for 30 m and 1 h RT and 37°C

KTM53 incubation: 1:200 for 1 h RT; 1:500 o/n 4°C

Anti-HRP secondary incubation: 1:100 and 1:500 1- 2 h RT

TDM-2 incubation: 1:1000, 1:1500 and 1:2000 4°C o/n

Anti-mouse secondary incubation: 1:200 – 1:500 2 h RT; 1:1000 30 m 37°C

A.2.2 Results

The KTM53 antibody did not produce a fluorescent signal from nuclear and mitochondrial DNA in UVC treated cells under any of the conditions tested. TDM-2 produced a strong nDNA signal in UVC treated cells when HCl denaturation was used (Figure 27). HCl denaturation eliminates picogreen staining in a dose-dependent fashion. Mitotracker Red is sufficiently excited by 633 nm laser to create a signal in the far red channel. I would not recommended use of this dye in combination with far red. Acetone permeabilization significantly decreases the background associated with Mitotracker Red and produces clear mitochondrial staining; however, it blurs picogreen staining. None of the conditions produced a reliable mtDNA signal.

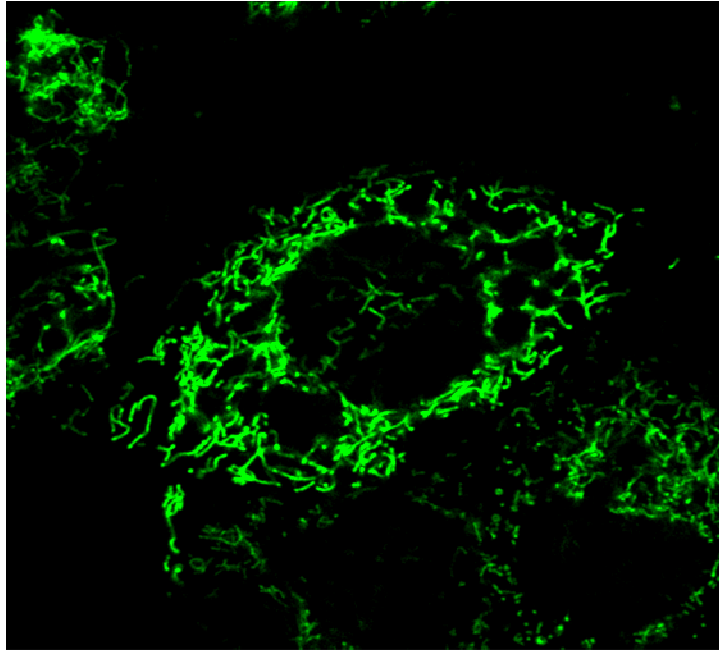


Figure 26: Mito-N378S-GFP localizes to the mitochondrial network in MEFs

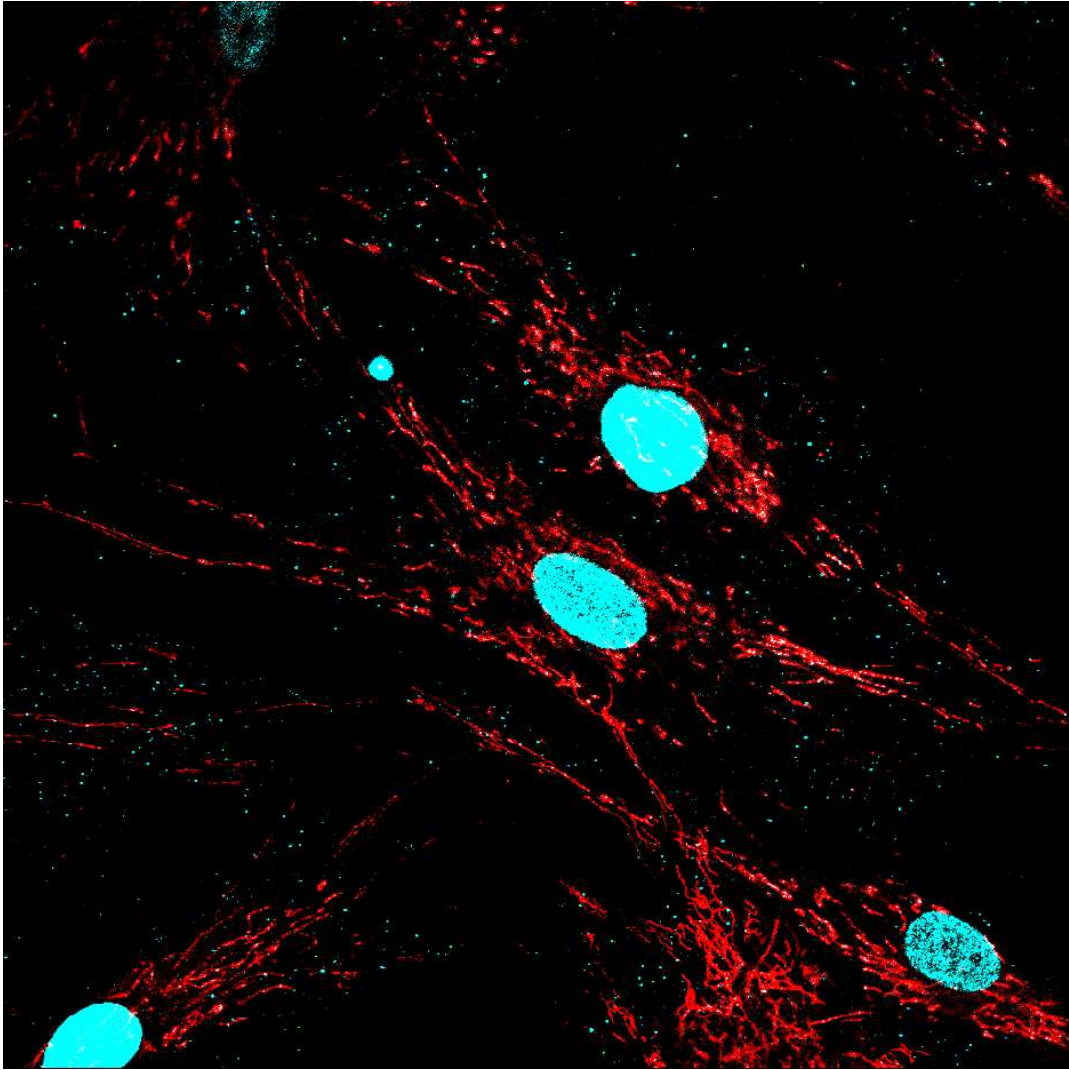


Figure 27: UVC treated cells with a CPD signal in nDNA and Mitotracker Red stained mitochondria.

Appendix B – Effects of UVC exposure on mitochondrial membrane potential, mass, relative superoxide level and mtDNA copy number in replicating primary human fibroblasts

Effects of UVC exposure on mitochondrial MP, mass and level of superoxide were analyzed by flow cytometry in replicating primary human fibroblasts without a thymidine block.

B.1 Methods

Mitochondrial MP, mitochondrial mass and mtDNA copy number analyses were performed as described above in Chapter 3 without use of thymidine in order to allow nDNA synthesis. To measure the relative level of superoxide, cells were stained with MitoSox (5 μ M) for 30 min at 37°C, collected via trypsinization **without EDTA**, resuspended in FACS buffer and fluorescence intensity was measured using a FACSVantage Sorter.

B.2 Results and Discussion

A dose dependent increase in mitochondrial MP and mass was observed at 48 and 72 h post exposure to UVC (two-way ANOVA, treatment x time point $P < 0.0001$; Fisher's PLSD, effect of treatment at each time point $P < 0.05$; Figure 28a-b).

Additionally, there was an overall increase in the relative superoxide level in cells exposed to UVC 10 J/m² irrespective of time point (two-way ANOVA, effect of treatment

$P < 0.0001$, treatment x time point $P = 0.1323$; Figure 28c). However, an increase in mitochondrial mass may increase the amount of TMRE and MitoSox accumulated in the cell, thus the increased fluorescence may be the result of more dye accumulation rather than increased MP or superoxide. Therefore, mitochondrial mass should be measured simultaneously along with fluorescence of mitochondrial specific, lipophilic dyes and used to normalize for differential dye accumulation.

Removal of damaged mtDNA in the absence of thymidine in UVC treated cells was demonstrated in Chapter 3. mtDNA content was not affected by UVC exposure therefore we concluded that mtDNA replication replaces degraded damaged mtDNA. Interestingly, the increase in mitochondrial mass did not result in an increase in mtDNA content.

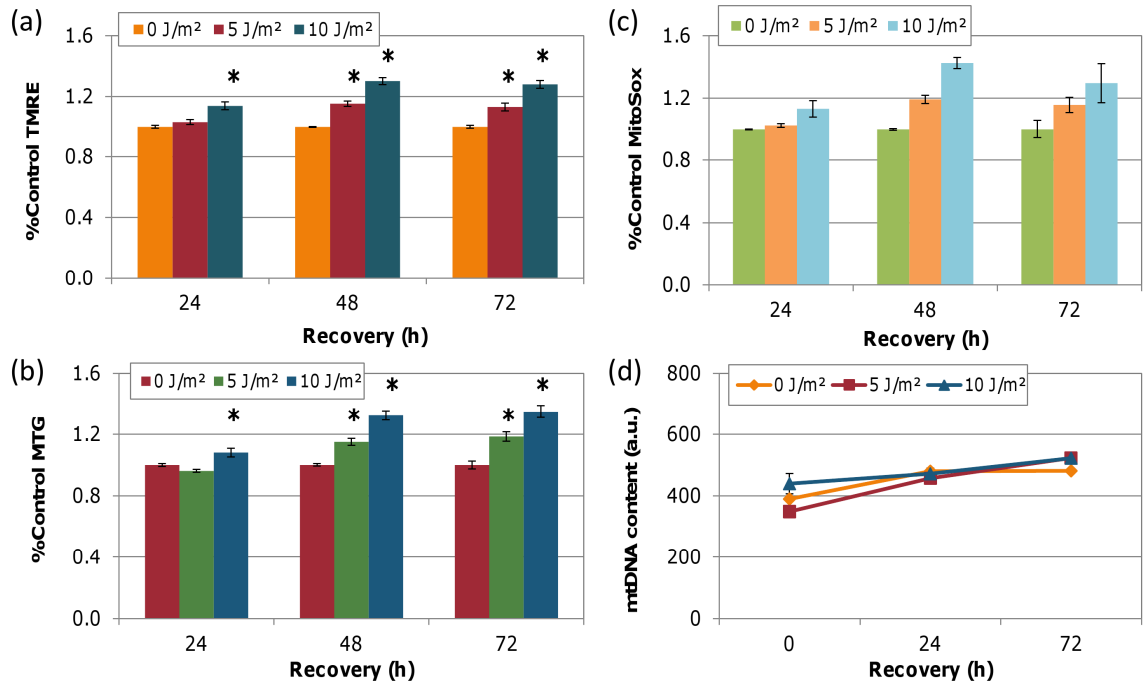


Figure 28: Mitochondrial MP, mass and relative level of superoxide increase after UVC exposure without changes in mtDNA copy number.

Appendix C – Studies with low-dose rapamycin and mtDNA damage removal and mitochondrial mass, membrane potential and ROS.

If damaged mtDNAs are removed by autophagy, I hypothesized that an increase in autophagy would accelerate removal of mitochondria and mtDNA damage and protect against changes in mitochondrial function. To test this hypothesis, I attempted to induce autophagy with rapamycin, an inhibitor of mTOR.

C.1 Methods

Thymidine blocked cells were treated with 100 nM rapamycin (ready-made solution in DMSO; Sigma) immediately after UVC exposure and throughout the recovery period. Thymidine + rapamycin media was replaced daily. FACS analysis of MP, ROS and mass and mtDNA damage and copy number assays were performed as described above in Chapter 3. Two biological reps of rapamycin plus UVC and 1-2 biological reps of rapamycin only were performed in these analyses.

C.2 Results and Discussion

Rapamycin at 100 nM did not significantly reduce mitochondrial mass alone or in conjunction with UVC (Figure 29). mtDNA content was not affected by rapamycin treatment alone to any significant degree nor did rapamycin significantly change mtDNA content in UVC-treated cells. These data suggest that either rapamycin is not inducing autophagy or that mitochondrial biogenesis and mtDNA replication are able to

compensate for increased mitochondrial and mtDNA degradation. Additionally, there was little effect of rapamycin treatment on MP or ROS in control or UVC-treated cells (Figure 29).

If rapamycin (100 nM) is increasing mtDNA turnover in UVC-treated cells, then mtDNA damage removal should be accelerated; however, we did not observe a significant difference in the removal rate (Figure 30). Therefore, we concluded that rapamycin is not inducing autophagy in UVC treated cells either because the concentration is not sufficient to do this or UVC exposure has maximized the autophagic response and further inhibition of mTOR with rapamycin has no additional effect.

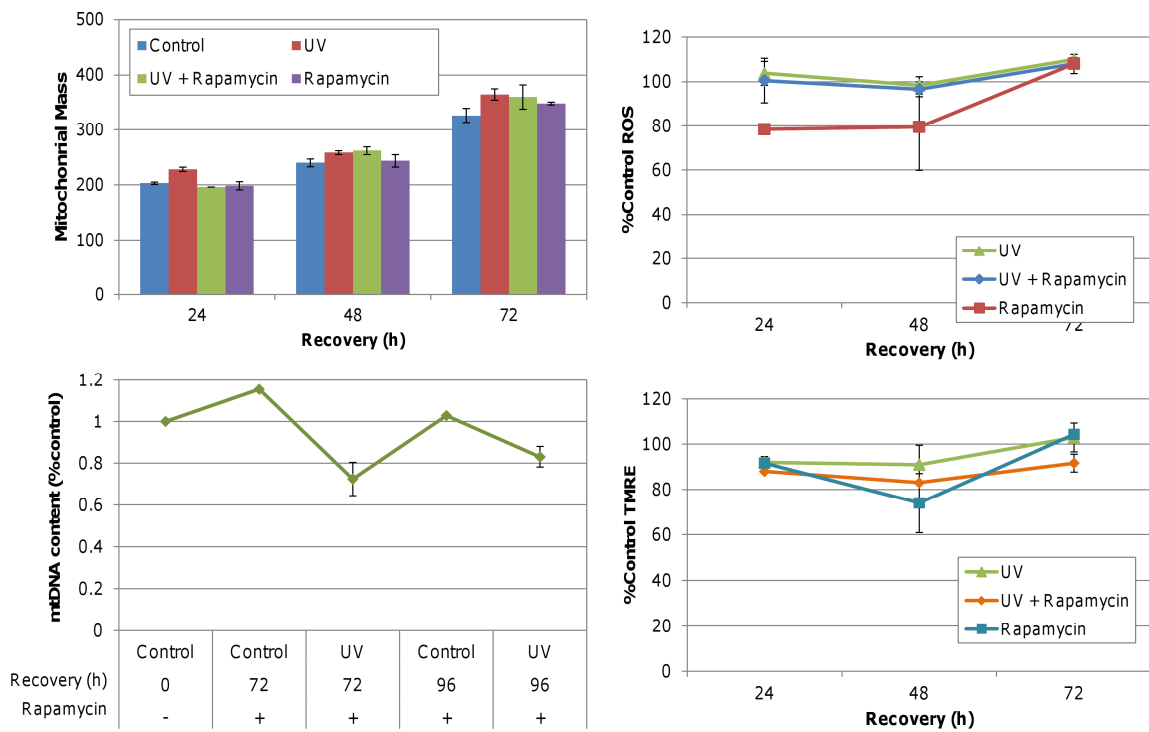


Figure 29: Low-dose rapamycin treatment has little effect on mitochondrial mass, MP or ROS in control or UVC exposed cells.

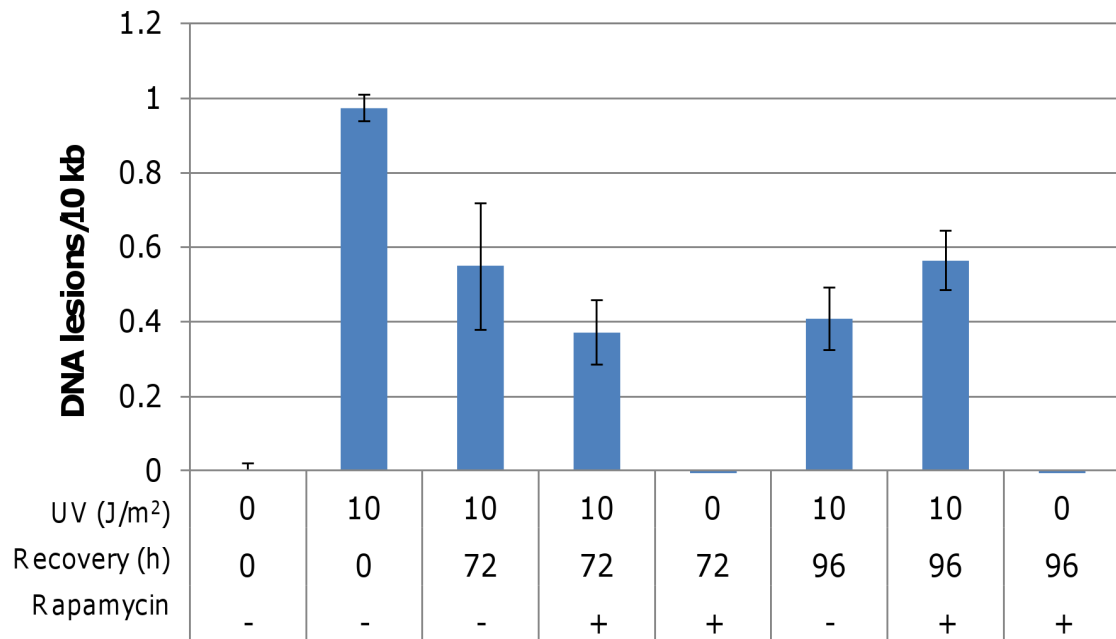


Figure 30: Low-dose rapamycin does not significantly affect the rate of mtDNA damage removal.

References

1. Greaves, L.C., et al., *Mitochondrial DNA and Disease*. J Pathol, 2011.
2. Jin, S., *Autophagy, mitochondrial quality control, and oncogenesis*. Autophagy, 2006. **2**(2): p. 80-4.
3. Brandon, M., P. Baldi, and D.C. Wallace, *Mitochondrial mutations in cancer*. Oncogene, 2006. **25**(34): p. 4647-62.
4. Chinnery, P.F., et al., *Accumulation of mitochondrial DNA mutations in ageing, cancer, and mitochondrial disease: is there a common mechanism?* The Lancet, 2002. **360**(9342): p. 1323-1325.
5. Bossy-Wetzel, E., et al., *Mitochondrial fission in apoptosis, neurodegeneration and aging*. Curr Opin Cell Biol, 2003. **15**(6): p. 706-16.
6. Lin, M.T. and M.F. Beal, *Mitochondrial dysfunction and oxidative stress in neurodegenerative diseases*. Nature, 2006. **443**(7113): p. 787-95.
7. Chen, H. and D.C. Chan, *Mitochondrial dynamics--fusion, fission, movement, and mitophagy--in neurodegenerative diseases*. Hum Mol Genet, 2009. **18**(R2): p. R169-76.
8. Weissman, L., et al., *DNA repair, mitochondria, and neurodegeneration*. Neuroscience, 2007. **145**(4): p. 1318-29.
9. Lowell, B.B. and G.I. Shulman, *Mitochondrial dysfunction and type 2 diabetes*. Science, 2005. **307**(5708): p. 384-7.
10. Dai, D.-F., P.S. Rabinovitch, and Z. Ungvari, *Mitochondria and Cardiovascular Aging*. Circulation Research, 2012. **110**(8): p. 1109-1124.
11. Terman, A., et al., *Mitochondrial turnover and aging of long-lived postmitotic cells: the mitochondrial-lysosomal axis theory of aging*. Antioxid Redox Signal, 2010. **12**(4): p. 503-35.
12. Wang, C.-Y. and Z.-B. Zhao, *Somatic mtDNA mutations in lung tissues of pesticide-exposed fruit growers*. Toxicology, 2012. **291**(1): p. 51-55.
13. Greenamyre, J.T., R. Betarbet, and T.B. Sherer, *The rotenone model of Parkinson's disease: genes, environment and mitochondria*. Parkinsonism & Related Disorders, 2003. **9**, **Supplement 2**(0): p. 59-64.
14. Lim, S., et al., *Persistent organic pollutants, mitochondrial dysfunction, and metabolic syndrome*. Ann N Y Acad Sci, 2010. **1201**: p. 166-76.
15. Kirkman, M.A., et al., *Gene-environment interactions in Leber hereditary optic neuropathy*. Brain, 2009. **132**(Pt 9): p. 2317-26.
16. Edwards, T.M. and J.P. Myers, *Environmental exposures and gene regulation in disease etiology*. Cien Saude Colet, 2008. **13**(1): p. 269-81.
17. Salazar, J.J. and B. Van Houten, *Preferential mitochondrial DNA injury caused by glucose oxidase as a steady generator of hydrogen peroxide in human fibroblasts*. Mutation Research, 1997. **385**(2): p. 139-49.

18. Yakes, F. and B. Van Houten, *Mitochondrial DNA damage is more extensive and persists longer than nuclear DNA damage in human cells following oxidative stress*. 1997, National Acad Sciences. p. 514-519.
19. Ballinger, S.W., et al., *Hydrogen Peroxide- and Peroxynitrite-Induced Mitochondrial DNA Damage and Dysfunction in Vascular Endothelial and Smooth Muscle Cells*. *Circ Res*, 2000. **86**(9): p. 960-966.
20. Barja, G. and A. Herrero, *Oxidative damage to mitochondrial DNA is inversely related to maximum life span in the heart and brain of mammals*. *FASEB J.*, 2000. **14**(2): p. 312-318.
21. Bohr, V.A. and G.L. Dianov, *Oxidative DNA damage processing in nuclear and mitochondrial DNA*. *Biochimie*, 1999. **81**(1-2): p. 155-160.
22. Palmeira, C.M., et al., *Preferential oxidation of cardiac mitochondrial DNA following acute intoxication with doxorubicin*. *Biochimica et Biophysica Acta (BBA) - Bioenergetics*, 1997. **1321**(2): p. 101-106.
23. Richter, C., J.W. Park, and B.N. Ames, *Normal oxidative damage to mitochondrial and nuclear DNA is extensive*. *Proc Natl Acad Sci U S A*, 1988. **85**(17): p. 6465-7.
24. Wunderlich, V., et al., *Preferential alkylation of mitochondrial deoxyribonucleic acid by N-methyl-N-nitrosourea*. *Biochem J*, 1970. **118**(1): p. 99-109.
25. Wunderlich, V., I. Tetzlaff, and A. Graffi, *Studies on nitrosodimethylamine: Preferential methylation of mitochondrial DNA in rats and hamsters*. *Chemico-Biological Interactions*, 1972. **4**(2): p. 81-89.
26. Allen, J.A. and M.M. Coombs, *Covalent binding of polycyclic aromatic compounds to mitochondrial and nuclear DNA*. *Nature*, 1980. **287**: p. 244-245.
27. Divi, R.L., et al., *Highly sensitive chemiluminescence immunoassay for benzo[a]pyrene-DNA adducts: validation by comparison with other methods, and use in human biomonitoring*. *Carcinogenesis*, 2002. **23**(12): p. 2043-2049.
28. Stairs, P.W., P.S. Guzelian, and G.C. Van Tuyle, *Benzo[a]pyrene differentially alters mitochondrial and nuclear DNA synthesis in primary hepatocyte cultures*. *Res Commun Chem Pathol Pharmacol*, 1983. **42**(1): p. 95-106.
29. Backer, J.M. and I.B. Weinstein, *Mitochondrial DNA is a major cellular target for a dihydrodiol-epoxide derivative of benzo[a]pyrene*. *Science*, 1980. **209**(4453): p. 297-9.
30. Sawyer, D.E. and B. Van Houten, *Repair of DNA damage in mitochondria*. *Mutat Res*, 1999. **434**(3): p. 161-76.
31. Murata, T., et al., *Preferential binding of cisplatin to mitochondrial DNA and suppression of ATP generation in human malignant melanoma cells*. *Biochem Int*, 1990. **20**(5): p. 949-55.
32. Olivero, O.A., et al., *Preferential formation and decreased removal of cisplatin-DNA adducts in Chinese hamster ovary cell mitochondrial DNA as compared to nuclear DNA*. *Mutat Res*, 1997. **391**(1-2): p. 79-86.

33. Giurgiovich, A.J., et al., *Elevated mitochondrial cisplatin-DNA adduct levels in rat tissues after transplacental cisplatin exposure*. *Carcinogenesis*, 1997. **18**(1): p. 93-96.
34. Jung, D., et al., *Effects of benzo[a]pyrene on mitochondrial and nuclear DNA damage in Atlantic killifish (*Fundulus heteroclitus*) from a creosote-contaminated and reference site*. *Aquat Toxicol*, 2009. **95**(1): p. 44-51.
35. Balansky, R., et al., *Induction by Carcinogens and Chemoprevention by N-Acetylcysteine of Adducts to Mitochondrial DNA in Rat Organs*. *Cancer Res*, 1996. **56**(7): p. 1642-1647.
36. Niranjana, B.G., N.K. Bhat, and N.G. Avadhani, *Preferential attack of mitochondrial DNA by aflatoxin B1 during hepatocarcinogenesis*. *Science*, 1982. **215**(4528): p. 73-5.
37. Bedard, L.L. and T.E. Massey, *Aflatoxin B1-induced DNA damage and its repair*. *Cancer Lett*, 2006. **241**(2): p. 174-83.
38. Jeong, Y.C., et al., *Pyrimido[1,2-*a*]-purin-10(3H)-one, M1G, is less prone to artifact than base oxidation*. *Nucleic Acids Res*, 2005. **33**(19): p. 6426-34.
39. Chen, R.H., et al., *Preferential repair and strand-specific repair of benzo a pyrene diol epoxide adducts in the HPRT gene of diploid human fibroblasts* *Proceedings of the National Academy of Sciences of the United States of America*, 1992. **89**(12): p. 5413-5417.
40. Braithwaite, E., X. Wu, and Z. Wang, *Repair of DNA lesions: mechanisms and relative repair efficiencies*. *Mutat Res*, 1999. **424**(1-2): p. 207-19.
41. Sinha, R.P. and D.P. Hader, *UV-induced DNA damage and repair: a review*. *Photochem Photobiol Sci*, 2002. **1**(4): p. 225-36.
42. Balajee, A.S. and V.A. Bohr, *Genomic heterogeneity of nucleotide excision repair*. *Gene*, 2000. **250**(1-2): p. 15-30.
43. Hanawalt, P.C., *Subpathways of nucleotide excision repair and their regulation*. *Oncogene*, 2002. **21**(58): p. 8949-56.
44. Chen, H. and D.C. Chan, *Mitochondrial dynamics in mammals*. *Curr Top Dev Biol*, 2004. **59**: p. 119-44.
45. Benard, G., et al., *Mitochondrial bioenergetics and structural network organization*. *Journal of Cell Science*, 2007. **120**(5): p. 838.
46. Malka, F., et al., *Separate fusion of outer and inner mitochondrial membranes*. *EMBO reports*, 2005. **6**(9): p. 853.
47. Tondera, D., et al., *SLP-2 is required for stress-induced mitochondrial hyperfusion*. *Embo J*, 2009. **28**(11): p. 1589-600.
48. Malakhova, L., et al., *The increase in mitochondrial DNA copy number in the tissues of gamma-irradiated mice*. *Cell Mol Biol Lett*, 2005. **10**(4): p. 721-32.
49. Griparic, L., T. Kanazawa, and A. van der Bliek, *Regulation of the mitochondrial dynamin-like protein Opa1 by proteolytic cleavage*. *Journal of Cell Biology*, 2007.

50. Gandre-Babbe, S. and A. van der Blik, *The novel tail-anchored membrane protein Mff controls mitochondrial and peroxisomal fission in mammalian cells*. *Molecular biology of the cell*, 2008. **19**(6): p. 2402.
51. Arnold, B., et al., *Integrating multiple aspects of mitochondrial dynamics in neurons: age-related differences and dynamic changes in a chronic rotenone model*. *Neurobiol Dis*, 2011. **41**(1): p. 189-200.
52. De la Mata, M., et al., *Recovery of MERRF Fibroblasts and Cybrids Pathophysiology by Coenzyme Q(10)*. *Neurotherapeutics*, 2012. **9**(2): p. 446-63.
53. Koopman, W.J.H., et al., *Inhibition of complex I of the electron transport chain causes O₂-mediated mitochondrial outgrowth*. *American Journal of Physiology - Cell Physiology*, 2005. **288**(6): p. C1440-C1450.
54. Koopman, W.J.H., et al., *Human NADH:ubiquinone oxidoreductase deficiency: radical changes in mitochondrial morphology?* *American Journal of Physiology - Cell Physiology*, 2007. **293**(1): p. C22-C29.
55. Barsoum, M.J., et al., *Nitric oxide-induced mitochondrial fission is regulated by dynamin-related GTPases in neurons*. *Embo J*, 2006. **25**(16): p. 3900-11.
56. Jendrach, M., et al., *Short- and long-term alterations of mitochondrial morphology, dynamics and mtDNA after transient oxidative stress*. *Mitochondrion*, 2008. **8**(4): p. 293-304.
57. Kim, I., S. Rodriguez-Enriquez, and J.J. Lemasters, *Selective degradation of mitochondria by mitophagy*. *Arch Biochem Biophys*, 2007. **462**(2): p. 245-53.
58. Lemasters, J.J., *Selective mitochondrial autophagy, or mitophagy, as a targeted defense against oxidative stress, mitochondrial dysfunction, and aging*. *Rejuvenation Res*, 2005. **8**(1): p. 3-5.
59. Rodriguez-Enriquez, S., L. He, and J.J. Lemasters, *Role of mitochondrial permeability transition pores in mitochondrial autophagy*. *Int J Biochem Cell Biol*, 2004. **36**(12): p. 2463-72.
60. Rodriguez-Enriquez, S., et al., *Tracker dyes to probe mitochondrial autophagy (mitophagy) in rat hepatocytes*. *Autophagy*, 2006. **2**(1): p. 39-46.
61. Peters, C., et al., *Mutual control of membrane fission and fusion proteins*. *Cell*, 2004. **119**(5): p. 667-78.
62. Twig, G., et al., *Fission and selective fusion govern mitochondrial segregation and elimination by autophagy*. *Embo J*, 2008. **27**(2): p. 433-46.
63. Narendra, D., et al., *Parkin is recruited selectively to impaired mitochondria and promotes their autophagy*. *J Cell Biol*, 2008. **183**(5): p. 795-803.
64. Narendra, D.P., et al., *PINK1 is selectively stabilized on impaired mitochondria to activate Parkin*. *PLoS Biol*, 2010. **8**(1): p. e1000298.
65. Ding, W.X., et al., *Nix is critical to two distinct phases of mitophagy, reactive oxygen species-mediated autophagy induction and Parkin-ubiquitin-p62-mediated mitochondrial priming*. *J Biol Chem*, 2010. **285**(36): p. 27879-90.

66. Geisler, S., et al., *PINK1/Parkin-mediated mitophagy is dependent on VDAC1 and p62/SQSTM1*. *Nat Cell Biol*, 2010. **12**(2): p. 119-31.
67. Vives-Bauza, C., et al., *PINK1/Parkin direct mitochondria to autophagy*. *Autophagy*, 2010. **6**(2): p. 315-6.
68. Gerschenson, M., et al., *Cisplatin exposure induces mitochondrial toxicity in pregnant rats and their fetuses*. *Reprod Toxicol*, 2001. **15**(5): p. 525-31.
69. Zhu, H., Y.B. Li, and M.A. Trush, *Characterization of Benzo[a]pyrene Quinone-Induced Toxicity to Primary Cultured Bone Marrow Stromal Cells from DBA/2 Mice: Potential Role of Mitochondrial Dysfunction*. *Toxicology and Applied Pharmacology*, 1995. **130**(1): p. 108-120.
70. Xia, T., et al., *Quinones and Aromatic Chemical Compounds in Particulate Matter Induce Mitochondrial Dysfunction: Implications for Ultrafine Particle Toxicity*. *Environmental Health Perspectives*, 2004. **112**(14): p. 1347-1358.
71. Ko, C.-B., et al., *Benzo(a)pyrene-induced apoptotic death of mouse hepatoma Hepa1c1c7 cells via activation of intrinsic caspase cascade and mitochondrial dysfunction*. *Toxicology*, 2004. **199**(1): p. 35-46.
72. Sajan, M.P., J.G. Satav, and R.K. Bhattacharya, *Activity of some respiratory enzymes and cytochrome contents in rat hepatic mitochondria following aflatoxin B1 administration*. *Toxicology Letters*, 1995. **80**(1-3): p. 55-60.
73. Obidoa, O., E.A. Bababunmi, and O. Bassir, *Action of dihydroaflatoxins on rat liver mitochondria. 1. Membrane-dependent osmotic and redox effects of aflatoxins B2 and G2*. *Toxicology*, 1978. **11**: p. 29-36.
74. Li, N., et al., *Ultrafine particulate pollutants induce oxidative stress and mitochondrial damage*. *Environ Health Perspect*, 2003. **111**(4): p. 455-60.
75. Nelson, D.L. and M.M. Cox, *Principles of Biochemistry*. Fourth ed. 2005, New York City: W.H. Freeman and Company.
76. Bereiter-Hahn, J. and M. Voth, *Dynamics of mitochondria in living cells: shape changes, dislocations, fusion, and fission of mitochondria*. *Microsc Res Tech*, 1994. **27**(3): p. 198-219.
77. Chan, D., *Mitochondrial fusion and fission in mammals*. 2006.
78. Margineantu, D.H., et al., *Cell cycle dependent morphology changes and associated mitochondrial DNA redistribution in mitochondria of human cell lines*. *Mitochondrion*, 2002. **1**(5): p. 425-35.
79. Robin, E.D. and R. Wong, *Mitochondrial DNA molecules and virtual number of mitochondria per cell in mammalian cells*. *Journal of Cellular Physiology*, 1988. **136**(3): p. 507-513.
80. Di Giulio, R.T. and J.N. Meyer, *Reactive Oxygen Species and Oxidative Stress*, in *Toxicology of Fishes*. 2008, CRC Press Taylor and Francis Group: Boca Raton.
81. Turrens, J.F., *Mitochondrial formation of reactive oxygen species*. *The Journal of Physiology*, 2003. **552**(2): p. 335-344.

82. Chance, B., H. Sies, and A. Boveris, *Hydroperoxide metabolism in mammalian organs*. *Physiol Rev*, 1979. **59**(3): p. 527-605.
83. Dykens, J.A., Will, Yvonne ed. *Drug-Induced Mitochondrial Dysfunction*. 2008, John Wiley & Sons: New Jersey.
84. Stuart, J.A. and M.F. Brown, *Mitochondrial DNA maintenance and bioenergetics*. *Biochim Biophys Acta*, 2006. **1757**(2): p. 79-89.
85. Beckman, K.B. and B.N. Ames, *The free radical theory of aging matures*. *Physiol Rev*, 1998. **78**(2): p. 547-81.
86. St-Pierre, J., et al., *Topology of Superoxide Production from Different Sites in the Mitochondrial Electron Transport Chain*. *Journal of Biological Chemistry*, 2002. **277**(47): p. 44784-44790.
87. Fukui, H. and C.T. Moraes, *The mitochondrial impairment, oxidative stress and neurodegeneration connection: reality or just an attractive hypothesis?* *Trends Neurosci*, 2008. **31**(5): p. 251-6.
88. Kukat, C., et al., *Super-resolution microscopy reveals that mammalian mitochondrial nucleoids have a uniform size and frequently contain a single copy of mtDNA*. *Proc Natl Acad Sci U S A*, 2011. **108**(33): p. 13534-9.
89. Iborra, F., H. Kimura, and P. Cook, *The functional organization of mitochondrial genomes in human cells*. *BMC biology*, 2004. **2**(1): p. 9.
90. Scheffler, I.E., *Mitochondria*. second ed. 2008, Hoboken: John Wiley and Sons.
91. Bogenhagen, D. and D. Clayton, *The number of mitochondrial deoxyribonucleic acid genomes in mouse L and human HeLa cells. Quantitative isolation of mitochondrial deoxyribonucleic acid*. *Journal of Biological Chemistry*, 1974. **249**(24): p. 7991.
92. Carling, P.J., L.M. Cree, and P.F. Chinnery, *The implications of mitochondrial DNA copy number regulation during embryogenesis*. *Mitochondrion*, 2011. **11**(5): p. 686-92.
93. Miller, F.J., et al., *Precise determination of mitochondrial DNA copy number in human skeletal and cardiac muscle by a PCR-based assay: lack of change of copy number with age*. *Nucl. Acids Res.*, 2003. **31**(11): p. e61-.
94. Casula, M., et al., *Mitochondrial DNA and RNA Increase in Peripheral Blood Mononuclear Cells from HIV-1-Infected Patients Randomized to Receive Stavudine-Containing or Stavudine-Sparing Combination Therapy*. *The Journal of Infectious Diseases*, 2005. **192**(10): p. 1794-1800.
95. Piko, L. and K.D. Taylor, *Amounts of mitochondrial DNA and abundance of some mitochondrial gene transcripts in early mouse embryos*. *Dev Biol*, 1987. **123**(2): p. 364-74.
96. Piko, L. and L. Matsumoto, *Number of mitochondria and some properties of mitochondrial DNA in the mouse egg*. *Dev Biol*, 1976. **49**(1): p. 1-10.
97. May-Panloup, P., et al., *Mitochondrial DNA in the oocyte and the developing embryo*. *Curr Top Dev Biol*, 2007. **77**: p. 51-83.

98. Bogenhagen, D. and D.A. Clayton, *Mouse L cell mitochondrial DNA molecules are selected randomly for replication throughout the cell cycle*. *Cell*, 1977. **11**(4): p. 719-27.
99. Lee, H.C. and Y.H. Wei, *Mitochondrial biogenesis and mitochondrial DNA maintenance of mammalian cells under oxidative stress*. *Int J Biochem Cell Biol*, 2005. **37**(4): p. 822-34.
100. Wu, Z., et al., *Mechanisms controlling mitochondrial biogenesis and respiration through the thermogenic coactivator PGC-1*. *Cell*, 1999. **98**(1): p. 115-24.
101. Kang, D., S.H. Kim, and N. Hamasaki, *Mitochondrial transcription factor A (TFAM): roles in maintenance of mtDNA and cellular functions*. *Mitochondrion*, 2007. **7**(1-2): p. 39-44.
102. Vina, J., et al., *Mitochondrial biogenesis in exercise and in ageing*. *Advanced Drug Delivery Reviews*, 2009. **61**(14): p. 1369-1374.
103. Civitarese, A.E., S.R. Smith, and E. Ravussin, *Diet, energy metabolism and mitochondrial biogenesis*. *Curr Opin Clin Nutr Metab Care*, 2007. **10**(6): p. 679-87.
104. Lynn, E.G., et al., *The regulation, control, and consequences of mitochondrial oxygen utilization and disposition in the heart and skeletal muscle during hypoxia*. *Antioxid Redox Signal*, 2007. **9**(9): p. 1353-61.
105. Spiegelman, B.M., *Transcriptional control of mitochondrial energy metabolism through the PGC1 coactivators*. *Novartis Found Symp*, 2007. **287**: p. 60-3; discussion 63-9.
106. Castellino, N. and S. Aloj, *Intracellular distribution of lead in the liver and kidney of the rat*. *Br J Ind Med*, 1969. **26**(2): p. 139-43.
107. Gavin, C.E., K.K. Gunter, and T.E. Gunter, *Mn²⁺ sequestration by mitochondria and inhibition of oxidative phosphorylation*. *Toxicology and Applied Pharmacology*, 1992. **115**(1): p. 1-5.
108. Sokolova, I.M., A.H. Ringwood, and C. Johnson, *Tissue-specific accumulation of cadmium in subcellular compartments of eastern oysters *Crassostrea virginica* Gmelin (*Bivalvia: Ostreidae*)*. *Aquatic Toxicology*, 2005. **74**(3): p. 218-228.
109. Anandatheerthavarada, H.K., et al., *Localization of Multiple Forms of Inducible Cytochromes P450 in Rat Liver Mitochondria: Immunological Characteristics and Patterns of Xenobiotic Substrate Metabolism*. *Archives of Biochemistry and Biophysics*, 1997. **339**(1): p. 136-150.
110. Niranjan, B.G., et al., *Hepatic mitochondrial cytochrome P-450 system. Distinctive features of cytochrome P-450 involved in the activation of aflatoxin B1 and benzo(a)pyrene*. *Journal of Biological Chemistry*, 1984. **259**(20): p. 12495-12501.
111. Jung, D. and R.T. Di Giulio, *Identification of mitochondrial cytochrome P450 induced in response to polycyclic aromatic hydrocarbons in the mummichog (*Fundulus heteroclitus*)*. *Comp Biochem Physiol C Toxicol Pharmacol*, 2010. **151**(1): p. 107-12.
112. LeDoux, S.P., et al., *Repair of mitochondrial DNA after various types of DNA damage in Chinese hamster ovary cells*. *Carcinogenesis*, 1992. **13**(11): p. 1967-1973.

113. Voulgaridou, G.P., et al., *DNA damage induced by endogenous aldehydes: current state of knowledge*. *Mutat Res*, 2011. **711**(1-2): p. 13-27.
114. Podratz, J.L., et al., *Cisplatin induced mitochondrial DNA damage in dorsal root ganglion neurons*. *Neurobiol Dis*, 2011. **41**(3): p. 661-8.
115. Salazar, I., et al., *The effect of benzo[a]pyrene on DNA synthesis and DNA polymerase activity of rat liver mitochondria*. *FEBS Lett*, 1982. **138**(1): p. 45-9.
116. Clayton, D., J. Doda, and E. Friedberg, *The absence of a pyrimidine dimer repair mechanism in mammalian mitochondria*. *Proceedings of the National Academy of Sciences*, 1974. **71**(7): p. 2777.
117. Pascucci, B., et al., *DNA repair of UV photoproducts and mutagenesis in human mitochondrial DNA*. *J Mol Biol*, 1997. **273**(2): p. 417-27.
118. Graziewicz, M.A., et al., *Nucleotide incorporation by human DNA polymerase gamma opposite benzo[a]pyrene and benzo[c]phenanthrene diol epoxide adducts of deoxyguanosine and deoxyadenosine*. *Nucleic Acids Res*, 2004. **32**(1): p. 397-405.
119. Tornaletti, S. and P.C. Hanawalt, *Effect of DNA lesions on transcription elongation*. *Biochimie*, 1999. **81**(1-2): p. 139-46.
120. Mitchell, D.L., G.M. Adair, and R.S. Nairn, *Inhibition of transient gene expression in Chinese hamster ovary cells by triplet-sensitized UV-B irradiation of transfected DNA*. *Photochem Photobiol*, 1989. **50**(5): p. 639-46.
121. Shen, H.M., et al., *Aflatoxin B1-Induced Lipid Peroxidation in Rat Liver*. *Toxicology and Applied Pharmacology*, 1994. **127**(1): p. 145-150.
122. Huc, L., et al., *Multiple apoptotic pathways induced by p53-dependent acidification in benzo[a]pyrene-exposed hepatic F258 cells*. *Journal of Cellular Physiology*, 2006. **208**(3): p. 527-537.
123. Bess, A.S., et al., *Mitochondrial dynamics and autophagy aid in removal of persistent mitochondrial DNA damage in *Caenorhabditis elegans**. *Nucleic Acids Res*, 2012.
124. Baird, W.M., L.A. Hooven, and B. Mahadevan, *Carcinogenic polycyclic aromatic hydrocarbon-DNA adducts and mechanism of action*. *Environmental and Molecular Mutagenesis*, 2005. **45**(2-3): p. 106-114.
125. Pfeifer, G.P., Y.H. You, and A. Besaratinia, *Mutations induced by ultraviolet light*. *Mutat Res*, 2005. **571**(1-2): p. 19-31.
126. Kasiviswanathan, R., et al., *Human mitochondrial DNA polymerase gamma exhibits potential for bypass and mutagenesis at UV-induced cyclobutane thymine dimers*. *J Biol Chem*, 2012.
127. Mita, S., R.J. Monnat, Jr., and L.A. Loeb, *Resistance of HeLa cell mitochondrial DNA to mutagenesis by chemical carcinogens*. *Cancer Res*, 1988. **48**(16): p. 4578-83.
128. Partridge, M.A., et al., *Environmental mutagens induced transversions but not transitions in regulatory region of mitochondrial DNA*. *J Toxicol Environ Health A*, 2009. **72**(5): p. 301-4.

129. Bogenhagen, D.F., *Repair of mtDNA in vertebrates*. Am J Hum Genet, 1999. **64**(5): p. 1276-81.
130. Croteau, D.L., R.H. Stierum, and V.A. Bohr, *Mitochondrial DNA repair pathways*. Mutat Res, 1999. **434**(3): p. 137-48.
131. Chen, H., et al., *Mitofusins Mfn1 and Mfn2 coordinately regulate mitochondrial fusion and are essential for embryonic development*. J Cell Biol, 2003. **160**(2): p. 189-200.
132. Delille, H., R. Alves, and M. Schrader, *Biogenesis of peroxisomes and mitochondria: linked by division*. Histochemistry and Cell Biology, 2009. **131**(4): p. 441-446.
133. Alavi, M., et al., *A splice site mutation in the murine Opa1 gene features pathology of autosomal dominant optic atrophy*. Brain, 2007. **130**(4): p. 1029.
134. Kim, J.Y., et al., *Mitochondrial DNA content is decreased in autosomal dominant optic atrophy*. Neurology, 2005. **64**(6): p. 966-72.
135. Jones, B. and W. Fangman, *Mitochondrial DNA maintenance in yeast requires a protein containing a region related to the GTP-binding domain of dynamin*. Genes & Development, 1992. **6**(3): p. 380.
136. Garrido, N., et al., *Composition and dynamics of human mitochondrial nucleoids*. Mol Biol Cell, 2003. **14**(4): p. 1583-96.
137. Ono, T., et al., *Human cells are protected from mitochondrial dysfunction by complementation of DNA products in fused mitochondria*. Nat Genet, 2001. **28**(3): p. 272-5.
138. Gilkerson, R.W., et al., *Mitochondrial nucleoids maintain genetic autonomy but allow for functional complementation*. J Cell Biol, 2008. **181**(7): p. 1117-28.
139. Busch, K., et al., *Mitochondrial dynamics generate equal distribution but patchwork localization of respiratory Complex I*. Molecular membrane biology, 2006. **23**(6): p. 509-520.
140. Chen, H., J.M. McCaffery, and D.C. Chan, *Mitochondrial fusion protects against neurodegeneration in the cerebellum*. Cell, 2007. **130**(3): p. 548-62.
141. Chen, H., et al., *Mitochondrial fusion is required for mtDNA stability in skeletal muscle and tolerance of mtDNA mutations*. Cell, 2010. **141**(2): p. 280-9.
142. Elachouri, G., et al., *OPA1 links human mitochondrial genome maintenance to mtDNA replication and distribution*. Genome Res, 2011. **21**(1): p. 12-20.
143. Rouzier, C., et al., *The MFN2 gene is responsible for mitochondrial DNA instability and optic atrophy 'plus' phenotype*. Brain, 2012. **135**(Pt 1): p. 23-34.
144. Zuchner, S., et al., *Mutations in the mitochondrial GTPase mitofusin 2 cause Charcot-Marie-Tooth neuropathy type 2A*. Nat Genet, 2004. **36**(5): p. 449-51.
145. Alexander, C., et al., *OPA1, encoding a dynamin-related GTPase, is mutated in autosomal dominant optic atrophy linked to chromosome 3q28*. nature genetics, 2000. **26**(2): p. 211-215.
146. Delettre, C., et al., *Nuclear gene OPA1, encoding a mitochondrial dynamin-related protein, is mutated in dominant optic atrophy*. Nat Genet, 2000. **26**(2): p. 207-10.

147. Labrousse, A.M., et al., *C. elegans* Dynamin-Related Protein DRP-1 Controls Severing of the Mitochondrial Outer Membrane. *Molecular cell*, 1999. **4**(5): p. 815-826.
148. Waterham, H., et al., *A lethal defect of mitochondrial and peroxisomal fission*. *The New England journal of medicine*, 2007. **356**(17): p. 1736.
149. Breckenridge, D.G., et al., *Caenorhabditis elegans drp-1 and fis-2 regulate distinct cell-death execution pathways downstream of ced-3 and independent of ced-9*. *Mol Cell*, 2008. **31**(4): p. 586-97.
150. Lee, Y.-j., et al., *Roles of the Mammalian Mitochondrial Fission and Fusion Mediators Fis1, Drp1, and Opa1 in Apoptosis*. *Mol. Biol. Cell*, 2004. **15**(11): p. 5001-5011.
151. Frank, S., et al., *The Role of Dynamin-Related Protein 1, a Mediator of Mitochondrial Fission, in Apoptosis*. *Developmental Cell*, 2001. **1**(4): p. 515-525.
152. Kuznetsov, A.V., et al., *The cell-type specificity of mitochondrial dynamics*. *Int J Biochem Cell Biol*, 2009. **41**(10): p. 1928-39.
153. Kuznetsov, A.V. and R. Margreiter, *Heterogeneity of mitochondria and mitochondrial function within cells as another level of mitochondrial complexity*. *Int J Mol Sci*, 2009. **10**(4): p. 1911-29.
154. Rossignol, R., et al., *Mitochondrial threshold effects*. *Biochem J*, 2003. **370**(Pt 3): p. 751-62.
155. Yoneda, M., T. Miyatake, and G. Attardi, *Complementation of mutant and wild-type human mitochondrial DNAs coexisting since the mutation event and lack of complementation of DNAs introduced separately into a cell within distinct organelles*. *Mol Cell Biol*, 1994. **14**(4): p. 2699-712.
156. Nakada, K., et al., *Inter-mitochondrial complementation: Mitochondria-specific system preventing mice from expression of disease phenotypes by mutant mtDNA*. *Nat Med*, 2001. **7**(8): p. 934-40.
157. Ashley, N. and J. Poulton, *Anticancer DNA intercalators cause p53-dependent mitochondrial DNA nucleoid re-modelling*. *Oncogene*, 2009. **28**(44): p. 3880-3891.
158. Lee, H.C., et al., *Increase in mitochondrial mass in human fibroblasts under oxidative stress and during replicative cell senescence*. *J Biomed Sci*, 2002. **9**(6 Pt 1): p. 517-26.
159. Zanchetta, L.M., et al., *Mitophagy and mitochondrial morphology in human melanoma-derived cells post exposure to simulated sunlight*. *Int J Radiat Biol*, 2011. **87**(5): p. 506-17.
160. van der Blik, A., *Fussy mitochondria fuse in response to stress*. *The EMBO journal*, 2009. **28**(11): p. 1533.
161. Fletcher, M.J. and D.R. Sanadi, *Turnover of rat-liver mitochondria*. *Biochim Biophys Acta*, 1961. **51**: p. 356-60.
162. Beattie, D.S., R.E. Basford, and S.B. Koritz, *The turnover of the protein components of mitochondria from rat liver, kidney, and brain*. *J Biol Chem*, 1967. **242**(20): p. 4584-6.
163. Menzies, R.A. and P.H. Gold, *The turnover of mitochondria in a variety of tissues of young adult and aged rats*. *J Biol Chem*, 1971. **246**(8): p. 2425-9.

164. Gross, N.J., G.S. Getz, and M. Rabinowitz, *Apparent turnover of mitochondrial deoxyribonucleic acid and mitochondrial phospholipids in the tissues of the rat*. J Biol Chem, 1969. **244**(6): p. 1552-62.
165. Lipsky, N.G. and P.L. Pedersen, *Mitochondrial turnover in animal cells. Half-lives of mitochondria and mitochondrial subfractions of rat liver based on [14C]bicarbonate incorporation*. J Biol Chem, 1981. **256**(16): p. 8652-7.
166. Miwa, S., C. Lawless, and T. von Zglinicki, *Mitochondrial turnover in liver is fast in vivo and is accelerated by dietary restriction: application of a simple dynamic model*. Aging Cell, 2008. **7**(6): p. 920-3.
167. Kai, Y., et al., *Rapid and random turnover of mitochondrial DNA in rat hepatocytes of primary culture*. Mitochondrion, 2006. **6**(6): p. 299-304.
168. Ashford, T.P. and K.R. Porter, *Cytoplasmic components in hepatic cell lysosomes*. J Cell Biol, 1962. **12**: p. 198-202.
169. Wong, A.S., Z.H. Cheung, and N.Y. Ip, *Molecular machinery of macroautophagy and its deregulation in diseases*. Biochim Biophys Acta, 2011. **1812**(11): p. 1490-7.
170. Rabinowitz, J.D. and E. White, *Autophagy and Metabolism*. Science, 2010. **330**(6009): p. 1344-1348.
171. Sarbassov, D.D., S.M. Ali, and D.M. Sabatini, *Growing roles for the mTOR pathway*. Current Opinion in Cell Biology, 2005. **17**(6): p. 596-603.
172. Kristensen, A.R., et al., *Ordered organelle degradation during starvation-induced autophagy*. Mol Cell Proteomics, 2008. **7**(12): p. 2419-28.
173. Gomes, L.C., G.D. Benedetto, and L. Scorrano, *During autophagy mitochondria elongate, are spared from degradation and sustain cell viability*. Nat Cell Biol, 2011. **13**(5): p. 589-598.
174. Rambold, A.S., et al., *Tubular network formation protects mitochondria from autophagosomal degradation during nutrient starvation*. Proc Natl Acad Sci U S A, 2011. **108**(25): p. 10190-5.
175. Kim, I. and J.J. Lemasters, *Mitochondrial degradation by autophagy (mitophagy) in GFP-LC3 transgenic hepatocytes during nutrient deprivation*. Am J Physiol Cell Physiol, 2011. **300**(2): p. C308-17.
176. Lemasters, J.J., et al., *The mitochondrial permeability transition in cell death: a common mechanism in necrosis, apoptosis and autophagy*. Biochim Biophys Acta, 1998. **1366**(1-2): p. 177-96.
177. Twig, G., B. Hyde, and O.S. Shirihai, *Mitochondrial fusion, fission and autophagy as a quality control axis: the bioenergetic view*. Biochim Biophys Acta, 2008. **1777**(9): p. 1092-7.
178. Valente, E.M., et al., *Hereditary early-onset Parkinson's disease caused by mutations in PINK1*. Science, 2004. **304**(5674): p. 1158-60.
179. Kitada, T., et al., *Mutations in the parkin gene cause autosomal recessive juvenile parkinsonism*. Nature, 1998. **392**(6676): p. 605-8.

180. Geisler, S., et al., *The PINK1/Parkin-mediated mitophagy is compromised by PD-associated mutations*. *Autophagy*, 2010. **6**(7): p. 871-8.
181. Vives-Bauza, C., et al., *PINK1-dependent recruitment of Parkin to mitochondria in mitophagy*. *Proc Natl Acad Sci U S A*, 2010. **107**(1): p. 378-83.
182. Matsuda, N., et al., *PINK1 stabilized by mitochondrial depolarization recruits Parkin to damaged mitochondria and activates latent Parkin for mitophagy*. *J Cell Biol*, 2010. **189**(2): p. 211-21.
183. Vila, M., D. Ramonet, and C. Perier, *Mitochondrial alterations in Parkinson's disease: new clues*. *J Neurochem*, 2008. **107**(2): p. 317-28.
184. Gil, J.M. and A.C. Rego, *Mechanisms of neurodegeneration in Huntington's disease*. *Eur J Neurosci*, 2008. **27**(11): p. 2803-20.
185. Santos, R.X., et al., *A Synergistic Dysfunction of Mitochondrial Fission/Fusion Dynamics and Mitophagy in Alzheimer's Disease*. *Journal of Alzheimer's Disease*, 2010. **20**: p. 401-412.
186. Kim, I. and J.J. Lemasters, *Mitophagy Selectively Degrades Individual Damaged Mitochondria After Photoirradiation*. *Antioxid Redox Signal*, 2011.
187. Van Laar, V.S., et al., *Bioenergetics of neurons inhibit the translocation response of Parkin following rapid mitochondrial depolarization*. *Hum Mol Genet*, 2011. **20**(5): p. 927-40.
188. Gilkerson, R.W., et al., *Mitochondrial autophagy in cells with mtDNA mutations results from synergistic loss of transmembrane potential and mTORC1 inhibition*. *Hum Mol Genet*, 2012. **21**(5): p. 978-90.
189. Arnoult, D., et al., *Bax/Bak-dependent release of DDP/TIMM8a promotes Drp1-mediated mitochondrial fission and mitoptosis during programmed cell death*. *Curr Biol*, 2005. **15**(23): p. 2112-8.
190. Parone, P.A., et al., *Preventing mitochondrial fission impairs mitochondrial function and leads to loss of mitochondrial DNA*. *PLoS ONE*, 2008. **3**(9): p. e3257.
191. Chen, L.H., et al., *Targeting Protective Autophagy Exacerbates UV-Triggered Apoptotic Cell Death*. *Int J Mol Sci*, 2012. **13**(1): p. 1209-24.
192. Eid, N., Y. Ito, and Y. Otsuki, *Enhanced mitophagy in Sertoli cells of ethanol-treated rats: morphological evidence and clinical relevance*. *J Mol Histol*, 2012. **43**(1): p. 71-80.
193. Crouser, E.D., et al., *Carbamoyl phosphate synthase-1: a marker of mitochondrial damage and depletion in the liver during sepsis*. *Crit Care Med*, 2006. **34**(9): p. 2439-46.
194. Pan, T., et al., *Rapamycin protects against rotenone-induced apoptosis through autophagy induction*. *Neuroscience*, 2009. **164**(2): p. 541-51.
195. Cotan, D., et al., *Secondary coenzyme Q10 deficiency triggers mitochondria degradation by mitophagy in MELAS fibroblasts*. *The FASEB Journal*, 2011. **25**(8): p. 2669-2687.
196. Rodriguez-Hernandez, A., et al., *Coenzyme Q deficiency triggers mitochondria degradation by mitophagy*. *Autophagy*, 2009. **5**(1): p. 19-32.

197. Marino, M.L., et al., *Proton pump inhibition induces autophagy as a survival mechanism following oxidative stress in human melanoma cells*. *Cell Death Dis*, 2010. **1**(10): p. e87.
198. Hamacher-Brady, A., et al., *Autophagy as a protective response to Bnip3-mediated apoptotic signaling in the heart*. *Autophagy*, 2006. **2**(4): p. 307-9.
199. Pridgeon, J.W., et al., *PINK1 Protects against Oxidative Stress by Phosphorylating Mitochondrial Chaperone TRAP1*. *PLoS Biol*, 2007. **5**(7): p. e172.
200. Dagda, R.K. and C.T. Chu, *Mitochondrial quality control: insights on how Parkinson's disease related genes PINK1, parkin, and Omi/HtrA2 interact to maintain mitochondrial homeostasis*. *J Bioenerg Biomembr*, 2009. **41**(6): p. 473-9.
201. Clark, I.E., et al., *Drosophila pink1 is required for mitochondrial function and interacts genetically with parkin*. *Nature*, 2006. **441**(7097): p. 1162-6.
202. Scheibye-Knudsen, M., et al., *Cockayne syndrome group B protein prevents the accumulation of damaged mitochondria by promoting mitochondrial autophagy*. *J Exp Med*, 2012. **209**(4): p. 855-69.
203. Monick, M.M., et al., *Identification of an autophagy defect in smokers' alveolar macrophages*. *J Immunol*, 2010. **185**(9): p. 5425-35.
204. Wu, J.J., et al., *Mitochondrial dysfunction and oxidative stress mediate the physiological impairment induced by the disruption of autophagy*. *Aging (Albany NY)*, 2009. **1**(4): p. 425-37.
205. Tal, M.C., et al., *Absence of autophagy results in reactive oxygen species-dependent amplification of RLR signaling*. *Proc Natl Acad Sci U S A*, 2009. **106**(8): p. 2770-5.
206. Cotan, D., et al., *Secondary coenzyme Q10 deficiency triggers mitochondria degradation by mitophagy in MELAS fibroblasts*. *FASEB J*, 2011. **25**(8): p. 2669-87.
207. Settembre, C., et al., *A block of autophagy in lysosomal storage disorders*. *Hum Mol Genet*, 2008. **17**(1): p. 119-29.
208. Gonzalez, C.D., et al., *The emerging role of autophagy in the pathophysiology of diabetes mellitus*. *Autophagy*, 2011. **7**(1): p. 2-11.
209. Dutta, D., et al., *Contribution of Impaired Mitochondrial Autophagy to Cardiac Aging*. *Circulation Research*, 2012. **110**(8): p. 1125-1138.
210. Kiontke, K. and W. Sudhaus (2006) *Ecology of Caenorhabditis species*. *WormBook*, 1-14.
211. Antoshechkin, I. and P.W. Sternberg, *The versatile worm: genetic and genomic resources for Caenorhabditis elegans research*. *Nat Rev Genet*, 2007. **8**(7): p. 518-32.
212. Wood, W.B., *The Nematode Caenorhabditis elegans*. *Monograph Series*. 1988, Cold Spring Harbor, NY: Cold Spring Harbor Laboratory Press.
213. Hope, I.A., *Background of Caenorhabditis elegans*, in *C. elegans: A practical approach*, I.A. Hope, Editor. 1999, Oxford University Press: New York.

214. The C. elegans Sequencing Consortium, *Genome Sequence of the Nematode C. elegans: A Platform for Investigating Biology*. Science, 1998. **282**(5396): p. 2012-2018.
215. Leung, M.C., et al., *Caenorhabditis elegans: an emerging model in biomedical and environmental toxicology*. Toxicol Sci, 2008. **106**(1): p. 5-28.
216. Murfitt, R.R., K. Vogel, and D.R. Sanadi, *Characterization of the mitochondria of the free-living nematode, Caenorhabditis elegans*. Comp Biochem Physiol B, 1976. **53**(4): p. 423-30.
217. Okimoto, R., et al., *The mitochondrial genomes of two nematodes, Caenorhabditis elegans and Ascaris suum*. Genetics, 1992. **130**(3): p. 471-98.
218. Tsang, W.Y. and B.D. Lemire, *The role of mitochondria in the life of the nematode, Caenorhabditis elegans*. Biochim Biophys Acta, 2003. **1638**(2): p. 91-105.
219. Breton, S., D.T. Stewart, and W.R. Hoeh, *Characterization of a mitochondrial ORF from the gender-associated mtDNAs of Mytilus spp. (Bivalvia: Mytilidae): identification of the "missing" ATPase 8 gene*. Mar Genomics, 2010. **3**(1): p. 11-8.
220. Tsang, W.Y. and B.D. Lemire, *Mitochondrial genome content is regulated during nematode development*. Biochem Biophys Res Commun, 2002. **291**(1): p. 8-16.
221. Mouli, P.K., G. Twig, and O.S. Shirihai, *Frequency and selectivity of mitochondrial fusion are key to its quality maintenance function*. Biophys J, 2009. **96**(9): p. 3509-18.
222. Backer, J.M. and I.B. Weinstein, *Interaction of benzo(a)pyrene and its dihydrodiol-epoxide derivative with nuclear and mitochondrial DNA in C3H10T 1/2 cell cultures*. Cancer Res, 1982. **42**(7): p. 2764-9.
223. Al Rawi, S., et al., *Postfertilization autophagy of sperm organelles prevents paternal mitochondrial DNA transmission*. Science, 2011. **334**(6059): p. 1144-7.
224. Sato, M. and K. Sato, *Degradation of paternal mitochondria by fertilization-triggered autophagy in C. elegans embryos*. Science, 2011. **334**(6059): p. 1141-4.
225. Zhang, J., M. Kundu, and P.A. Ney, *Mitophagy in mammalian cells: the reticulocyte model*. Methods Enzymol, 2009. **452**: p. 227-45.
226. Elmore, S., et al., *The mitochondrial permeability transition initiates autophagy in rat hepatocytes*. The FASEB Journal, 2001: p. 102061.
227. Mijaljica, D., M. Prescott, and R.J. Devenish, *Different fates of mitochondria: alternative ways for degradation?* Autophagy, 2007. **3**(1): p. 4-9.
228. Tolkovsky, A.M., et al., *Mitochondrial disappearance from cells: a clue to the role of autophagy in programmed cell death and disease?* Biochimie, 2002. **84**(2-3): p. 233-240.
229. Boya, P., et al., *Inhibition of Macroautophagy Triggers Apoptosis*. Mol. Cell. Biol., 2005. **25**(3): p. 1025-1040.
230. Malhi, H., G.J. Gores, and J.J. Lemasters, *Apoptosis and necrosis in the liver: A tale of two deaths?* Hepatology, 2006. **43**(S1): p. S31-S44.

231. Addo, M.G., et al., *Caenorhabditis elegans*, a pluricellular model organism to screen new genes involved in mitochondrial genome maintenance. *Biochim Biophys Acta*, 2010. **1802**(9): p. 765-73.
232. Rea, S.L., n. Ventura, and T.E. Johnson, *Relationship Between Mitochondrial Electron Transport Chain Dysfunction, Development, and Life Extension in Caenorhabditis elegans*, in *PLoS Biology*. 2007, Public Library of Science. p. e259.
233. Tsang, W.Y., et al., *Mitochondrial Respiratory Chain Deficiency in Caenorhabditis elegans Results in Developmental Arrest and Increased Life Span*. *J. Biol. Chem.*, 2001. **276**(34): p. 32240-32246.
234. Boyd, W.A., et al., *Nucleotide excision repair genes are expressed at low levels and are not detectably inducible in Caenorhabditis elegans somatic tissues, but their function is required for normal adult life after UVC exposure*. *Mutation Research/Fundamental and Molecular Mechanisms of Mutagenesis*, 2009. **683**(1-2): p. 57-67.
235. Hunter, S.E., et al., *The QPCR assay for analysis of mitochondrial DNA damage, repair, and relative copy number*. *Methods*, 2010. **51**(4): p. 444-451.
236. Santos, J.H., et al., *Quantitative PCR-based measurement of nuclear and mitochondrial DNA damage and repair in mammalian cells*. *Methods Mol Biol*, 2006. **314**: p. 183-99.
237. Bratic, I., et al., *Mitochondrial DNA level, but not active replicase, is essential for Caenorhabditis elegans development*. *Nucleic Acids Res*, 2009. **37**(6): p. 1817-28.
238. Rual, J.F., et al., *Toward improving Caenorhabditis elegans phenome mapping with an ORFeome-based RNAi library*. *Genome Res*, 2004. **14**(10B): p. 2162-8.
239. Kamath, R.S. and J. Ahringer, *Genome-wide RNAi screening in Caenorhabditis elegans*. *Methods*, 2003. **30**(4): p. 313-21.
240. Kodoyianni, V., E.M. Maine, and J. Kimble, *Molecular basis of loss-of-function mutations in the glp-1 gene of Caenorhabditis elegans*. *Mol Biol Cell*, 1992. **3**(11): p. 1199-213.
241. Kanazawa, T., et al., *The C. elegans Opa1 homologue EAT-3 is essential for resistance to free radicals*. *PLoS Genet*, 2008. **4**(2): p. e1000022.
242. Dagda, R.K., et al., *Loss of PINK1 function promotes mitophagy through effects on oxidative stress and mitochondrial fission*. *J Biol Chem*, 2009. **284**(20): p. 13843-55.
243. Merrill, R.A., et al., *Mechanism of neuroprotective mitochondrial remodeling by PKA/AKAP1*. *PLoS Biol*, 2011. **9**(4): p. e1000612.
244. Lagido, C., et al., *Bridging the phenotypic gap: real-time assessment of mitochondrial function and metabolism of the nematode Caenorhabditis elegans*. *BMC Physiol*, 2008. **8**: p. 7.
245. Grad, L.I., L.C. Sayles, and B.D. Lemire, *Isolation and functional analysis of mitochondria from the nematode Caenorhabditis elegans*. *Methods Mol Biol*, 2007. **372**: p. 51-66.
246. Rochette, P.J. and D.E. Brash, *Human telomeres are hypersensitive to UV-induced DNA Damage and refractory to repair*. *PLoS Genet*, 2010. **6**(4): p. e1000926.

247. Meyer, J.N., et al., *Decline of nucleotide excision repair capacity in aging Caenorhabditis elegans*. *Genome Biol*, 2007. **8**(5): p. R70.
248. Austin, J. and J. Kimble, *glp-1 is required in the germ line for regulation of the decision between mitosis and meiosis in C. elegans*. *Cell*, 1987. **51**(4): p. 589-99.
249. Simsek, D., et al., *Crucial role for DNA ligase III in mitochondria but not in Xrcc1-dependent repair*. *Nature*, 2011. **471**(7337): p. 245-248.
250. Braeckman, B.P., et al., *Assaying metabolic activity in ageing Caenorhabditis elegans*. *Mech Ageing Dev*, 2002. **123**(2-3): p. 105-19.
251. Melendez, A., et al., *Autophagy genes are essential for dauer development and life-span extension in C. elegans*. *Science*, 2003. **301**(5638): p. 1387-91.
252. Hansen, M., et al., *A role for autophagy in the extension of lifespan by dietary restriction in C. elegans*. *PLoS Genet*, 2008. **4**(2): p. e24.
253. Morck, C. and M. Pilon, *C. elegans feeding defective mutants have shorter body lengths and increased autophagy*. *BMC Dev Biol*, 2006. **6**: p. 39.
254. Florez-McClure, M.L., et al., *Decreased insulin-receptor signaling promotes the autophagic degradation of beta-amyloid peptide in C. elegans*. *Autophagy*, 2007. **3**(6): p. 569-80.
255. Kang, C., Y.J. You, and L. Avery, *Dual roles of autophagy in the survival of Caenorhabditis elegans during starvation*. *Genes Dev*, 2007. **21**(17): p. 2161-71.
256. Blommaert, E.F.C., et al., *The Phosphatidylinositol 3-Kinase Inhibitors Wortmannin and LY294002 Inhibit Autophagy in Isolated Rat Hepatocytes*. *European Journal of Biochemistry*, 1997. **243**(1-2): p. 240-246.
257. Samokhvalov, V., B.A. Scott, and C.M. Crowder, *Autophagy protects against hypoxic injury in C. elegans*. *Autophagy*, 2008. **4**(8): p. 1034-41.
258. Piko, L. and D.G. Chase, *Role of the mitochondrial genome during early development in mice. Effects of ethidium bromide and chloramphenicol*. *J Cell Biol*, 1973. **58**(2): p. 357-78.
259. Astin, J.W., N.J. O'Neil, and P.E. Kuwabara, *Nucleotide excision repair and the degradation of RNA pol II by the Caenorhabditis elegans XPA and Rsp5 orthologues, RAD-3 and WWP-1*. *DNA Repair*, 2008. **7**(2): p. 267-280.
260. Gaines, G. and G. Attardi, *Intercalating drugs and low temperatures inhibit synthesis and processing of ribosomal RNA in isolated human mitochondria*. *J Mol Biol*, 1984. **172**(4): p. 451-66.
261. Yasuhira, S. and A. Yasui, *Alternative excision repair pathway of UV-damaged DNA in Schizosaccharomyces pombe operates both in nucleus and in mitochondria*. *J Biol Chem*, 2000. **275**(16): p. 11824-8.
262. Kalinowski, D.P., S. Illenye, and B. Van Houten, *Analysis of DNA damage and repair in murine leukemia L1210 cells using a quantitative polymerase chain reaction assay*. *Nucleic Acids Res*, 1992. **20**(13): p. 3485-94.

263. Ved, R., et al., *Similar Patterns of Mitochondrial Vulnerability and Rescue Induced by Genetic Modification of α -Synuclein, Parkin, and DJ-1 in *Caenorhabditis elegans**. *Journal of Biological Chemistry*, 2005. **280**(52): p. 42655-42668.
264. Samann, J., et al., *Caenorhabditis elegans LRK-1 and PINK-1 act antagonistically in stress response and neurite outgrowth*. *J Biol Chem*, 2009. **284**(24): p. 16482-91.
265. Kamp, F., et al., *Inhibition of mitochondrial fusion by alpha-synuclein is rescued by PINK1, Parkin and DJ-1*. *Embo J*, 2010. **29**(20): p. 3571-89.
266. Twig, G. and O.S. Shirihai, *The interplay between mitochondrial dynamics and mitophagy*. *Antioxid Redox Signal*, 2011. **14**(10): p. 1939-51.
267. White, K.E., et al., *OPA1 Deficiency Associated with Increased Autophagy in Retinal Ganglion Cells in a Murine Model of Dominant Optic Atrophy*. *Invest. Ophthalmol. Vis. Sci.*, 2009. **50**(6): p. 2567-2571.
268. Choi, S.E., et al., *Protective role of autophagy in palmitate-induced INS-1 beta-cell death*. *Endocrinology*, 2009. **150**(1): p. 126-34.
269. Gomes, L.C. and L. Scorrano, *High levels of Fis1, a pro-fission mitochondrial protein, trigger autophagy*. *Biochimica et Biophysica Acta (BBA) - Bioenergetics*, 2008. **1777**(7-8): p. 860-866.
270. Gispert, S., et al., *Parkinson phenotype in aged PINK1-deficient mice is accompanied by progressive mitochondrial dysfunction in absence of neurodegeneration*. *PLoS ONE*, 2009. **4**(6): p. e5777.
271. Yu, W., et al., *The PINK1/Parkin pathway regulates mitochondrial dynamics and function in mammalian hippocampal and dopaminergic neurons*. *Hum Mol Genet*, 2011. **20**(16): p. 3227-40.
272. Chen, H., A. Chomyn, and D.C. Chan, *Disruption of Fusion Results in Mitochondrial Heterogeneity and Dysfunction*. *Journal of Biological Chemistry*, 2005. **280**(28): p. 26185-26192.
273. Zanna, C., et al., *OPA 1 mutations associated with dominant optic atrophy impair oxidative phosphorylation and mitochondrial fusion*. *Brain*, 2008. **131**(2): p. 352.
274. Olichon, A., et al., *Loss of OPA1 perturbs the mitochondrial inner membrane structure and integrity, leading to cytochrome c release and apoptosis*. *J Biol Chem*, 2003. **278**(10): p. 7743-6.
275. Yang, C.C., et al., *The dynamin-related protein DRP-1 and the insulin signaling pathway cooperate to modulate *C. elegans* longevity*. *Aging Cell*, 2011.
276. Aamann, M.D., et al., *Cockayne syndrome group B protein promotes mitochondrial DNA stability by supporting the DNA repair association with the mitochondrial membrane*. *FASEB J*, 2010. **24**(7): p. 2334-46.
277. Kamenisch, Y., et al., *Proteins of nucleotide and base excision repair pathways interact in mitochondria to protect from loss of subcutaneous fat, a hallmark of aging*. *J Exp Med*, 2010. **207**(2): p. 379-90.

278. Scheibye-Knudsen, M., et al., *Cockayne syndrome group B protein prevents the accumulation of damaged mitochondria by promoting mitochondrial autophagy*. J Exp Med, 2012. **209**(4): p. 855-69.
279. Davies, A.M., et al., *A Ca²⁺-induced mitochondrial permeability transition causes complete release of rat liver endonuclease G activity from its exclusive location within the mitochondrial intermembrane space. Identification of a novel endo-exonuclease activity residing within the mitochondrial matrix*. Nucleic Acids Res, 2003. **31**(4): p. 1364-73.
280. Ikeda, S. and K. Ozaki, *Action of Mitochondrial Endonuclease G on DNA Damaged by-Ascorbic Acid, Peplomycin, and cis-Diamminedichloroplatinum (II)*. Biochemical and Biophysical Research Communications, 1997. **235**(2): p. 291-294.
281. Shokolenko, I., et al., *Oxidative stress induces degradation of mitochondrial DNA*. Nucleic Acids Res, 2009. **37**(8): p. 2539-48.
282. Tann, A.W., et al., *Apoptosis induced by persistent single-strand breaks in mitochondrial genome: critical role of EXOG (5'-EXO/endonuclease) in their repair*. J Biol Chem, 2011. **286**(37): p. 31975-83.
283. Brooks, P.J., *The case for 8,5'-cyclopurine-2'-deoxynucleosides as endogenous DNA lesions that cause neurodegeneration in xeroderma pigmentosum*. Neuroscience, 2007. **145**(4): p. 1407-17.
284. Furda, A., Bess, AS, Meyer, JN, Van Houten, B, *Analysis of DNA damage and repair in nuclear and mitochondrial DNA of animal cells using quantitative PCR*. , in *Methods in Molecular Biology: DNA repair protocols*, L. Bjergbæk, Editor. 2012, Springer Science+Business Media New York, USA.
285. Venegas, V. and M.C. Halberg, *Measurement of mitochondrial DNA copy number*. Methods Mol Biol, 2012. **837**: p. 327-35.
286. Koopman, W.J., et al., *Mitochondrial network complexity and pathological decrease in complex I activity are tightly correlated in isolated human complex I deficiency*. Am J Physiol Cell Physiol, 2005. **289**(4): p. C881-90.
287. Jackman, J. and P.M. O'Connor, *Methods for Synchronizing Cells at Specific Stages of the Cell Cycle*, in *Current Protocols in Cell Biology*. 2001, John Wiley & Sons, Inc.
288. Ryba, T., et al., *Genome-scale analysis of replication timing: from bench to bioinformatics*. Nat. Protocols, 2011. **6**(6): p. 870-895.
289. Klionsky, D.J., et al., *Guidelines for the use and interpretation of assays for monitoring autophagy in higher eukaryotes*. Autophagy, 2008. **4**(2): p. 151-75.
290. Rubinsztein, D.C., et al., *In search of an "autophagometer"*. Autophagy, 2009. **5**(5): p. 585-9.
291. Metivier, D., et al., *Cytofluorometric detection of mitochondrial alterations in early CD95/Fas/APO-1-triggered apoptosis of Jurkat T lymphoma cells. Comparison of seven mitochondrion-specific fluorochromes*. Immunology Letters, 1998. **61**(2-3): p. 157-163.

292. Pendergrass, W., N. Wolf, and M. Poot, *Efficacy of MitoTracker Green and CMXRosamine to measure changes in mitochondrial membrane potentials in living cells and tissues*. *Cytometry A*, 2004. **61**(2): p. 162-9.
293. Larsson, N.G., et al., *Mitochondrial transcription factor A is necessary for mtDNA maintenance and embryogenesis in mice*. *Nat Genet*, 1998. **18**(3): p. 231-6.
294. Hock, M.B. and A. Kralli, *Transcriptional Control of Mitochondrial Biogenesis and Function*. *Annual Review of Physiology*, 2009. **71**(1): p. 177-203.
295. Chazotte, B., *Labeling mitochondria with TMRM or TMRE*. *Cold Spring Harb Protoc*, 2011. **2011**(7): p. 895-7.
296. Kuznetsov, A.V., et al., *Mitochondrial ROS production under cellular stress: comparison of different detection methods*. *Anal Bioanal Chem*, 2011. **400**(8): p. 2383-90.
297. Unsal-Kacmaz, K., et al., *Preferential binding of ATR protein to UV-damaged DNA*. *Proc Natl Acad Sci U S A*, 2002. **99**(10): p. 6673-8.
298. Hurley, P.J. and F. Bunz, *ATM and ATR: components of an integrated circuit*. *Cell Cycle*, 2007. **6**(4): p. 414-7.
299. Suzuki, K., S. Kodama, and M. Watanabe, *Recruitment of ATM protein to double strand DNA irradiated with ionizing radiation*. *J Biol Chem*, 1999. **274**(36): p. 25571-5.
300. Sengupta, S., T.R. Peterson, and D.M. Sabatini, *Regulation of the mTOR complex 1 pathway by nutrients, growth factors, and stress*. *Mol Cell*, 2010. **40**(2): p. 310-22.
301. Alexander, A., et al., *ATM signals to TSC2 in the cytoplasm to regulate mTORC1 in response to ROS*. *Proc Natl Acad Sci U S A*, 2010. **107**(9): p. 4153-8.
302. Robert, T., et al., *HDACs link the DNA damage response, processing of double-strand breaks and autophagy*. *Nature*, 2011. **471**(7336): p. 74-9.
303. Valentin-Vega, Y.A., et al., *Mitochondrial dysfunction in ataxia-telangiectasia*. *Blood*, 2012. **119**(6): p. 1490-500.
304. Cartoni, R., et al., *Mitofusins 1/2 and ERR α expression are increased in human skeletal muscle after physical exercise*. *The Journal of Physiology*, 2005. **567**(1): p. 349-358.
305. Merlo Pich, M., et al., *Increased transcription of mitochondrial genes for Complex I in human platelets during ageing*. *FEBS Letters*, 2004. **558**(1-3): p. 19-22.
306. Manczak, M., M.J. Calkins, and P.H. Reddy, *Impaired mitochondrial dynamics and abnormal interaction of amyloid beta with mitochondrial protein Drp1 in neurons from patients with Alzheimer's disease: implications for neuronal damage*. *Human Molecular Genetics*, 2011. **20**(13): p. 2495-2509.
307. Lavin, M.F., *Ataxia-telangiectasia: from a rare disorder to a paradigm for cell signalling and cancer*. *Nat Rev Mol Cell Biol*, 2008. **9**(10): p. 759-69.
308. Eaton, J.S., et al., *Ataxia-telangiectasia mutated kinase regulates ribonucleotide reductase and mitochondrial homeostasis*. *J Clin Invest*, 2007. **117**(9): p. 2723-34.
309. Holt, I.J., *Zen and the art of mitochondrial DNA maintenance*. *Trends Genet*, 2010. **26**(3): p. 103-9.

310. Bourdon, A., et al., *Mutation of RRM2B, encoding p53-controlled ribonucleotide reductase (p53R2), causes severe mitochondrial DNA depletion*. *Nat Genet*, 2007. **39**(6): p. 776-80.
311. Rufa, A., et al., *Leber hereditary optic neuropathy in 2 of 4 siblings with 11778 mtDNA mutation: clinical variability or effect of toxic environmental exposure?* *Eur Neurol*, 2005. **53**(1): p. 32-4.
312. Xu, L., et al., *Active site of Escherichia coli DNA photolyase: Asn378 is crucial both for stabilizing the neutral flavin radical cofactor and for DNA repair*. *Biochemistry*, 2008. **47**(33): p. 8736-43.

Biography

Amanda Michelle Smith Bess was born in Webster, Texas, USA on April 28, 1984 to Judith and Jeffrey Smith. She received her Bachelor of Science degree, summa cum laude, in Biology from North Georgia College and State University in August of 2006.

Publications:

Bess, Amanda S., Crocker, Tracey L., Ryde, Ian T., Meyer, Joel N. 2012.

Mitochondrial dynamics and autophagy aid in removal of persistent mitochondrial DNA damage. *Nucleic Acids Res.* 10.1093/nar/gks532.

A. Furda, **A. S. Bess**, J. N. Meyer, B. Van Houten. Quantitative Analysis of DNA damage and repair in nuclear and mitochondrial DNA of animal cells using quantitative PCR. IN DNA Repair Protocols, Third Edition. Ed. Lotte Bjergbaek Springer Science+Business Medical LLC, NY, NY, in press 2012.

Powers CM, Wrench N, Ryde IT, **Smith AM**, Seidler FJ, Slotkin TA. 2009. Silver Impairs Neurodevelopment: Studies in PC12 Cells. *Environ Health Perspect* 118(1): 73-9.

Honors and Awards:

Burroughs Wellcome Travel Scholarship. Mitochondrial Medicine 2011, 2011.

Student Travel Award. Environmental Mutagenesis Society, Fort Worth, TX, Oct. 2010.

Best Poster Presentation. Genetics and Environmental Mutagenesis Society, 2009.

Duke University Graduate Student Travel Award, 2009 – 2011.

Nicholas School of the Environment Student Travel Award, 2009 – 2011.